

Università degli Studi di Padova

DIPARTIMENTO DI INGEGNERIA CIVILE,

EDILE ED AMBIENTALE



Tesi di Laurea

**EXPLOITING HYDROLOGIC MEASUREMENTS
FOR IRRIGATION WATER MANAGEMENT: A
CASE STUDY**

Relatore: Prof. Gianluca BOTTER

Correlatore: Prof. Mario PUTTI

Laureanda: Elisa NEGRETTO

ANNO ACCADEMICO 2013-2014

Al mio nonno Renzo

Contents

1	Introduction	1
2	Soil Moisture Dynamics	5
2.1	Soil Water Balance Equations	7
2.1.1	The FAO method for ET evaluation	9
2.1.2	ET in water stress conditions	10
2.2	Soil Moisture Dynamics	12
2.3	Irrigation	15
2.3.1	Sprinkler irrigation	16
2.3.2	Irrigation Schemes	19
3	Materials and Methods	25
3.1	Time Domain Reflectometry	25
3.1.1	Basic Principles	26
3.1.2	Probe configuration	28
3.1.3	Construction of the probes	29
4	Results of the experiment	31
4.1	Description of the site	31
4.2	Positioning of the probes	34
4.3	Hydrologic data	35
4.3.1	First period	42
4.3.2	First irrigation	48
4.3.3	Second period	55
4.3.4	Second irrigation	56

4.3.5	Third irrigation	65
4.3.6	Third period	75
5	Interpretation of the results and discussion	81
6	Conclusions	97

Chapter 1

Introduction

Globally, irrigation is one of the primary use of fresh-water, accounting for nearly 85% of total water consumption [*Jury and Vaux, 2007*] and providing about 40% of the total food production [*Fereres and Soriano, 2007*]. Considering the ‘Millennium Development’ goals of halving the proportion of malnourished people in the world by 2015 while ensuring environmental sustainability not only is a tremendous agricultural endeavor but represents also the world largest water-resource challenge [*Vico e Porporato, 2010*]. In this perspective, improvements in irrigation management and water delivery methods are very important, because they may significantly increase the overall efficiency of irrigation and water productivity. Moreover, agriculture-related water demand is expected to increase in the near future due to foreseen alterations of rainfall regimes owing to climate change and increased need for food, fiber and biofuel.

Along with the need to minimize the amount of irrigation water per cultivated area, there is the interest for farmers in maximizing profits, through balancing crop yields and irrigation costs adapting water applications to plant water requirements. This tasks are highly complicated due to hydro-climatic variability and rainfall unpredictability both within single seasons and among different years. The hydro-climatic fluctuations have an extensive impact on irrigation requirements, crop productivity and profitability, as well as water resources availability. The inherent rainfall unpredictability calls for a probabilistic framework, which is necessary to fully assess the feasibility of different irrigation strategies.

In fact, an optimal irrigation schedule requires the determination of the right

amount and timing of water supplement to avoid crop stress in case of water scarcity and water wasting if too much water is given through irrigation. Another important issue to consider in irrigation scheduling is the increasing cost of diesel oil needed for irrigation applications.

There are three mainly used irrigation systems having different features: surface irrigation, sprinkler irrigation and drip irrigation. The former allows water to flow over the landcrop and naturally infiltrate into the soil driven by gravity. This is an old method and it is extremely inefficient due to the high water volumes required for a single application, the low spatial uniformity and the dependance on soil type which strongly impacts the wetting patterns. Sprinkler irrigation, instead, consists of water applied as an 'artificial rainfall' through sprinklers which spray the water over the crop. Sprinklers can be fixed, moving connected to a pipe or placed along a moving bar. This method ensures an high control of the volume and rates applied and a good uniformity of distribution. However, due to the need of high pressures to pump water through the pipes and the sprinklers, it is high energy-consuming. Other disadvantages related to the use of sprinkler irrigation are the water losses due to evaporation and wind disturbance. Drip irrigation consists of water dripped onto or into the soil at very slow rates from a system of plastic pipes featured by holes. There can be two ways of providing water using drip irrigation: the first method uses a system of pipes outside the soil, just resting on the surface, while the second method, called sub-irrigation, involves the presence of pipes located below the surface. The main advantages of this technique are the absence of wind disturbance and evaporation together with a higher control of the amount of water given to the crop. On the other hand, this method is nowadays suitable for row crops and most of all for high values crops, due to the high costs of the plant. In Italy, sprinkler irrigation is the most used irrigation technique as it represents the best trade off among efficiency, costs of the machinery and energy consumption, especially for the maize crops. Wind disturbance can affect the irrigation because the sprinkler can be deflected causing a non uniform irrigation pattern. Wind may ultimately force the farmer to delay the application, thereby increasing the time and costs of each application.

Hydrologic measurements can help significantly irrigation management allowing for a more rational use of water without reducing the crop productivity. In particular,

soil moisture measurements in a crop field provide precious information about the amount of water needed per application and help scheduling the applications. In fact, if the field capacity threshold is exceeded, water starts to be released from the rootzone implying water waste. On the other hand, low soil moisture levels should be avoided to reduce water stress that may ultimately determine an undesired reduction of plant growth and crop productivity. When the proper amount of water is provided to crop through irrigation, water consumption is minimized, with positive effects in terms of energy used and decreased costs for irrigation.

In the next years, water resource will become more and more limited due to increasing human needs and climate changes. Therefore, there will be the need for irrigation strategies with higher efficiencies in terms of energy and water consumption. In fact, jointly with a possibly reduced water availability, the world's population is likely to grow in the next decades with a consequent increasing need for maize and its derivatives. Hence, the availability of hydrologic measurements together with innovative methods, will help significantly the development of optimal strategies for water resources.

Chapter 2

Soil Moisture Dynamics

Soil is a heterogeneous medium whose physical properties strongly influence soil moisture dynamics. Soils are triphase media composed by air, water and solid particles in different percentages. Porosity n represents the ratio between the volume of voids V_v , which is given by the sum of the volume occupied by water V_w and air V_a , and the total volume of the medium obtained from the sum of the volumes occupied by the three components. The measure of the water content in the soil can be expressed as soil water content θ or as relative soil water content s . The former is given by the ratio between the water content and the total volume of the soil, as reported in equation (2.1), while the latter considers the water volume available scaled to the void volume.

$$\theta(t) = \frac{V_w}{V_{tot}} \quad (2.1)$$

$$s(t) = \frac{V_w}{V_v} = \frac{V_w}{V_a + V_w} \quad (2.2)$$

θ can assume values comprised between 0 (no water) and the porosity (saturation). Besides s assumes values equal to 0 (no water) and 1 (saturation). $s=1$ implies indeed that water is occupying all the available volume. Soil is usually unsaturated, so the water movement is governed by the Darcy's Law in unsaturated medium.

$$v_x(\vec{x}, t) = -K(\vec{x}, s(t)) \frac{\partial \psi_{tot}(\vec{x}, t)}{\partial x} \quad (2.3)$$

In which v_x represent the velocity in an arbitrary x direction at a point $\vec{x} = (x, y, z)$, K is the hydraulic conductivity at a point and it is a function of the time through

s . ψ_{tot} represents the overall soil water potential at a point \vec{x} and time t . Such a potential is given by the sum of the height z of the considered point above a reference plane and of the capillary matric potential which is negative and given by:

$$\psi(s(t)) = \frac{p_c(s(t))}{\gamma} \quad (2.4)$$

In this equation, p_c is the contribution to water pressure given by capillarity forces that is negative and depends on the soil water content and γ is the unit weight of water. When the soil is in unsaturated conditions, there are a lot of interfaces between water and air, so p_c increases as s decreases, meaning that ψ is close to 0 when s is close to 1 and much lower than 0 when s is almost equal to 0.

In order to estimate the values of ψ and K there are many available models, but the easier ones are those proposed by the Clapp-Hornberger model [*Clapp and Hornberger, 1978*] and reported below.

$$\psi(s) = \psi_{sat}s^{-b} \quad (2.5)$$

$$K(s) = K_{sat}s^{2b+3} \quad (2.6)$$

ψ_{sat} and K_{sat} are the capillary potential and the hydraulic conductivity at saturation and b is an empirical parameter determining the degree of non-linearity. Since b is usually higher than 1, the system emphasizes the changes in soil water content.

In unsaturated soils it is possible to define two different critical levels of soil water content: s_{fc} represents the field capacity that is the s value above which the movement of water is appreciable, meaning that below this level the hydraulic conductivity is too small and the water is strongly attracted to soil particles. It represents the inertia of the system against water movement and depends on soil type. s_h , instead, represents the hygroscopic point (i.e. the soil water content below which water molecules are so strongly attracted by soil particles that cannot be removed from soil). s_h is strongly dependent on soil type being strongly sensitive to the percentage of clay.

2.1 Soil Water Balance Equations

Spatial heterogeneity of soil and vegetation properties play a key role on soil moisture dynamics at different spatial and temporal scales. Since climatic and hydrological processes affecting the soil water balance display random features, stochastic approaches can be used to describe the soil water balance at a point (e.g. *Rod-It and Porporato, 2004*). The soil moisture balance in the root zone is expressed by:

$$nZ_r \frac{ds(t)}{dt} = I(s(t), t) - ET(s(t), t) - q(s(t), t) \quad (2.7)$$

Where n is the porosity, Z_r is the depth of the root zone which represents the uncompacted topsoil layer and s is the spatially averaged soil moisture as defined in equation (2.2) (with reference to the above mentioned control volume). The input term is represented by the rainfall infiltration I , while the output terms are the evapotranspiration ET and leakages q ones.

Infiltration from rainfall can be obtained as:

$$I(s(t), t) = P(t) - \omega(t) - O(s(t), t) \quad (2.8)$$

In which P is the total precipitation, ω is the precipitation intercepted by trees and O represents the overland flow. The rainfall that reaches the ground surface P_s is given by:

$$P_s(t) = P(t) - \omega(t) \quad (2.9)$$

Interception can be described by a mono-parametric model which sets Δ as the maximum rainfall intercepted by vegetation, meaning that until the precipitation is lower than Δ it is all intercepted by trees, while once the precipitation exceeds the threshold, only Δ is held by trees and the remaining precipitation can reach the ground surface. The value of Δ is a function of the type of vegetation and of the season. Much more complicated is the subdivision of P_s into infiltration and overflow. There are two main reasons for which rain is no more able to infiltrate into the soil: rainfall intensity can be too high causing the exceedance of the infiltration capacity at a given instant (Horton mechanism) or the cumulative rainfall volume is too high and the soil becomes completely saturated (Dunne mechanism). The

Horton mechanism usually dominates in arid and semiarid climates, where storms are concentrated in short periods and characterized by huge depths, while Dunne mechanism becomes more important in humid climates, when rainfall is characterized by large annual volumes but lower intensities. In order to calculate the infiltration volume, many infiltration models are available and they are all based on the Horton and/or Dunne mechanism.

Leakages can be considered as the sum of the lateral flow q_l and of the vertical flow q_v :

$$q(s(t), t) = q_l(s(t), t) + q_v(s(t), t) \quad (2.10)$$

Lateral flow is a function of spatial gradients of water matric potential φ_c , while the vertical flow represents the deep percolation which is mainly induced by gravity. In order to have lateral flow in the root zone, there should be heterogeneity of soil properties and the presence of sinks able to sustain the water matric potential gradient. Usually, in the root zone gravity dominates, so the vertical flow is more important than the lateral flow. As for the ET term, it is important to highlight that evapotranspiration is the sum of two distinct processes:

- evaporation E through which water is transformed into water vapor using solar energy to obtain the change of phase;
- transpiration T performed by plants which incorporate water through their roots and release it as water vapor through stomata.

Transpiration process is done by plants that need water to maintain cellular turgor, perform photosynthesis and incorporate nutrients from the ground. Even if plants need a continuous water supply, changes in the amount of water stored in their tissues are less important. Hence, plants only transfer water from the soil to the atmosphere through stomata. Stomata are small intracellular openings (some μm) in the epidermic tissue of the leaves through which water vapor is released and CO_2 is incorporated. These openings are present most of all in the lower part of the leaves to avoid direct exposition to the Sun and ensure a better control on the amount of water leaving the plant. Thanks to the action of guard cells, plants are able to regulate the quantity of released water depending on the quantity of available water through a compromise: in case of large water losses, also large amounts of CO_2 can be assimilated and viceversa. Stomatal openings create a

continuum from soil to the atmosphere which is necessary to ensure a proper water gradient and allow for the water rise against gravity forces. It is like having two reservoirs at different levels connected through a pipe. The first reservoir, the one having higher potential energy, is represented by water in the soil and the second one, having lower potential energy, is the atmosphere. The connection is ensured by the plant water.

The driving factors for these two phenomena are similar: temperature, solar radiation, air humidity and wind speed which plays an important role removing water vapor from the surface avoiding the creation of the equilibrium condition which would stop evapotranspiration. Also the type of vegetation and the life-cycle season are very important, besides soil water availability. Evaporation and transpiration are treated together because they are controlled by similar driving factors. Evaporation usually dominates in bare soils and lakes, while transpiration is prevalent in vegetated soils and during wet periods due to the high efficiency of plant in removing water from the soil.

2.1.1 The FAO method for ET evaluation

Over the last 50 years a large number of empirical methods have been developed to estimate evapotranspiration depending on different climatic variables. The problem was the local validity of the methods and the consequent need for rigorous calibrations, which are time-consuming and expensive. In order to solve this problems the FAO organization published on its website [www.fao.org] some guidelines in the ‘*FAO Irrigation and Drainage Paper No. 24 ‘Crop water requirements’’* [Allen et al, 1998]. The Penman-Monteith equation is the tool used to properly combine the surface energy balance with water vapor and sensible heat fluxes. The Penman-Monteith equation allows for the calculation of the potential evapotranspiration (ET_0), which is the evapotranspiration that a reference crop would produce during its growing season in the absence of limitations caused by water stress and under actual climate conditions. The reference crop is defined as an active grass-field with an assumed height of 0.12m, having a surface resistance of 70s/m and an albedo of 0.23. To obtain the actual evapotranspiration ET , ET_0 needs to be multiplied by a stress coefficient and a crop coefficient:

$$ET = k_s(s(t))k_c(t)ET_0 \quad (2.11)$$

In equation (2.11) k_s is the water stress coefficient which depends on the soil moisture and on soil vegetation and features, while k_c is the crop coefficient, dependent on the season and on the crop. During its life-cycle, a crop experiences different growing stages. In particular, the FAO manual identifies four different classes: initial, crop development, mid-season and late-season. The values for the crop coefficient considered by the FAO manual are: $k_{c,ini}$ for the initial stage, $k_{c,mid}$ for the mid season and $k_{c,end}$ at the end of the late season stage. The value for $k_{c,ini}$ is subject to the effects of large variations in wetting frequencies, therefore refinements to the value used for $k_{c,ini}$ are suggested. $k_{c,mid}$ and $k_{c,end}$ values are referred to a sub-humid climate, so these values should be modified for other conditions as explained in the FAO manual. Moreover, k_c values are referred to non-stressed crops cultivated under excellent agronomic and water management conditions and achieving maximum crop yield. The ‘*FAO Irrigation and Drainage Paper No. 24 ‘Crop water requirements’’* [Allen et al, 1998] provides also the lengths for the four distinct growth stages aforementioned. These lengths are given for various types of climates and locations, but they could vary with crop variety and crop conditions from region to region. The values for the three crop coefficients and the four lengths organized by type (i.e. small vegetables, legumes, cereals, etc.) and maize crop belongs to cereals. The values suggested by the FAO manual for the maize crop are reported in table 2.1 and in table 2.2.

Crop	$k_{c,ini}$	$k_{c,mid}$	$k_{c,end}$
Cereals	0.3	1.15	0.4
Maize (grain)		1.20	0.6 - 0.35

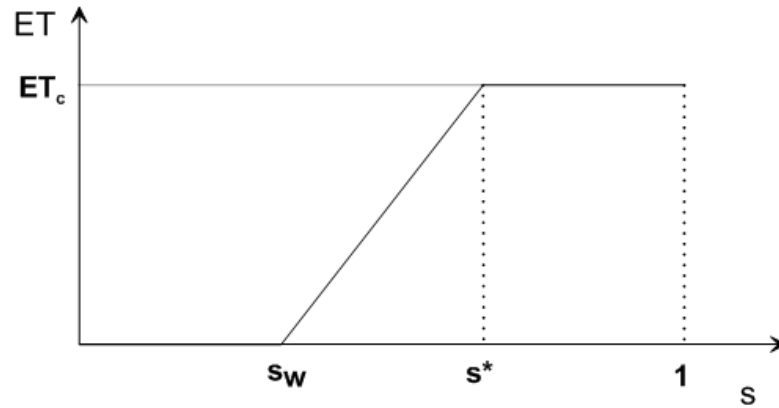
Table 2.1: Single (time-averaged) crop coefficients k_c

The behavior of the stress coefficients is discussed in the following paragraphs.

2.1.2 ET in water stress conditions

When soil water availability is limited, plants are able to reduce the speed at which they take water from the soil. This reduction of transpiration, from a mechanical

Crop	L_{ini}	L_{dev}	L_{mid}	L_{late}	Plant Date	Region
Maize (grain)	30	50	60	40	April	East Africa
	25	40	45	30	Dec/Jan	Arid Climate
	30	40	50	30	April	Spain; California

Table 2.2: Lengths of crop development stages**Figure 2.1:** ET curve

point of view, is performed by reducing the stomatal openings. When the decrease of water availability is low, reflected in a low decrease of the matric water potential φ , the reduction can be compensated by osmotic adaptation. Besides, when the decrease of soil water potential is significant, the guard cells lose turgor and the opening degree of the stomata is reduced. When the soil water content is too low, no flow can be sustained from the roots to the atmosphere, and the stomata are completely closed. The soil moisture level below which osmotic adaptation is insufficient to compensate the decrease of soil water availability and stomata start closing is the incipient stress point s^* . Its value depends on soil and vegetation features. The soil moisture level below which stomata are completely closed is the wilting point, s_w . The dependence of evapotranspiration rate of soil moisture can be modeled via a linear model, (Figure 2.1), where ET varies from 0 to the potential evapotranspiration ET_c .

ET_c can be related to effective evapotranspiration ET through the water stress coefficient k_s as stated by the FAO method expressed by equation (2.11). Moreover, the water stress coefficient can be related to relative soil moisture content s as

follows:

$$k_s = \begin{cases} 0 & (s < s_w) \\ \frac{s-s_w}{s^*-s_w} & (s_w < s < s^*) \\ 1 & (s > s^*) \end{cases}$$

Having a trend similar to the evapotranspiration one reported in Figure 2.1.

2.2 Soil Moisture Dynamics

Soil moisture dynamics are strictly related to the input and output terms of the water balance reported in equation (2.7). Rainfall (infiltration) and evapotranspiration are both stochastic due to the inherent rainfall and climate variability suggesting the need for a stochastic approach to describe how the dynamics of ET and I are reflected by the dynamics of soil moisture. Monte Carlo approaches allow the generation of stochastic long-term series of rainfall, and then study the temporal evolution of soil moisture forced by the synthetic rainfall. To this aim, it is necessary to specify how ET and I depend on $P(t)$ and $s(t)$. As per the infiltration I , it is assumed that the total precipitation P is equal to the rainfall on ground surface P_s thus neglecting plants interception ω and that infiltration is known from the stochastic rainfall model adopted. Two different cases are obtained when $s(t) < 1$:

$$I[s(t), t] = P_s(t) \quad (\text{if } P_s(t) < K_{h,sat}) \quad (2.12)$$

$$I[s(t), t] = K_{h,sat} \quad (\text{if } P_s(t) \geq K_{h,sat}) \quad (2.13)$$

Otherwise, if $s(t) = 1$:

$$I[s(t), t] = 0 \quad (2.14)$$

Potential evapotranspiration ET_c , can be then assumed as constant thereby focusing on a temporally averaged value representative of a given season at a given site.

In the root zone, it is assumed that the horizontal gradient is negligible with respect to the vertical one, so the dominant phenomenon in the root zone is vertical leaching which is governed by gravity and linked to soil moisture through horizontal hydraulic conductivity at saturation $k_{h,sat}$.

$$q[s(t), t] = L(s(t)) = k_{h,sat}s(t)^{2b+3} \quad (2.15)$$

This relation implies that L is low when s is close to 0, while the vertical leaching increases to $k_{h,sat}$ when soil moisture content is almost equal to 1. At this point, all the terms appearing in the soil-moisture water balance equation are linked to soil moisture s , so equation (2.7) can be written as follows:

$$nZ_r \frac{ds(t)}{dt} = I[s(t), t] - k_s(s(t))ET_c - k_{h,sat}s(t)^{2b+3} \quad (2.16)$$

The conceptual model briefly sketched above has seven parameters which can be suitably subdivided on the basis of their dependence on various factors:

- n , Z_r , $k_{h,sat}$, b depend on soil characteristics;
- s^* , s_w depend on soil type and vegetation features;
- ET_c depends on climate, location, vegetation type and period.

In between events infiltration is equal to zero, so as the mass balance equation (2.7) can be written as:

$$nZ_r \frac{ds(t)}{dt} = -k_s(s(t))ET_c - k_{h,sat}s(t)^{2b+3} \quad (2.17)$$

s decreases in time depending on the negative terms on the right-hand side that are evapotranspiration and vertical leakages. When climate is assumed to be constant, the decrease of soil moisture content does not depend on time. Focusing on the first output term ($-k_s(s(t))ET_c$) three different situations can be distinguished:

- when $s > s^*$, ET_c is constant, meaning that evapotranspiration removes every day the same quantity of water, producing a constant decrease of soil moisture content; equation (2.17) indeed becomes $ds/dt = -ET_c/nZ_r$, where k_s is equal to 1 (see Figure 2.1).
- when $s_w < s < s^*$, $ET = k_s ET_c$ and provided that ET_c has a linear behavior (Figure 2.1), the mass balance equation becomes $ds/dt = -\alpha s ET_c/nZ_r$, whose solution is exponential as shown in Figure 2.2, b).

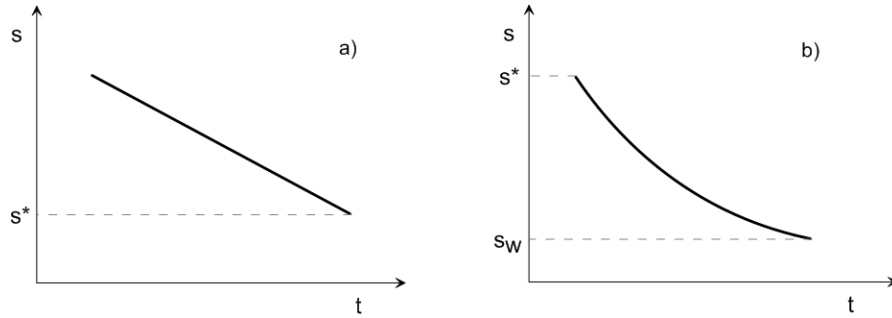


Figure 2.2: s dynamics: a) linear behavior, b) exponential behavior

Analogously, under the above assumptions, when $ET = 0$ the behavior of s induced by L can be analyzed. The result is that when soil is close to saturation (i.e. $s \approx 1$), ET is slow, while L becomes very important and the decrease of s is very fast. For lower values of s , L becomes negligible. During rainfall events, ET and L are much smaller than infiltration I and the mass balance equation becomes

$$nZ_r \frac{ds(t)}{dt} = I[s(t), t] \quad (2.18)$$

The typical response of soil moisture to a rainfall event is a ‘jump’, because soil is storing a big quantity of water in a small amount of time. An example of such behavior is reported in Figure 2.3.

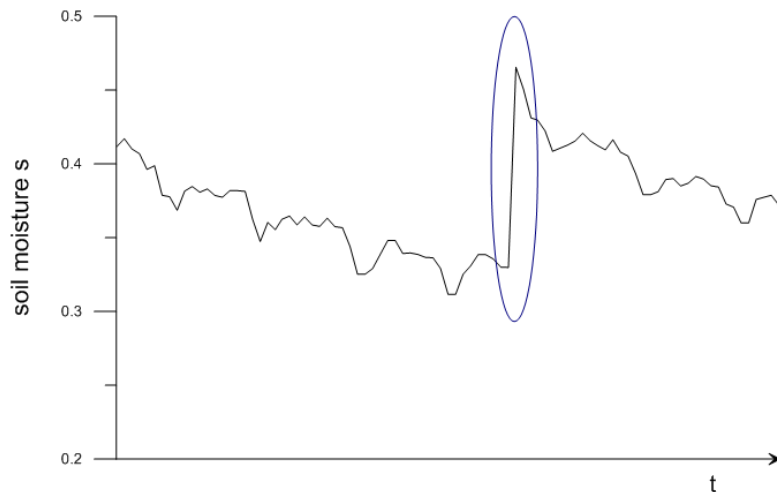


Figure 2.3: Example of a ‘jump’ in soil moisture dynamics due to rainfall

2.3 Irrigation

Irrigation consists of a series of operations through which water is taken from a source (i.e. lakes, rivers, reservoirs) and distributed to crops with the aim of increasing the productivity of the field. This practice is very useful when rain is a limiting factor, because it allows the avoidance (or reduction) of water stress in plants during the growing season, thereby maximizing crop production.

Water supplied through irrigation can be considered as an additional input in the soil water balance equation (equation (2.7)) which hence becomes:

$$nZ_r \frac{ds(t)}{dt} = I(s(t), t) + R - ET(s(t), t) - q(s(t), t) \quad (2.19)$$

In which R represents the irrigation rate.

The efficiency in water use for irrigation is evaluated as the amount of units of crop produced from each unit amount of available water used by plants and, in most cases, the amount of crop produced is directly proportional to the amount of available water. Water use efficiency measures the efficiency in the ratio between transpired water and CO_2 production. In fact, plants maximize their growth when transpiration and CO_2 production are maximum, hence, it is of enormous importance to determine the range of soil moisture content in which ET is maximized [s^* , 1]. It is also important to take into account that losses are given by the sum of ET and leakages L . Hence, there is the simultaneous need to maximize evapotranspiration and reduce the ratio ET/L .

Plotting soil water losses as a function of s , the resulting plot is the one reported in Figure 2.4.

From this plot, it is evident that until s is lower than soil field capacity, plants take all the water available in the soil, while once s exceeds such value L becomes dominant. Taking this into account and considering that ET is maximum when s is between s^* and 1, the region (s^*, s_{fc}) is the optimal range for s . In fact, evapotranspiration is unrestricted, all the water is efficiently used by plants (leakages $\cong 0$).

The goal of irrigation activities is to furnish water to the field in order to keep the relative soil moisture content within the aforementioned interval. The corresponding volume of water that needs to be provided to the field is called 'Readily

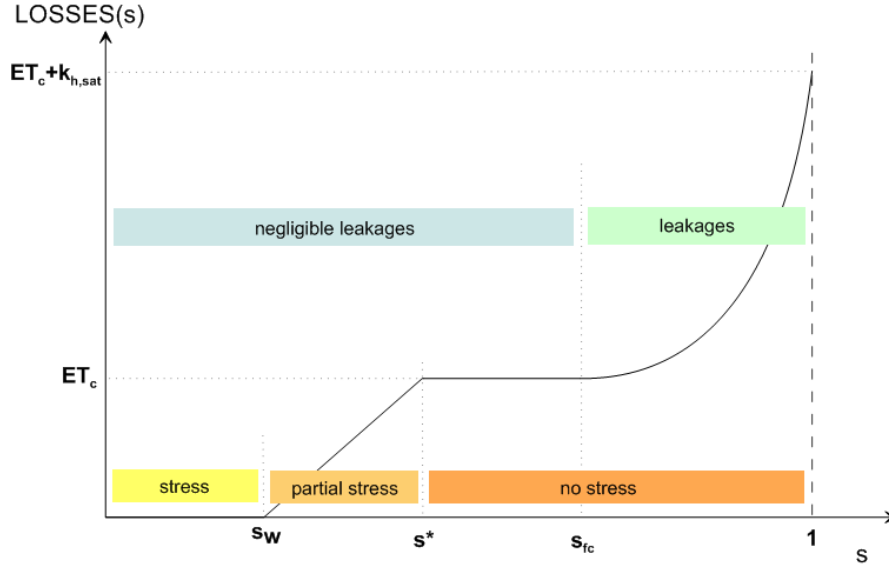


Figure 2.4: Water losses as a function of s

Available Water' (RAW). RAW can be calculated as follows:

$$RAW = nZ_r(s_{fc} - s^*) \quad (2.20)$$

The interaction between irrigation and rainfall (which is stochastic in terms of timing and amount) needs to be carefully considered. The goal is that of avoiding the following circumstances (Figure 2.5):

- decreasing of s below the stress point; hence, the farmer needs to add water through an irrigation application to delay the down crossing of s^* ;
- upcrossing the field capacity s_{fc} , due to irrigation or to the combined action of irrigation and rain which causes undesirable water losses due to leakages.

In the former case, plants can go in a stress condition, while in the latter case there can be water losses that cause waste of water.

2.3.1 Sprinkler irrigation

The irrigation time and amount within each crop depends on the type of irrigation devices. The three methods most used are: surface irrigation, which allows water to flow over the landcrop and naturally infiltrate into the soil driven by gravity, sprinkler irrigation, that will be described below, and drip irrigation, with which

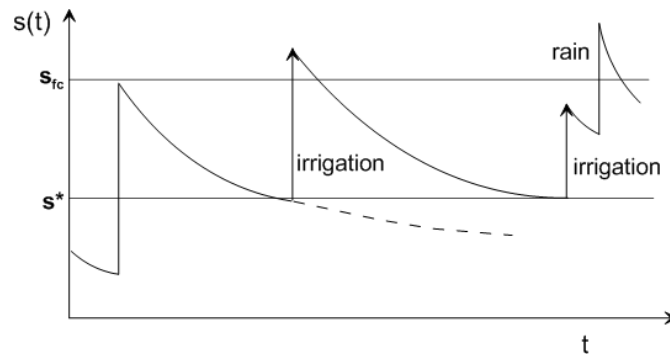


Figure 2.5: Possible risks related to irrigation applications

water is dripped onto or into the soil at very low rates from a system of plastic pipes fitted with outlets.

The sprinkler irrigation method consists in delivering water as an ‘artificial rainfall’ over the crop. Water is applied through sprinklers that can be fixed, moving or distributed along moving bars. Sprinklers applied along moving bars diffuse water very close to the soil, while single sprinklers diffuse water high above the crops. The water is pumped into a system of pipes and then diffused in form of drops. This kind of irrigation is suitable for many crops such as row, field and tree, but large sprinklers cannot be used for delicate crops. Each sprinkler distributes water through circular patterns in a non uniform way, because rates applied decrease with the distance from the sprinkler. Moreover, wetting patterns can be different depending on the network of sprinklers employed as reported in Figure 2.6 and if sprinklers are fixed, moving or on a moving bar.

The introduction in the seventies of a large transportable reel provided with a hose able to wrap on itself, has been a significant facilitation for irrigation operations. Indeed, this mobile machine represents the main irrigation system used in Italy [Bertocco, 2012]. Registered data highlighted that of the 2.5 million hectares of irrigation, more than 1 million is irrigated using sprinklers and, in particular, hose reels are more than the 80%. Modern technologies have lowered operating costs, because the pipes employed are able to reduce head losses and consequently reduce the operating pressures, which is reflected in a decrease of energy consumption. Another advantage of sprinkler irrigation is the uniformity of distribution of the water over the crop, which can reach the 90%, because the modern machineries are

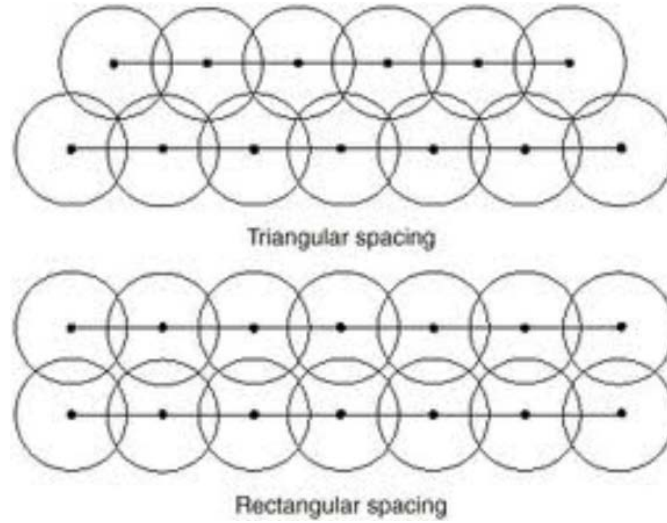


Figure 2.6: Different sprinklers patterns

able to reduce the quantity of water distributed in the central part with respect to the margins. Delivering water as an artificial rain has the disadvantage of involving high water losses due to evaporation and drift caused by wind, with a consequent reduction in the delivery efficiency. Also the wind effect can be countered using modern sprinklers, increasing the efficiency, while the only way to reduce evaporation effect is irrigate during the night or early in the morning and late in the afternoon.

The global irrigation efficiency E is the ratio between the water volume and rate taken from the source by the consortium destined to a given farm and the volume and rate of water usable by plants. Irrigation consortia have the role of storing water to be used from farmers during irrigation season. The amount of water to be stored is calculated on the basis of the different crops and on the extent of the cultivated areas to let farmers irrigate their fields avoiding water scarcity. Global irrigation efficiency depends on different factors and can be calculated as:

$$E = E_{de} \cdot E_f \cdot E_{di} \quad (2.21)$$

In 2.21 equation, E_{de} represents the global delivery efficiency, that is calculated as the ratio of the volume effectively received from the farmer and the volume of water taken from the consortium for that farmer; E_f is the farm efficiency, that is the ratio between the volume of water delivered to crops and the volume that

the farmer receives from the consortium; while E_{di} is the distribution efficiency, that is the ratio between the volume of water used by plants and the volume that the farmer delivers to them. Losses are distributed along the path of water from the consortium to the field and finally to the plants. Along consortium network there can be losses due to water evaporation or infiltration and, depending on the network efficiency and the bed permeability, the values of delivery efficiency can vary from 0.4 (low efficiency) to 0.9 (high efficiency). Farms can have losses along their distribution network and this can be due to an inefficient storage of water volume within the farm or to the delivery network itself. Values for the farm efficiency are usually close to one if the irrigation system is well maintained. The last factor determining the global delivery efficiency is the distribution efficiency. In this case losses can be due to several factors such as a non uniform water distribution, drift and creep outside the crop, runoff, leakages and evaporation. The values attributed to distribution efficiency vary depending on the irrigation system adopted. For example, sprinkler irrigation typically has an efficiency around 0.75.

2.3.2 Irrigation Schemes

Scheduling of irrigation application can be done according to three different approaches:

1. traditional scheme
2. water balance scheme
3. 'threshold' scheme

1. Traditional irrigation scheme provides a series of identical irrigations separated by constant intervals and during each application a water amount equal to the 'watering volume' W is released to the crop. W is the amount of water required to produce a jump of relative soil moisture from s^* to s_{fc} . Hence W is equal to the readily available volume RAW defined by equation (2.20). The time interval T between two subsequent applications is obtained as the ratio between the RAW and the potential evapotranspiration ET_c . The time required to provide to the crop

the established water volume W is obtained dividing such volume by the product of the application intensity IA and E_{di} . The application intensity IA is **in terms expressed** as the ratio between the sprinkler discharge q and the unit soil surface covered by each sprinkler. This method neglects precipitation and leakages are produced leading to an unefficient use of water resources (Figure 2.7).

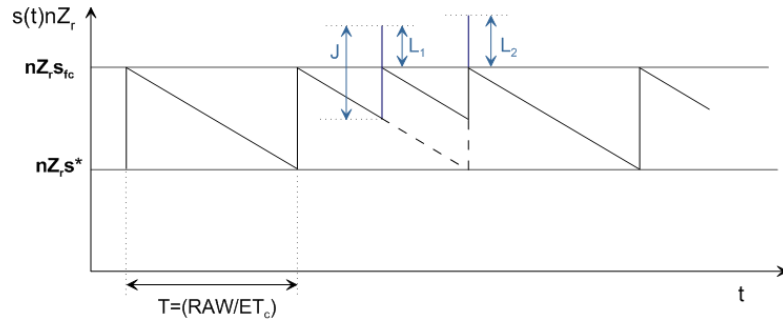


Figure 2.7: Traditional irrigation scheme

Indeed, in this way all the rainfall is lost as deep percolation, underlining the fact that this technique is not wise in terms of sustainable use of water resources.

2. Water balance scheme considers soil water balance providing irrigations at flexible intervals, because each rainfall event delays the subsequent application to avoid as much as possible the exceedance of the field capacity. In this way the total number of applications in a given period will be lower than the traditional scheme ones. At each irrigation, a volume of water equal to the watering volume is delivered to the crop as happens in the previous case, while the irrigation interval T becomes different, because both water coming from rainfall and from irrigation are considered. Each irrigation interval T_i is thus obtained as $(RAW + \Delta P_i)/ET_c$, in which ΔP_i represents the cumulated rain depth in between two consequent applications. The duration D of each application is calculated as in the above case. An example of water balance scheme application is given in Figure 2.8.

There can be also cases in which too much water is coming from rainfall events producing significant losses. In this case a fraction of the incoming rainfall is used to reduce the water volumes provided as irrigation.

3. 'Threshold' irrigation scheme consists in a continuous supply of water in order to maintain the soil moisture at the critical level s^* . Once rainfall events drive s above s^* , irrigation is suspended. According to this method, the irrigation

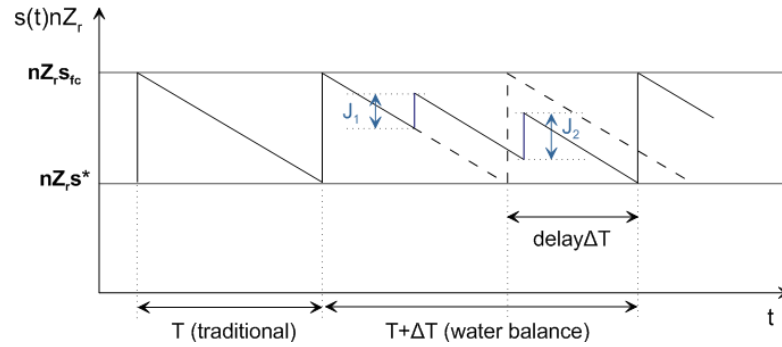


Figure 2.8: Water balance irrigation scheme

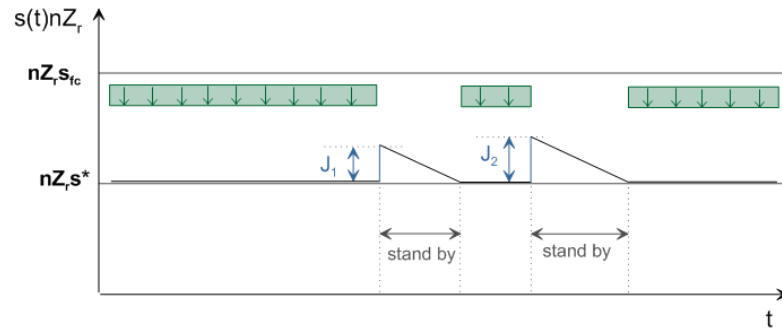


Figure 2.9: Threshold irrigation scheme

rate Q_{irr} is constant during dry periods (days in which $P \cong 0$). $Q \cong ET_c$, so as the plants are provided with a daily water volume which is equal to the volume uptaken in that day by plants for transpiration. The time D needed to provide the water volume to the crop is calculated as $(Q_{irr}24/E_{di})/IA$ and the result is that D is lower than 1 day. Once rainfall occurs, there is the need to calculate the time needed from the relative soil moisture s to go back to the critical value s^* and it can be done dividing ΔP by ET_c , that represents the velocity with which s decreases in time. Threshold irrigation scheme minimizes the risk of exceeding field capacity thus minimizing the risk of wasting water due to leakages. An example of this scheme application is reported below.

The choice of the optimal irrigation scheme is related to water saving purposes. Nevertheless the optimal scheme also depends on crop type and climate conditions. In fact, where rainfall is negligible fixed sprinkler irrigation can be less expensive than drip irrigation, provided that in this case the three methods are equivalent in terms of water consume.

Sprinkler irrigation coupled with a water balance scheme results to be the combination which ensures the best ratio efficiency/costs in most cases and this is the reason why sprinkler irrigation is the most used one worldwide.

As explained above, sprinkler irrigation is the most used method for crop irrigation in Italy and also in Veneto region. In particular, hose reels are employed to deliver water to the whole field, but, in most cases, they are not able to irrigate sufficiently the corners of the field and this is the reason why the corners are irrigated using fixed sprinklers. In this work sprinkler irrigation is employed using both types of sprinklers as explained above. The fixed sprinkler is a quite old machinery fixed on a pump which is directly connected to a tractor, while the hose reel is a modern machine which has a pipe with a diameter of 150mm to reduce head losses and thus reduce energy consumption.

The major part of the maize field considered is irrigated using the hose reel and irrigation timing and amount is based on the experience of the farmer. He decides when to start an irrigation observing the leaves of the maize plants and taking also into account the external temperature, moreover the farmer takes into account also the amount of water coming from rainfall, thus delaying irrigation applications when rainfall is enough to avoid water stress conditions for the crop. Since the same hose reel is used for the irrigation of several hectares of maize, it cannot be stopped during the hottest hours of the day and this implies higher water losses due to evapotranspiration. Besides, one of the advantages of using such machinery, is that the amount of water released to the crop is automatically measured by an internal computer and can be easily read on a display.

The fixed sprinkler mentioned above has been employed to irrigate only a small part of a maize field in which a water balance scheme was performed and soil moisture level was measured as better described in chapter 4. The advantage of the use of a fixed sprinkler only for a small portion of the field is that irrigation can be done early in the morning or in the evening, to minimize water losses due to evapotranspiration. On the other hand, the fixed sprinkler is not provided with a computer, so the amount of water delivered to the field is measured using a rain gauge (Figure 2.10).

Further explanations about soil moisture measurements and the case-study will be given in chapter 3 and chapter 4 respectively.



Figure 2.10: Rain gauge used in the maize field

Chapter 3

Materials and Methods

The amount of water provided during each irrigation application and the timing of each irrigation can be scheduled on the basis of soil moisture measurements. In fact, knowing the soil moisture content of a particular field and monitoring soil moisture dynamics can help the farmer to give water to the field at the better moment and in the right amount, in order to avoid water stress conditions in plants and water losses due to excessive water. In this thesis, the soil moisture content of a maize field is monitored. This field is irrigated in most part by a hose reel and in a corner by a fixed sprinkler. The irrigation timing and amount relative to the part of the field irrigated with the hose reel is decided by the farmer which cultivates such field. Indeed, for the field corner irrigated using the fixed sprinkler each irrigation application is decided evaluating the soil moisture level.

Relative soil moisture value can be experimentally obtained in different ways and the one chosen for this thesis is the time domain reflectometry which is better described in the following paragraph.

3.1 Time Domain Reflectometry

Time domain reflectometry (TDR) is a method for the determination of soil water content and electrical conductivity. Water content is inferred from the dielectric permittivity of the medium, whereas electrical conductivity is inferred from TDR signal attenuation. The main advantages of TDR over other measurement methods are the superior accuracy to within 1 or 2 % volumetric water content; the fact that

calibration requirements are minimal (in many cases soil-specific calibration is not needed); the lack of radiation hazard associated with other techniques. Moreover, TDR has excellent spatial and temporal resolution, measurements are simple to obtain and the method is capable of providing continuous measurements through automation and multiplexing.

3.1.1 Basic Principles

In the telecommunications industry TDR is used to identify locations of discontinuities in cables. The TDR instrument sends a pulse through the medium and compares the reflections from the unknown transmission environment to those produced by a standard impedance. The propagation velocity v_p of the signal that is a function of the cable dielectric constant, along with a typical reflection at a point of discontinuity in a cable, allows the operator to determine locations of line breaks or other damage to cables using travel time analysis. Using similar principles, a waveguide or probe of known length L may be embedded in soil and the travel time for a TDR-generated electromagnetic wave to traverse the probe length may be determined. From the travel time analysis the bulk dielectric constant of soil is computed from which the volumetric water content is inferred. The bulk dielectric constant of soil (ϵ_b) is a function of the propagation velocity according to the following equation

$$\epsilon_b = \left(\frac{c}{v}\right)^2 = \left(\frac{ct}{2L}\right)^2 \quad (3.1)$$

Where c is the velocity of electromagnetic waves in vacuum ($3 \cdot 10^8$ m/s) and t is the travel time for the pulse to travel the length of the embedded wave-guide (down and back). The travel time is evaluated on the base of the ‘apparent’ or electromagnetic length of the probe, which is characterized on the TDR output screen by diagnostic changes in the waveform.

In Figure 3.1, x_1 marks the reflection at the entry of the signal to the probe and x_2 marks the reflection at the end of the probe.

The dielectric constant definition given in equation (3.1) simply states that it is the ratio squared of propagation velocity in vacuum relative to that in the medium. Considering soil medium, the soil bulk dielectric constant ϵ_b is governed by the dielectric of liquid water $\epsilon_W \approx 81(20^\circ C)$, as the dielectric constants of other soil

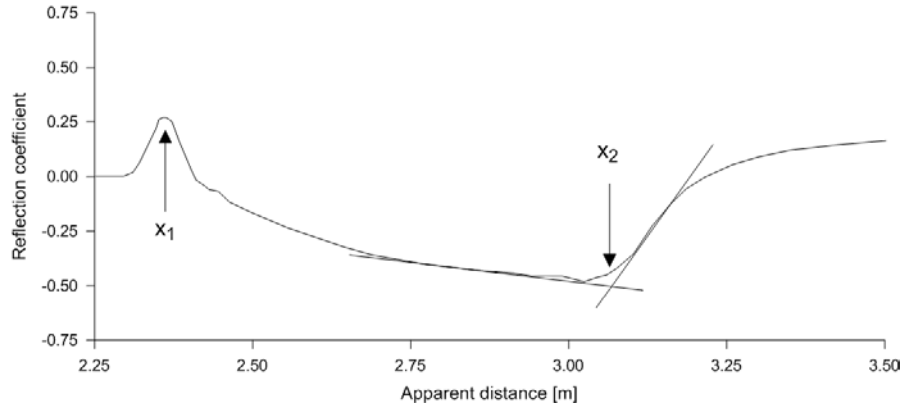


Figure 3.1: Example of TDR output waveform

constituents are much smaller, e.g., soil minerals $\epsilon_s = 3$ to 5, frozen water (ice) $\epsilon_i = 4$ and air $\epsilon_a = 1$. This large disparity of the dielectric constants makes the method relatively insensitive to soil composition and texture and thus a good method for liquid soil water measurement.

Several factors influence dielectric constant measurements such as soil porosity and bulk density, measurement frequency, temperature and water status. The need to relate water content θ_v to ϵ_b so as to account for the above mentioned factors has resulted in a variety of models. For this purpose, two basic approaches have been used. The first approach is empirical, whereby mathematical expressions are simply fitted to observed data without using any particular physical model. Such an approach was employed by Topp et al. (1980) who fitted a third order polynomial to the observed relationships between ϵ_b and θ_v for multiple soils. The second approach uses a model of the dielectric constants and the volume fractions of each of the soil components to derive a relationship between the composite (bulk) dielectric constant and soil water. Such a physically based approach, called a dielectric-mixing model, was adopted by Dobson et al. (1985) and by Roth et al. (1990). For this work, calibration is conducted using the empirical relationship proposed by Topp et al. (1980):

$$\theta_v = -5.310^{-2} + 2.9210^{-2}\epsilon_b - 5.510^{-4}\epsilon_b^2 + 4.310^{-6}\epsilon_b^3 \quad (3.2)$$

This equation provides an adequate description for water content lower than 0.5, which covers the entire range of interest in most mineral soils. The estimation of error is of about 0.013 for θ_v . On the other hand, equation (3.2) fails to adequately

describe the $\epsilon_b - \theta_v$ relationship for water contents exceeding 0.5 and for organic soils or mineral soils high in organic matter, mainly because the calibration of Topp was based on experimental results for mineral soils and concentrated in the range of $\theta_v < 0.5$. Limitations or disadvantages of the TDR method include relatively high equipment costs, potential limited applications under highly saline conditions due to signal attenuation.

3.1.2 Probe configuration

A number of different geometrical configurations have been proposed, which have a single central conductor and from one to six outer conducting rods, as shown in Figure 3.2. The two-wire probe has the advantage of minimal soil disturbance, but produces an unbalanced signal, leading to unwanted noise and signal loss [White and Zegelin, 1995]. The three or more rod probes provide a balanced signal,

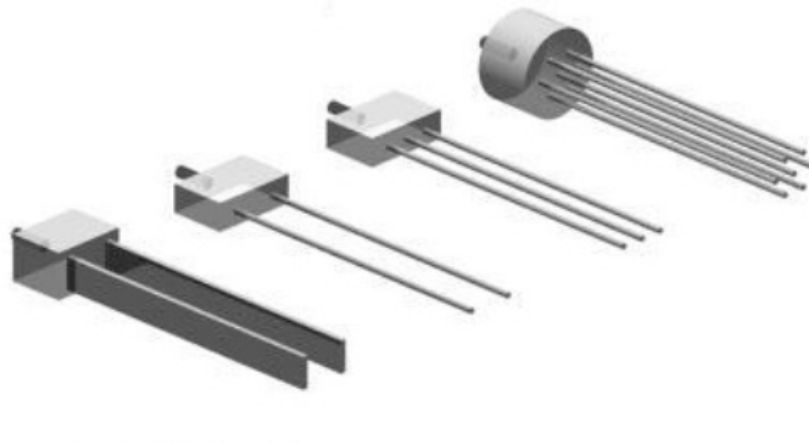


Figure 3.2: Different probes configurations

at the expense of some additional soil disturbance. Though not commonly used in soils, the parallel plate probe was shown by *Robinson and Friedman* (2000) to provide a highly uniform electrical field between plates. When using the multi-wire probes highly concentrated electrical field converging on the central conductor more heavily weights the dielectric constant of constituents within this region. Moreover, *Ferre et al.* (1998) found that two-rod probes have a larger sample area compared with three-rod probes, and that thin rod coatings (for reducing conductive losses)

for any probes will reduce the sampling area of the probe. The particular spatial sensitivities of different probe configurations can be used depending on specific research applications. Since a two or three-rod probe placed horizontally serves as an effective point (plane) measurement for water or solute fronts moving vertically through soil profiles, three-rod probes have been chosen for this work.

3.1.3 Construction of the probes

The three-rod probes required have been assembled in the laboratory using PVC blocks, stainless steel rods, coaxial cable and epoxy resin. The PVC block has been drilled in order to let the central part of the cable be in contact with the central rod and the two lateral rods to be in contact with the outer part of the cable. Once the cable is inserted into the PVC block, the steel rods are placed in the correspondent holes. In particular, the central hole is larger than the remaining holes, due to the fact that the central bar has a larger diameter (8mm versus 6mm). To fix the bars to the PVC block, a special clamp was used, as shown in Figure 3.3. Since the

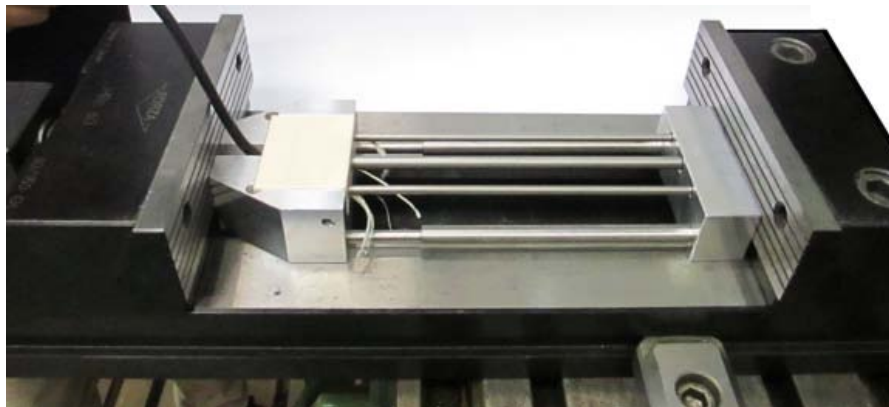


Figure 3.3: Particular clamp used to assembly the probes

probes will stay into the soil and thus also in contact with water, all the holes was filled with the epoxy resin. A bit of resin was put also in the point of insertion of the rods into the PVC block. In order to improve the stiffness at the point in which the cable enters the PVC block, a PVC cylinder was added, together with a thermosetting lining. The last step of the probes construction consisted in the connection with the multiplexer. In order to ensure a better protection against

infiltration, special cable holders have been adopted and fixed with epoxy resin. One of the resulting probes is reported in Figure 3.4.



Figure 3.4: Final probe configuration

Once the construction is completed, the correct functioning of the instrument is checked in laboratory before putting the probes in the site.

Chapter 4

Results of the experiment

On June 10 2013 a TDR instrument was placed in a maize field with the aim of monitoring soil moisture dynamics and scheduling irrigation based on a ‘water balance’ scheme.

4.1 Description of the site

The instrument has been installed in a maize field in Albettone (VI), as shown by Figure 4.1 where the location of the instrument is highlighted with a red dot.



Figure 4.1: Location of the TDR

The hybrid corn sown in the field in question is *P1758*, which is delivered by Pioneer. Such maize belongs to ‘class 700’, according to a classification proposed by the FAO. The FAO classification divides the different maize hybrids on the basis of their maturation period by assigning a label ranging from 100 (the most early) to 800 (the most late). Hence a value equal to 700 stands for a late corn with a maturation period from 130 to 140 days [Nelli *et al.*, 2013]. *P1758*, in particular, has an estimated maturation period of 132 days and it is considered to be one of the most productive corn [*Pioneer Hi-Bred Italia*]. Moreover, Pioneer suggests a plant density of about 7.0-7.8 plants/m² to ensure the best productivity for grain maize. Therefore, in the corn field used in this study plants are sown at a distance of 75cm in the longitudinal direction and 18cm in the transversal direction (Figure 4.2).

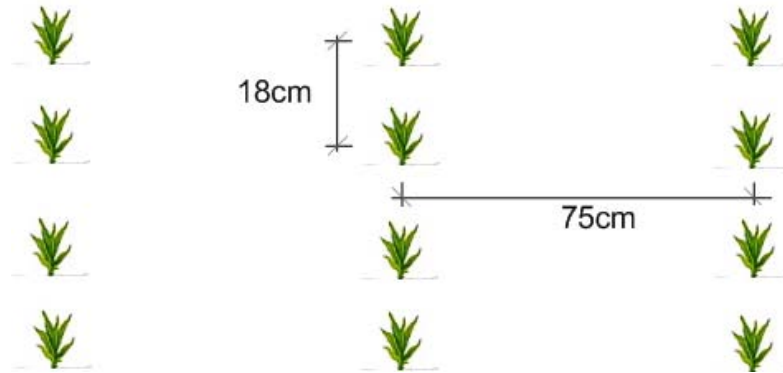


Figure 4.2: Scheme of the distance between corn plants in the field

The soil of the considered crop field has been analyzed by the Pioneer laboratory in autumn 2010 and the results in terms of grain size percentages (Table 4.1) show that it has a clay loam texture, as derived from the soil texture diagram (Figure 4.3) based on the USDA classification. The USDA diagrams classifies the different soils on the base of the underlying percentages of sand, silt and clay.

The porosity of this soil has been obtained from a weighted mean of the porosity with the percentages of each grain size. The porosity values for sand, silt and clay are taken from a Table given by *Laio et al.* [2001] and reported in Table 4.2.

To schedule irrigation based on a ‘water balance’ scheme, the values of hygroscopic point s_h , wilting point s_w , incipient stress point s^* and field capacity s_{fc} must be known. These values can be derived from the literature (*Laio et al.*, 2001).

<i>Gran size</i>	percentage
Skeleton ($\phi > 2\text{mm}$)	absent
Sand ($2.0 < \phi < 0.05\text{mm}$)	24.7 %
Silt ($0.05 < \phi < 0.002\text{mm}$)	44.5 %
Clay ($\phi < 0.002\text{mm}$)	30.7 %

Table 4.1: Grain size analysis of the soil

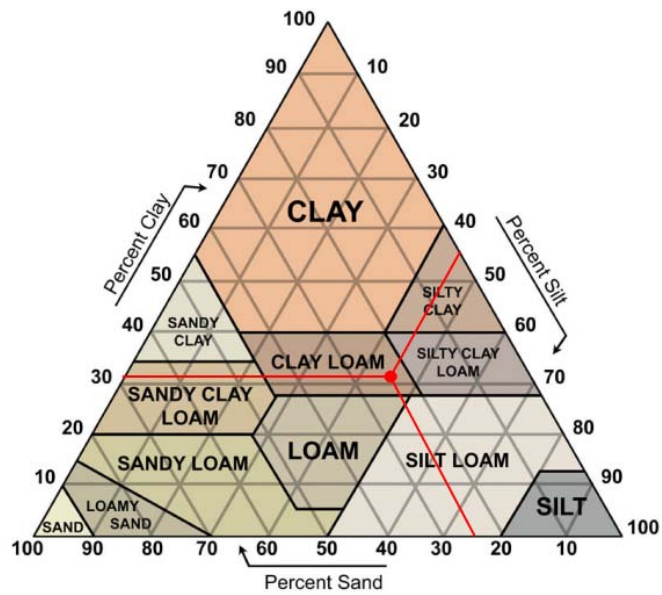


Figure 4.3: USDA soil classification

	n [-]
sand	0.35
silt	0.45
clay	0.50
soil	0.44

Table 4.2: Porosity of each grain size and of the soil mixture

Reference values are available for different soil types (Table 4.3) and the values characterizing the soil under investigation can be obtained as a weighted average of the values pertaining for each soil type.

<i>grain size</i>	s_h	s_w	s^*	s_{fc}
sand	0.08	0.11	0.33	0.35
silt	0.14	0.18	0.46	0.56
clay	0.47	0.52	0.78	1.00
soil	0.23	0.27	0.53	0.64

Table 4.3: Values of s_h , s_w , s^* and s_{fc} for the considered soil

The right amount of water to deliver to the crop at each irrigation is strongly dependent on the value of the RAW (equation (2.20)), which is then affected by the rootzone depth. Z_r is set equal to 40cm in this case, corresponding to the depth at which the field was plowed. The value obtained for the $RAW = nZ_r(s_{fc} - s^*)$ is equal to 21mm.

4.2 Positioning of the probes

The TDR instrument is provided with 6 probes that are subdivided into two groups: 3 of them are placed in a field part in which traditional sprinkler irrigation is applied relying on the farmer experience (uninformed irrigation), while the 3 remaining probes are positioned in a part of the maize field in which an informed water balance irrigation which accounts for the available hydrologic measurements is performed. The probes located in the site where uninformed irrigation is performed (hereafter ‘uninformed site’) are the probes number 4, 5 and 6, while probes 1, 2 and 3 are located in the ‘informed site’. In both groups the probes are positioned horizontally at three different depths and in different horizontal positions to avoid interferences as reported in Figure 4.4. In particular, for each group the probes at higher depth are those labeled by larger numbers (i.e. 3 and 6), while the probes labeled with 1 and 4 are the closest to the surface.

The holes made to position the probes were progressively filled with the soil removed to drill the holes. Each probe is connected to the TDR with a cable 15



Figure 4.4: Probes positioning horizontally and at different depths

meters long, thus allowing the positioning of the two distinct groups at a distance of about 30m from each other, hopefully enough to reduce the interferences between the two sites during irrigation operations.

The TDR instrument has been set to acquire data every 2 hours to better observe the daily trend of the measured variables but the acquisition frequency is increased up to one measure every 15 minutes during irrigations. The output of the instruments is, for each acquisition and for each probe, a curve made of 255 points. These curves are then elaborated via a Fortran code which calculates the volumetric water content (i.e. θ in equation (2.1)), the bulk dielectric constant and the electrical conductivity.

4.3 Hydrologic data

The acquisitions of the TDR instruments started on June 10 and ended on September 18 2013, just before the maize harvesting. In Figures 4.6 and 4.7 are reported all the acquisitions from the first to the last day, subdivided into two groups: informed and uninformed probes while the daily means for each probe are shown in Figures 4.8 and 4.9.

During this period, there have been three irrigations and several rainfall events. All these events are properly evidenced in the following graphs to better understand the behavior of all water content dynamics. The soil moisture trends in both sites are very similar, especially when daily means are considered, while considering the single probes their behavior is a bit different in terms of soil water content measured. For the informed site, the deepest probe (i.e. 3) has the lower water

content, while the larger water content is measured by probe 2. Conversely, for the uninformed site, there are periods in which the larger water contents are measured by probe 6 and other periods in which the probe which measure the larger soil water content is probe 4 or 5. Moreover, the water content range observed in the informed site is wider than that recorded in the uninformed site, implying that the water content of the uninformed site is more spatially uniform.

Figures 4.6 and 4.7 show how the water content changes in time and that the soil water contents decrease to a lesser extent from August 25, evidencing lower evapotranspiration of the maize plants which are going to die. This increase is more evident for the uninformed site in which the water content measured by the uninformed probes during the last period tends to coincide, while this does not happen for the informed site. From the water content values measured in the two sites, in the uninformed site there seems to be an higher water content compared to the informed site and this is further evidenced by Figure 4.5, in which the daily means of the water content for the two sites are reported. Since the water content of the uninformed site starts to become larger than for the informed site after the first irrigation, this difference can be due to the larger amount of irrigation water received by the uninformed site. In fact, this difference increases until the third irrigation and then remains almost the same.

In the periods between two significant events, the rate at which the soil water content measured by the six probes decreases is different and this can be due to several factors. For example, in the first period (from June 10 to 24) the water content in the uninformed site decreases faster than in the informed site, probably because the plants in the informed site were a bit smaller than in the uninformed site at the beginning of the experiment, with a lower evapotranspiration. This difference in the plants growth has become negligible in following days.

During the period of the acquisitions, the probe 6 has started to malfunction, providing water content values quite unreliable. In particular, after August 2 there have been entire days in which the probe 6 has not given acceptable values. For this reason, the water content measurements of the probe 6 have been neglected during the last period of acquisitions.

Figures 4.6 and 4.7

All the acquisitions have been subdivided into six different periods which are an-

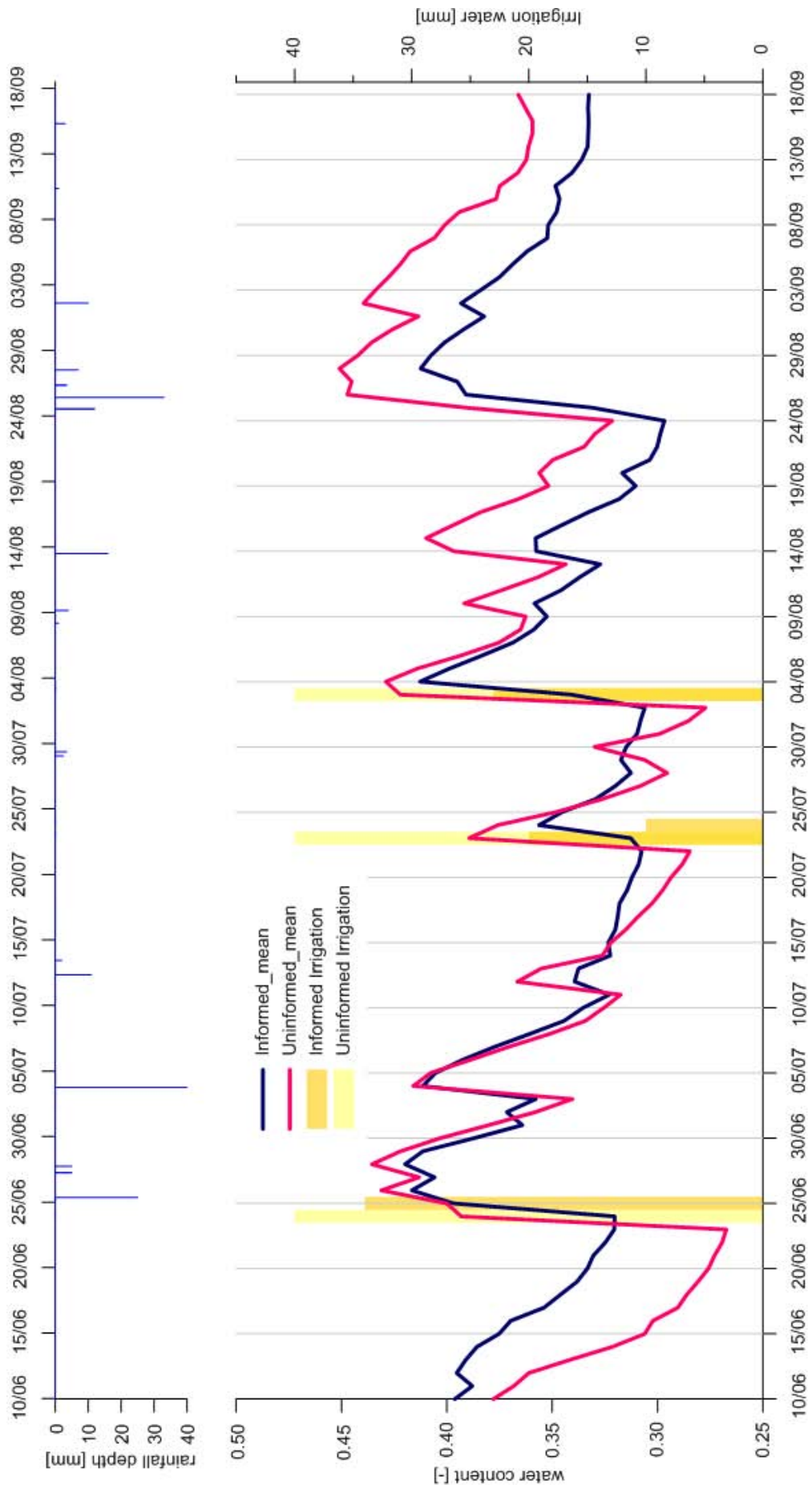


Figure 4.5: Daily means of the water contents measured in the two sites

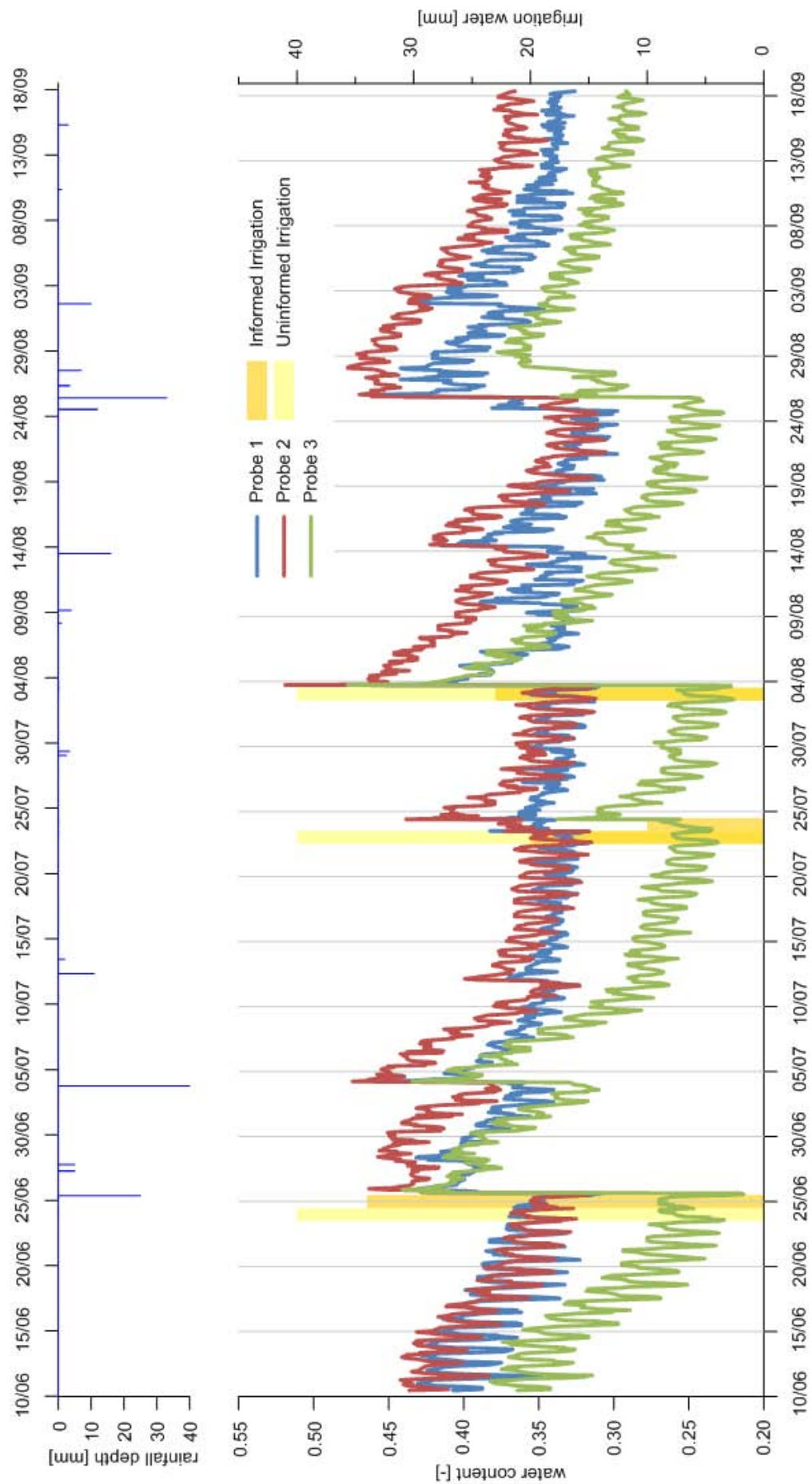


Figure 4.6: Water content of the hole period of acquisitions; informed probes

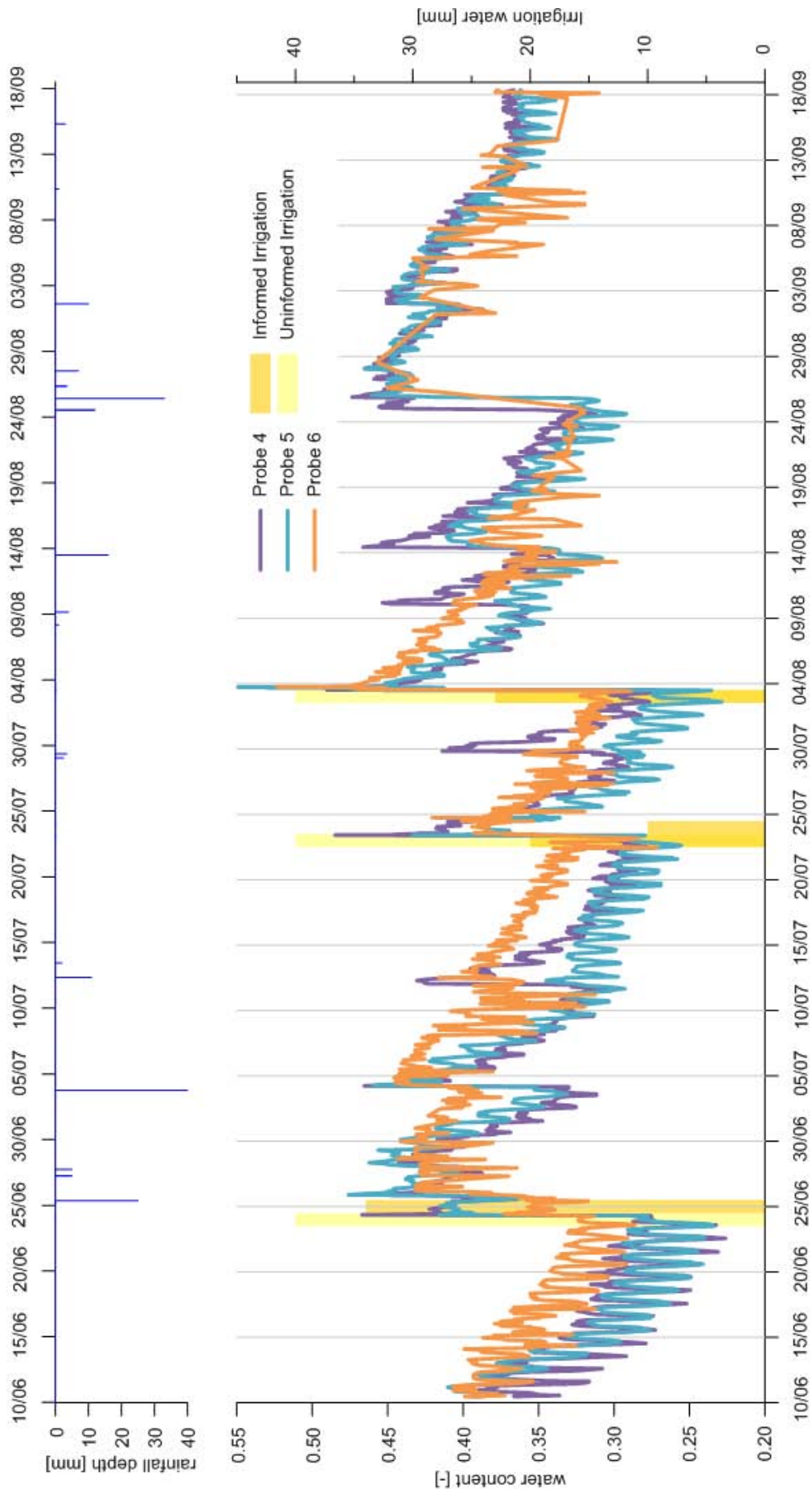


Figure 4.7: Water content of the hole period of acquisitions; uninformed probes

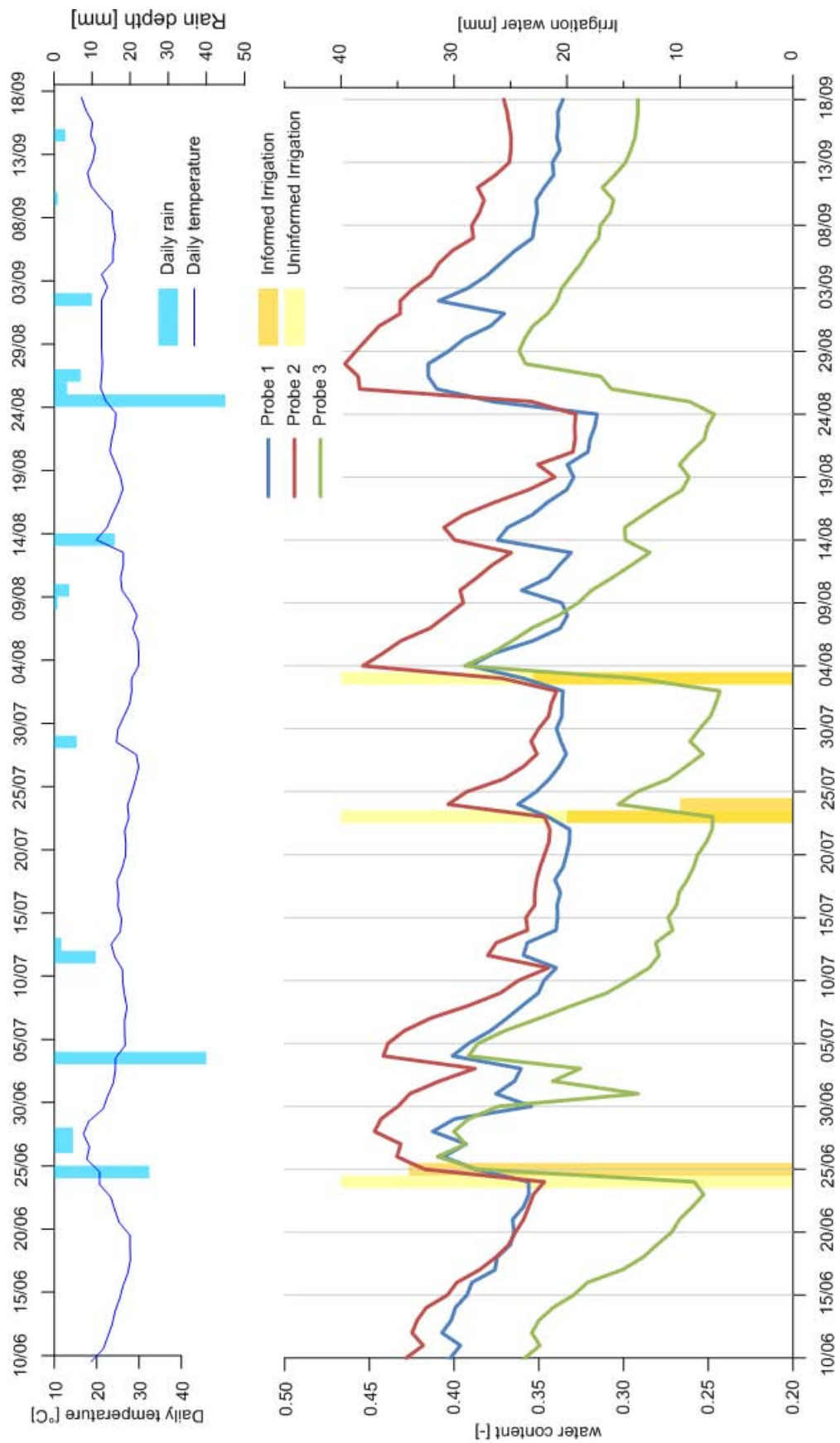


Figure 4.8: Daily means of the water content of the whole period of acquisitions; informed probes

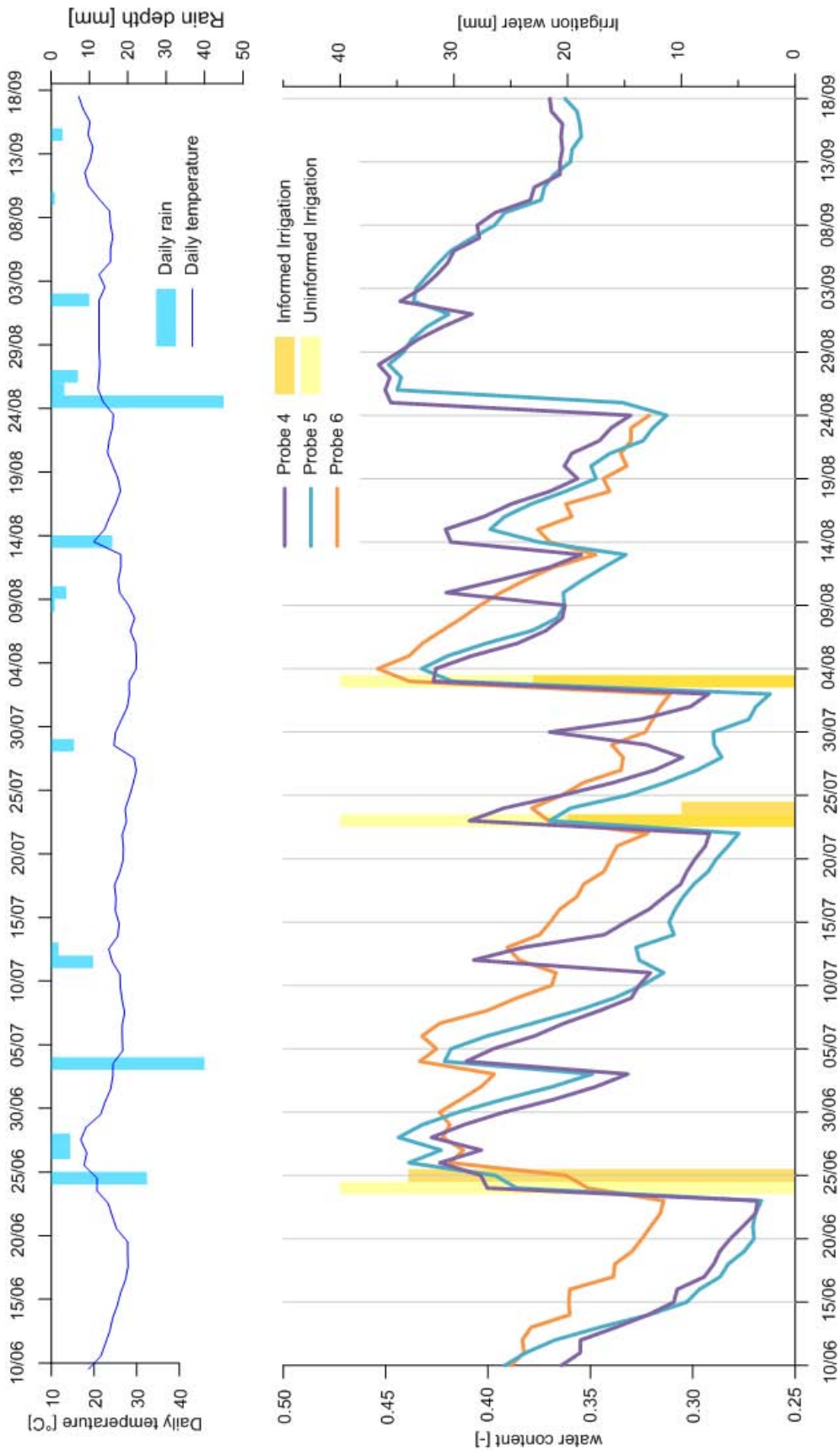


Figure 4.9: Daily means of the water content of the whole period of acquisitions; uninformed probes

alyzed in the following paragraphs:

1. *1st PERIOD*: from June 10 to 24;
2. *1st IRRIGATION*: from June 24 to July 3;
3. *2nd PERIOD*: from July 4 to 22;
4. *2nd IRRIGATION*: from July 23 to August 2;
5. *3rd IRRIGATION*: from August 2 to 23;
6. *3rd PERIOD*: from August 24 to September 18.

4.3.1 First period

The first period is characterized by the absence of external inputs of water (either through rainfall or irrigation). As a result, the daily average water content of the probes decreases as a consequence of the evapotranspiration of the maize plants. The water content measurements of the first period (from 11:25PM of June, 10 to 7:17AM of June, 24) are reported in Figures 4.10 and 4.11.

The plots of the temporal pattern of soil water content show a linear trend during the first days, meaning that evapotranspiration is taking place at a constant rate because s is above the critical value s^* . Besides, in the last part of the period, soil moisture content starts to decrease less than linearly, implying that ET is stressed due to the scarce water availability. For this reason, on June 24 the first irrigation application took place, as described in section 4.3.2.

After dividing the initial water content of each probe for the porosity (Table 4.2), the initial relative soil moisture content can be estimated. The daily means of s for the six probes at the beginning of the experiment and the correspondent values of the relative soil moisture are reported in Table 4.4, which shows that the soil was very close to saturation on June 10. In fact, in the days preceding the installation of the TDR instruments several rainfall events were observed. The initial saturation values reveal that the values of the field capacity and of the incipient stress point derived from laboratory measurements (Table 4.3) should be modified. In particular, the value of s_{fc} is set equal to the mean value of s recorded

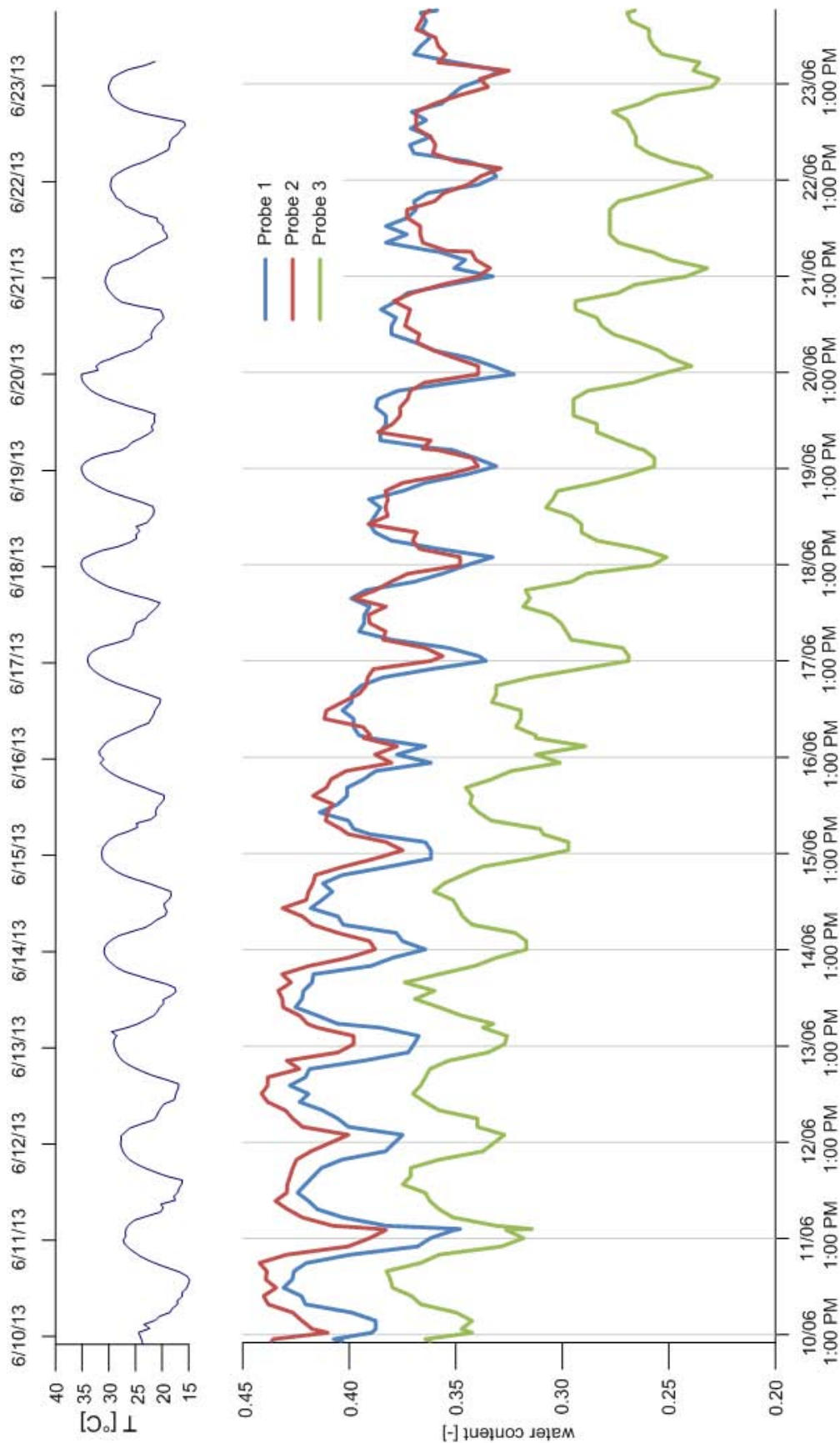


Figure 4.10: First period acquisitions; ‘informed probes’

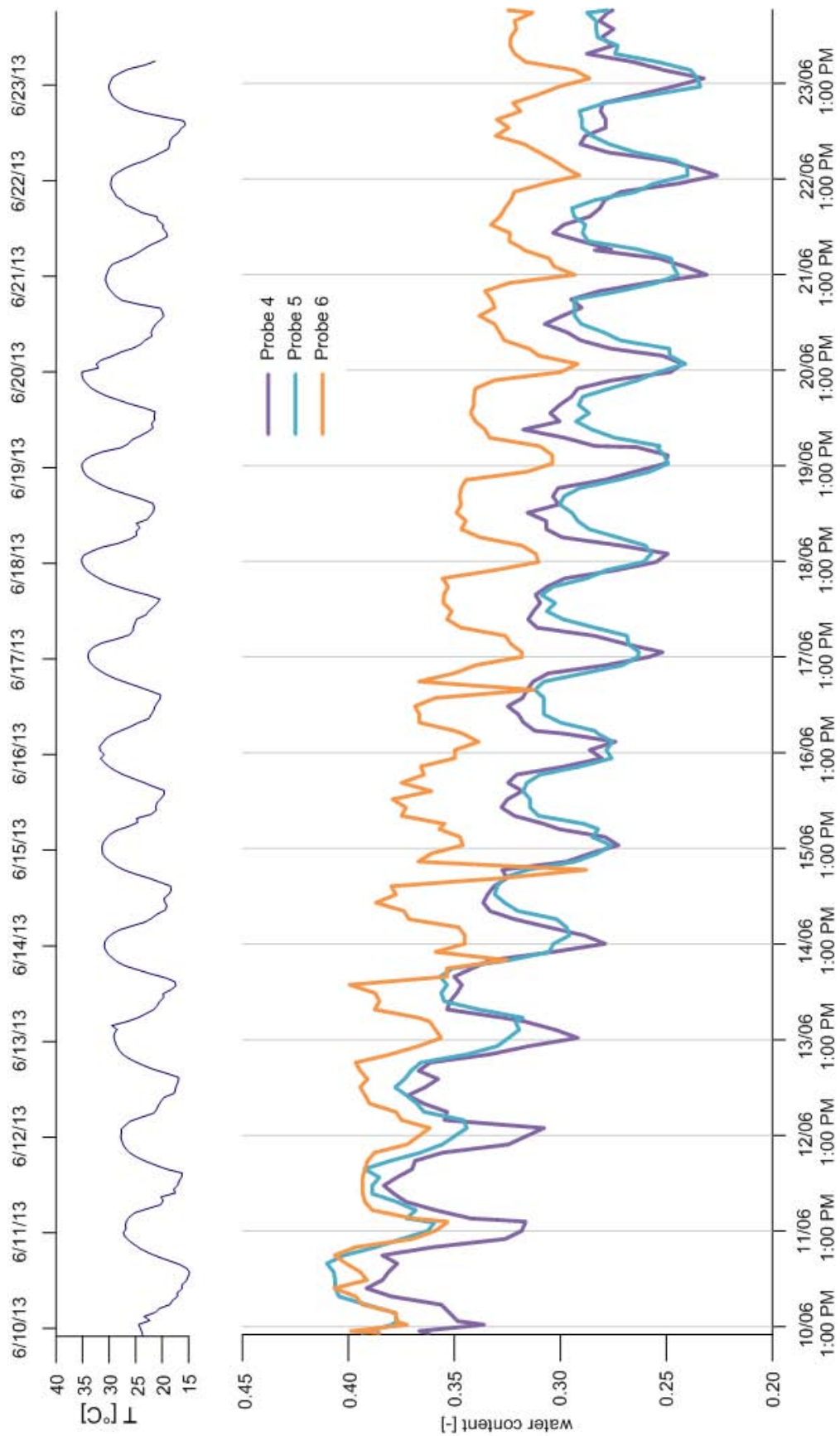


Figure 4.11: First period acquisitions; 'uninformed' probes

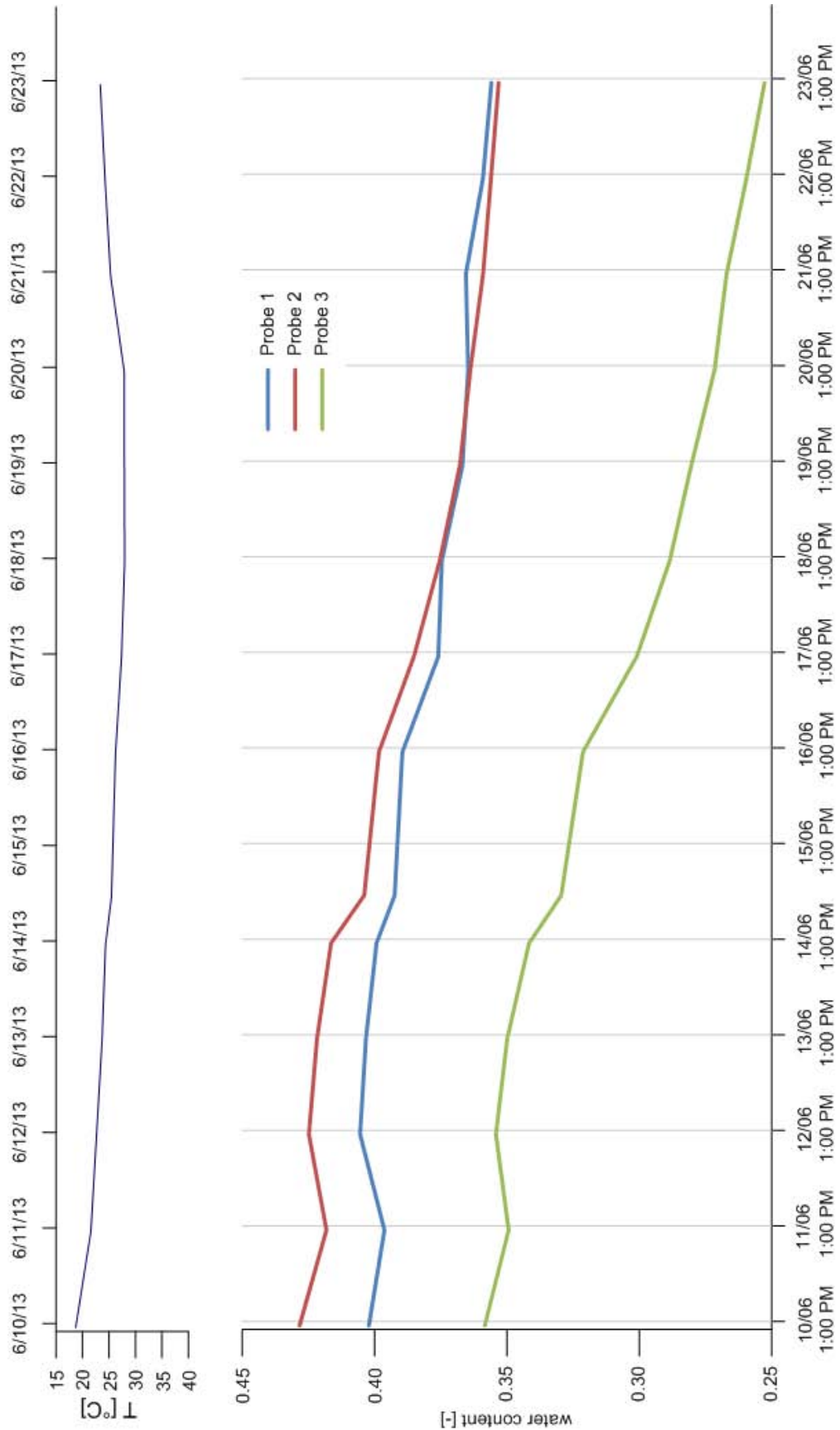


Figure 4.12: Daily means of the first period of acquisitions; ‘informed’ probes

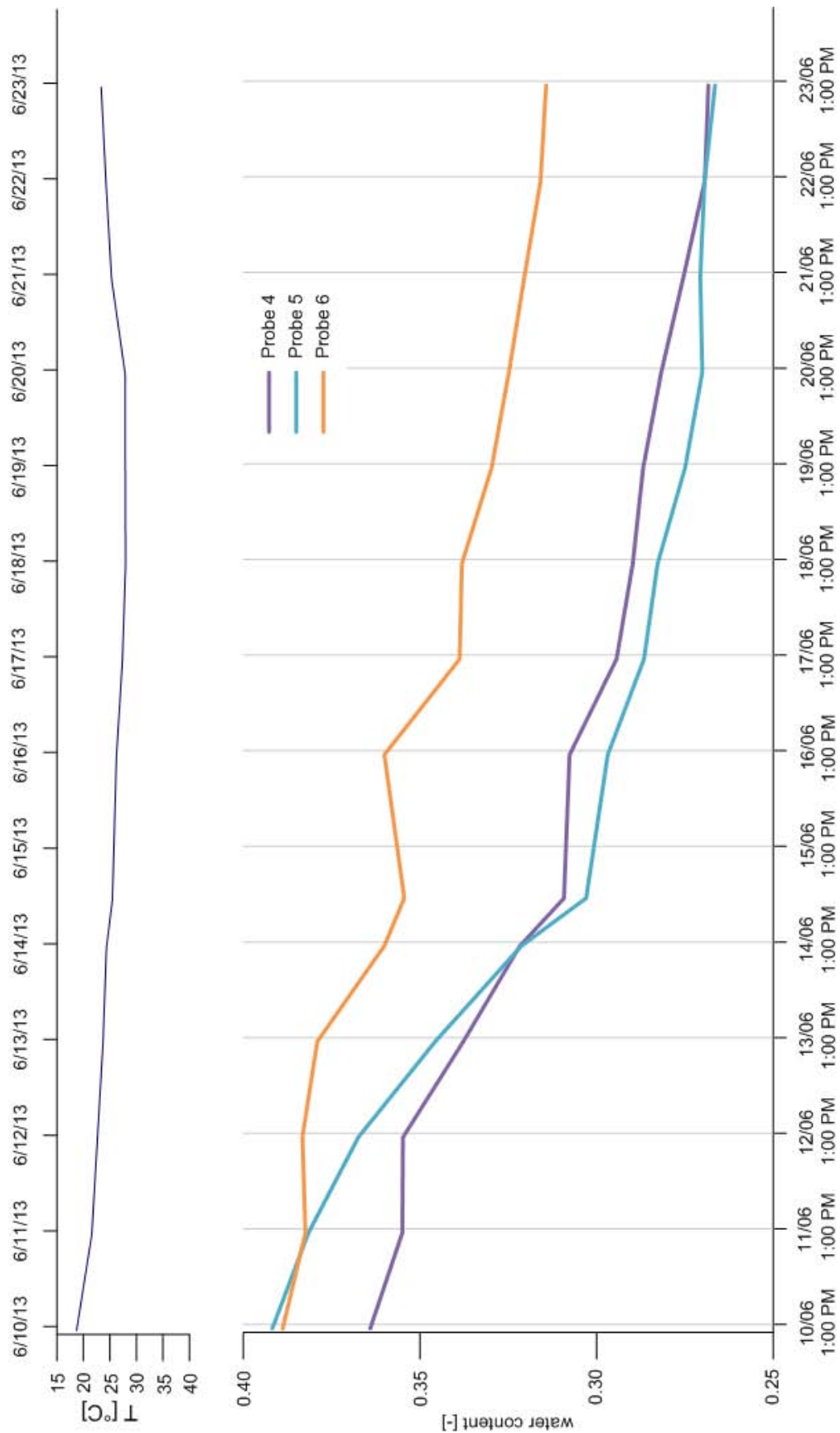


Figure 4.13: Daily means of the first period of acquisitions; ‘uninformed’ probes

by the six probes during the first day of measurements, while the incipient stress point value s^* for the two groups is obtained subtracting a quantity equal to 0.25 from s_{fc} , as suggested by *Laio et al*, [2001]. The soil of the field seems to be more clayey than how emerges from the results of the laboratory. Hence, the values of the field capacity and of the incipient stress point are quite similar to those characteristic of a clay soil. The values of s_{fc} and s^* assumed in this study are reported in Table 4.5.

<i>Probe</i>	θ	s
1	0.402	0.894
2	0.428	0.952
3	0.356	0.790
4	0.362	0.804
5	0.390	0.867
6	0.389	0.863

Table 4.4: Initial values for soil water content and relative soil moisture

	<i>field capacity</i>	<i>incipient stress</i>
s	0.85	0.60
θ	0.38	0.27

Table 4.5: Values assumed for s_{fc} and s^*

The water content measured by the six probes shows marked daily fluctuations. In particular, the water content is maximum during the night time when evapotranspiration is null and minimum at noon, when evapotranspiration is maximum. In Figures 4.12 and 4.13 it is evident that, for the informed group of probes, the two probes closer to the surface (probes 1 and 2) have similar water contents while probe 3 has a lower water content. Besides, for the uninformed group of probes, the probe which shows a larger water content is the probe 6 (the deepest one), while the other two probes have a lower and similar water content.

4.3.2 First irrigation

This period includes the first irrigation, and the first rainfall event since the beginning of the acquisitions. The first irrigation application began on June 24 at 8AM to avoid stress conditions for maize plants. First, the irrigation involved the part of the field in which ‘uninformed’ probes are placed, while the part containing the ‘informed’ probes has been irrigated the day after (June, 25) (Figures 4.14 and 4.15).

During the irrigation of the uninformed site, 40mm have been delivered to the field causing a substantial jump in the value of the surface soil moisture, followed by a noticeable drop down. This decrease suggests that the field capacity has been exceeded in the upper soil layer originating a leaching event. Given the reduced distance between the two groups of probes, also the soil moisture values of the informed probes are slightly affected by irrigation.

The informed irrigation started on June, 25 around 4PM. The amount of water delivered was 35mm subdivided into two subsequent applications of respectively 25mm and 9mm. Also in this case, the other group of probes was slightly influenced by the irrigation. Figures 4.18 and 4.19 show in detail the water content dynamics of the two groups of probes during this first irrigation. In particular, it is evident how the irrigation of each site influences the other site and that such influence is delayed with respect to the irrigation.

The soil moisture values just before irrigation and just after the irrigation are reported in Table 4.6. Soil moisture values before the irrigation were presumably just above the incipient stress point, except than for probe 3. After the irrigation instead the soil moisture content are all above the field capacity, except for the probe 6.

A few hours after the irrigation of the informed group of probes, a rainfall event started bringing 25mm of water which caused another positive jump in the water content clearly visible from the graphs. After, the water content started to decrease linearly (Figures 4.16 and 4.17) until the next rain event which started on June 27 and ended the following day bringing 10mm in all subdivided in two successive events of 5mm each. From June 29 to July 3 has not occurred any other event of rain and the water content started to decrease again.

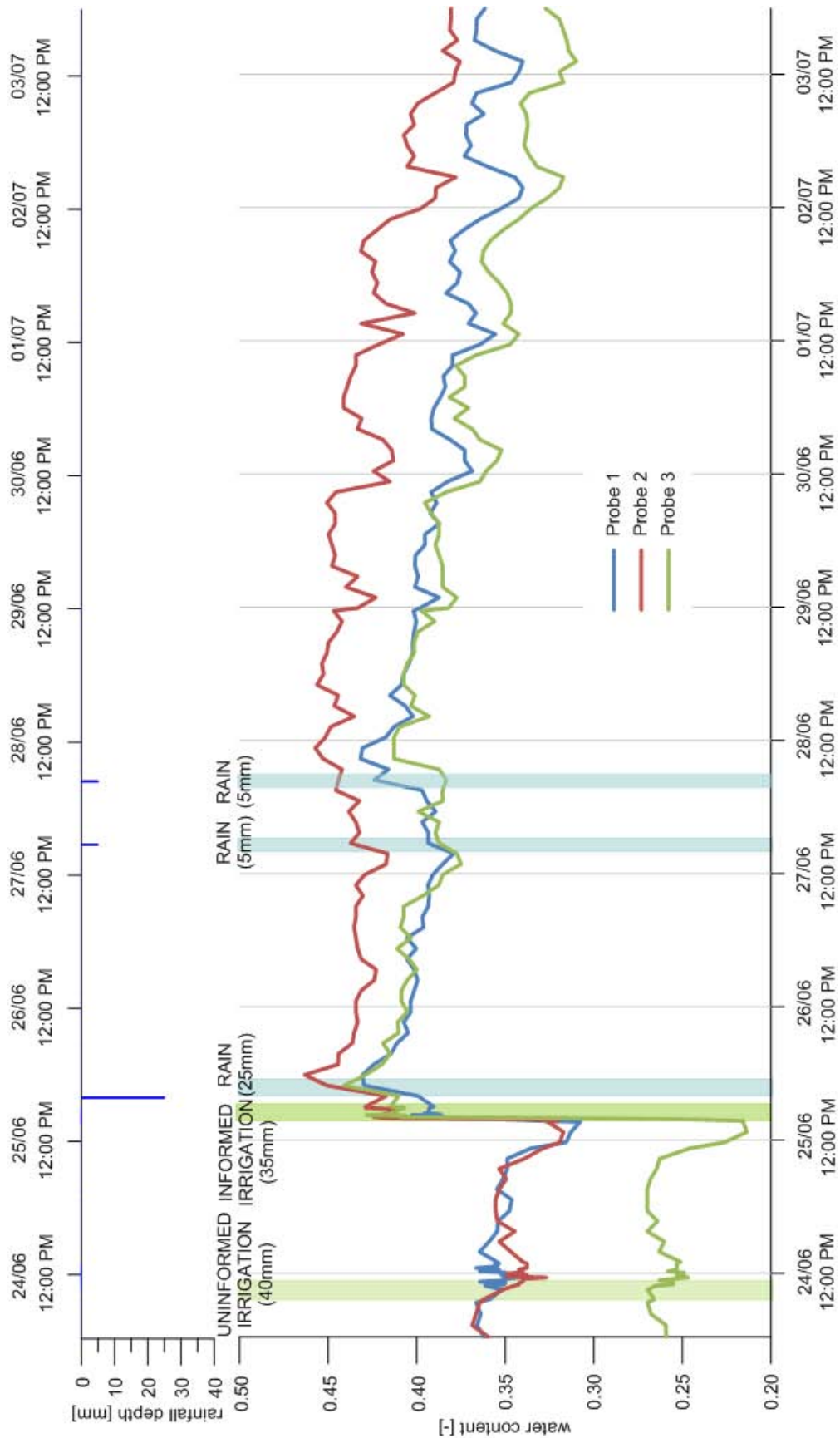


Figure 4.14: First irrigation period; ‘informed’ probes

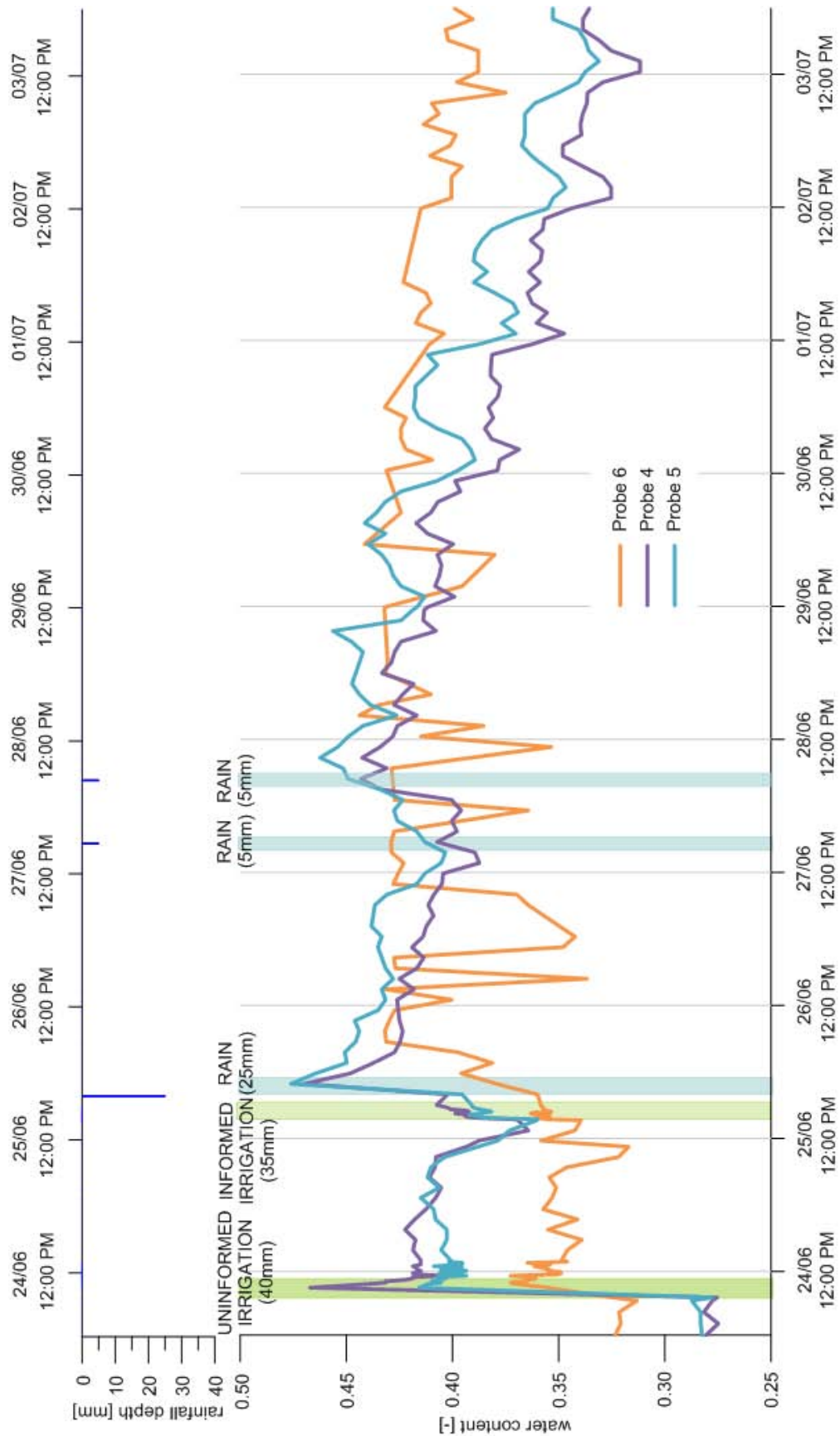


Figure 4.15: First irrigation period; ‘uninformed’ probes

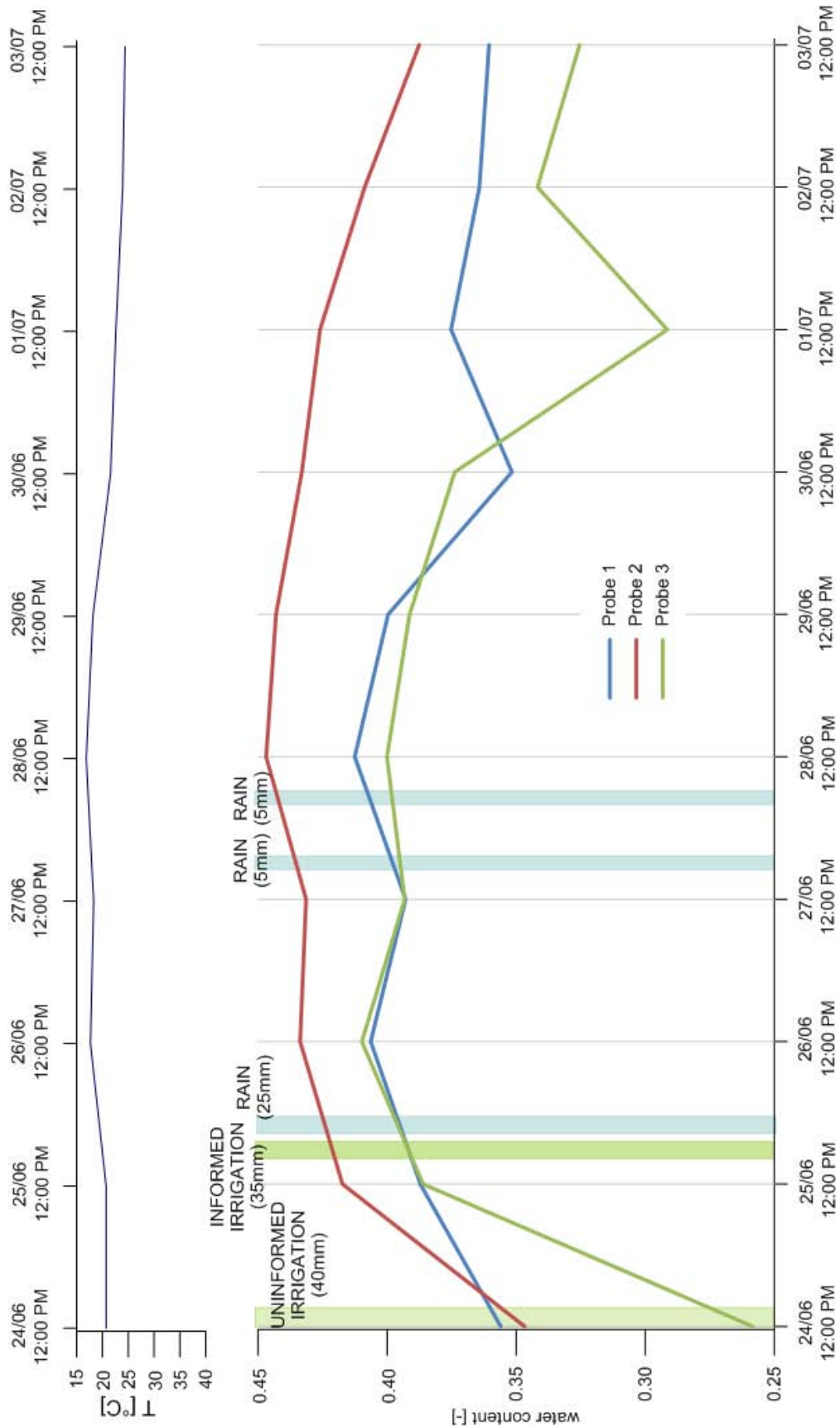


Figure 4.16: Daily means of the first irrigation period; ‘informed’ probes

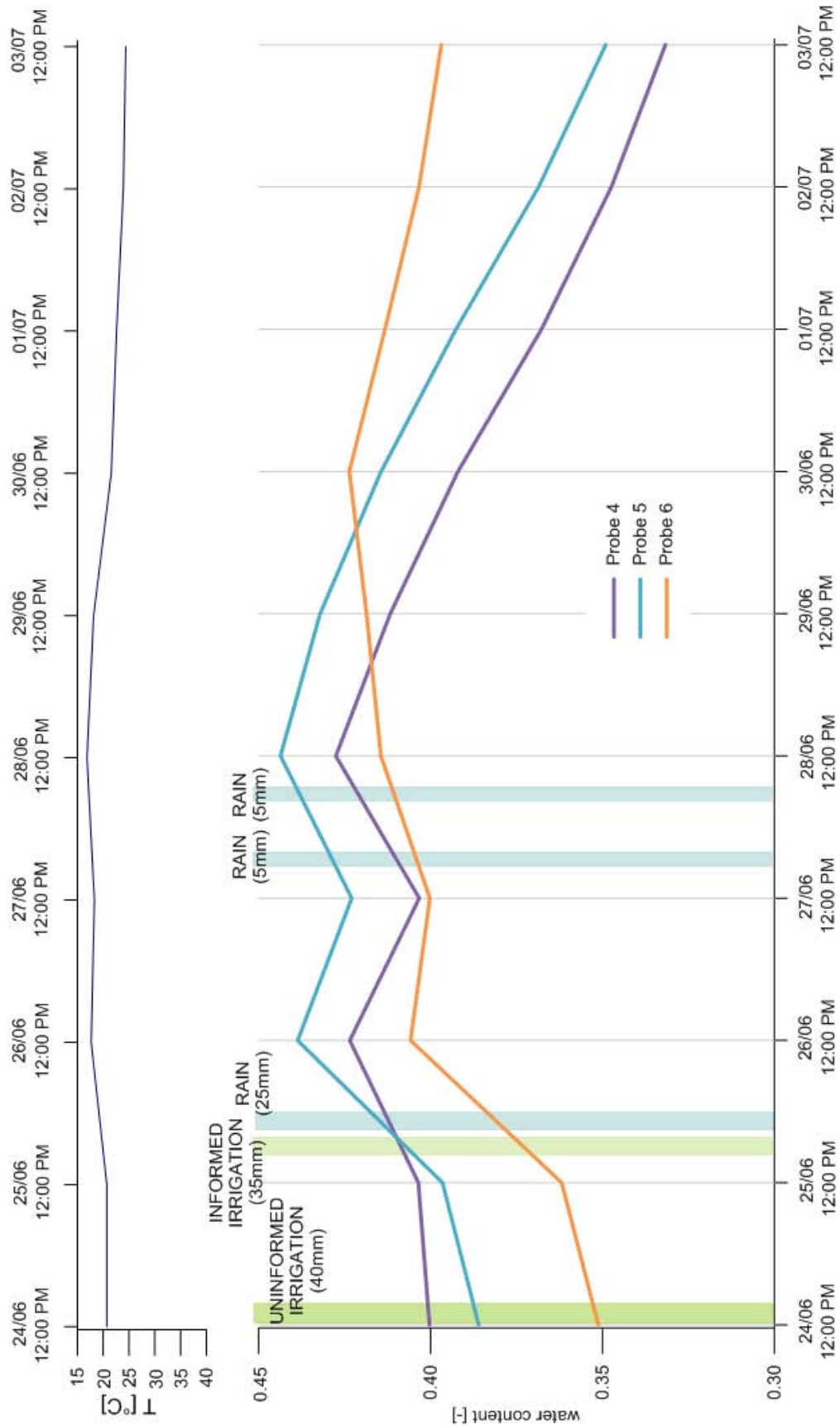


Figure 4.17: Daily means of the first irrigation period; ‘uninformed’ probes

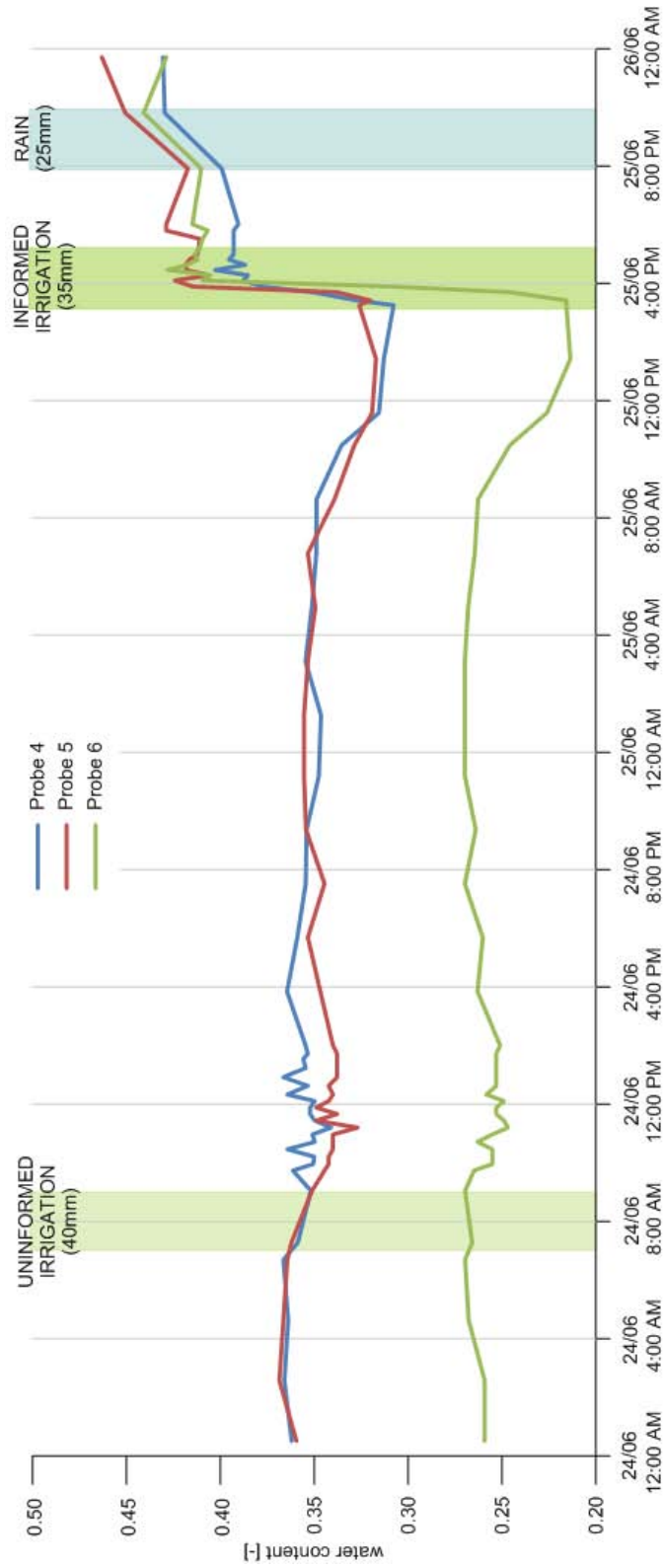


Figure 4.18: Focus on the first irrigation; ‘informed’ probes

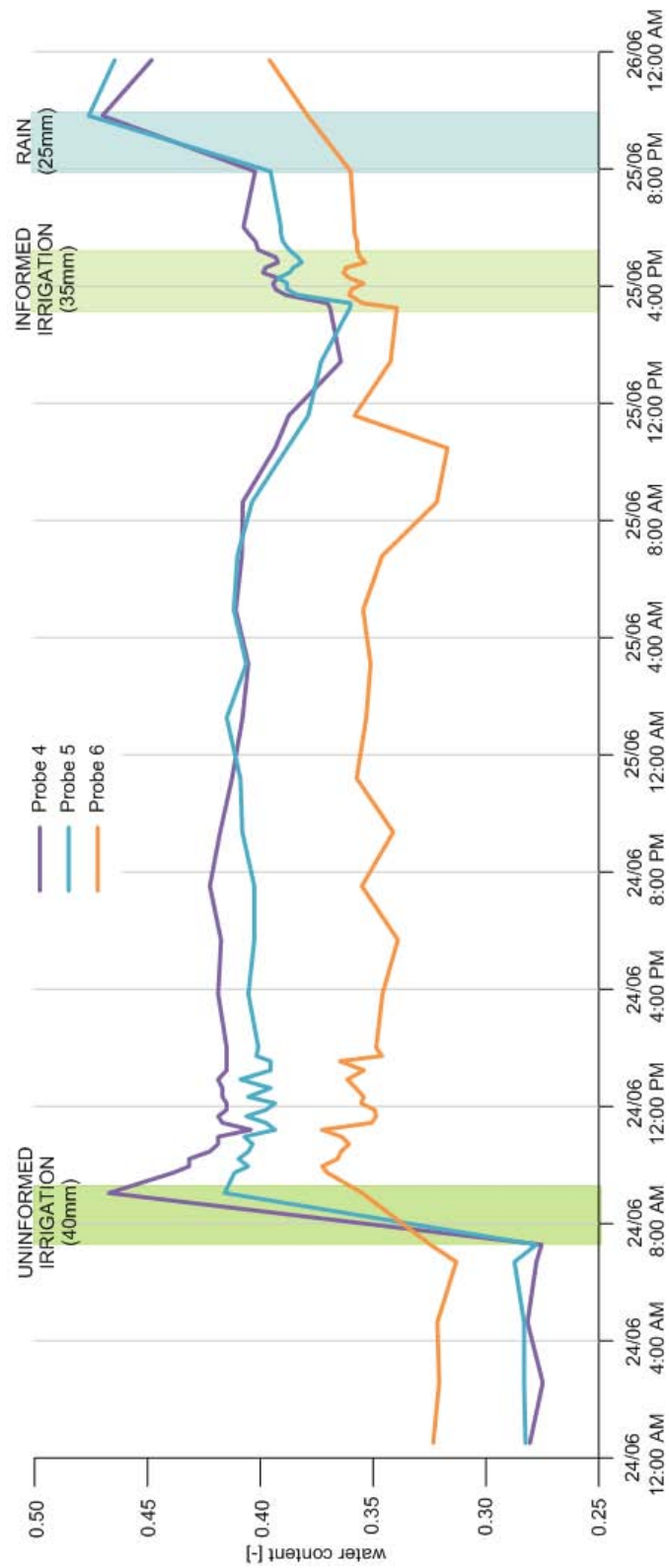


Figure 4.19: Focus on the first irrigation; ‘uninformed’ probes

<i>Probe</i>	θ_{before}	s_{before}	θ_{after}	s_{after}	$\Delta\theta$	Δs
1	0.308	0.699	0.395	0.899	0.088	0.195
2	0.326	0.741	0.416	0.947	0.090	0.201
3	0.216	0.490	0.412	0.937	0.197	0.437
average	0.283	0.629	0.408	0.907	0.125	0.278
4	0.275	0.626	0.432	0.981	0.156	0.347
5	0.278	0.631	0.410	0.931	0.132	0.293
6	0.325	0.738	0.366	0.831	0.041	0.091
average	0.293	0.650	0.402	0.894	0.110	0.244

Table 4.6: Water content and soil moisture values before and after the first irrigation

4.3.3 Second period

The second period considered is characterized by 3 rainfall events and prolonged droughts with average daily temperature above 25C. On July, 4 a rainfall event brought 40mm causing a large jump in the water content (Figures 4.20 and 4.21) and the consequent exceedance of the field capacity. The exceedance of the field capacity is evidenced by a sharp decrease of the water content just after rainfall. After the event, the water content decreased linearly for the first 3 days (Figures 4.22 and 4.23) and thereafter exponentially until July 12 when a new event bringing 11mm was observed. As a consequence, the water contents of the probes 1, 2, 4 and 5 increased immediately, while for the probes 3 and 6 (i.e. the deepest probes) showed a delayed increase. Another rainfall event of 2mm was recorded on July 13 with very limited effects on the water content (Figures 4.20 and 4.21). During the dry period from July 14 to 23, the water content of the ‘uninformed’ probes decreased more than linearly for probe 4 and almost linearly for probes 5 and 6, while the water content of the ‘informed’ probes remains almost constant as evidenced by Figures 4.22 and 4.23. In the informed site there are a lot of fractures through which water moves towards the side of the field in which uninformed probes have been positioned. This explains why, even if the two different sites have received the same amount of rain, the soil water content of the uninformed site shows a larger peak. The water movement through the fractures is allowed by the gentle slope of the field. Fields usually have a slight slope to avoid water

stagnation over the soil; in the field considered here the slope is towards the side of the field in which uninformed probes are positioned.

4.3.4 Second irrigation

This period is characterized by the second irrigation of the maize field which is followed by a dry period, interrupted only by two small rainfall events. The second irrigation for the maize field started on July 23. First, the ‘uninformed’ site was irrigated (40mm) starting from 9:25AM using the hose reel. Then, the ‘informed’ site was irrigated using a fixed sprinkler. The irrigation of the informed probes has been split into two applications: the first one started at 11:30AM delivering 20mm of water, while the second application started the following day (July 24) at 9:20AM providing 10mm as shown by Figures 4.24 and 4.25.

The 40 millimeters of water delivered to the part of the field where uninformed probes are placed caused a huge peak in the values of the water contents measured by probes 4 and 5 (Figure 4.27) and a consequent sharp decrease of the soil water content value just after the irrigation. Since probe 6 is the deepest probe, the peak observed in the corresponding soil moisture content is delayed with respect to the probes closer to the surface. No leakages were observed in the deep soil layer. The total amount of water delivered to the informed probes determined the exceedance of the field capacity (Figure 4.26). The peaks of the three informed probes due to the 10mm are simultaneous, while for the first 20mm only probes 1 and 2 show an increase of the water content. In the deepest probe the water content starts to increase only after the second irrigation. The irrigation of each site influenced the value of the water content of other site. The most evident effect is those of the uninformed probes after the second part of the irrigation of the informed probes; the peaks are contemporary for the probes 4, 5 and 6 and delayed of few hours after the end of the irrigation. The water contents and the relative soil moisture values for the six probes before and after the irrigation of each group are reported in Table 4.7.

After the second irrigation, the water contents of the probes started to decrease more than linearly (Figures 4.28 and 4.29) until July 29 when a rainfall event was observed that brought 2.5mm plus 3.5mm in the evening. These two contributions

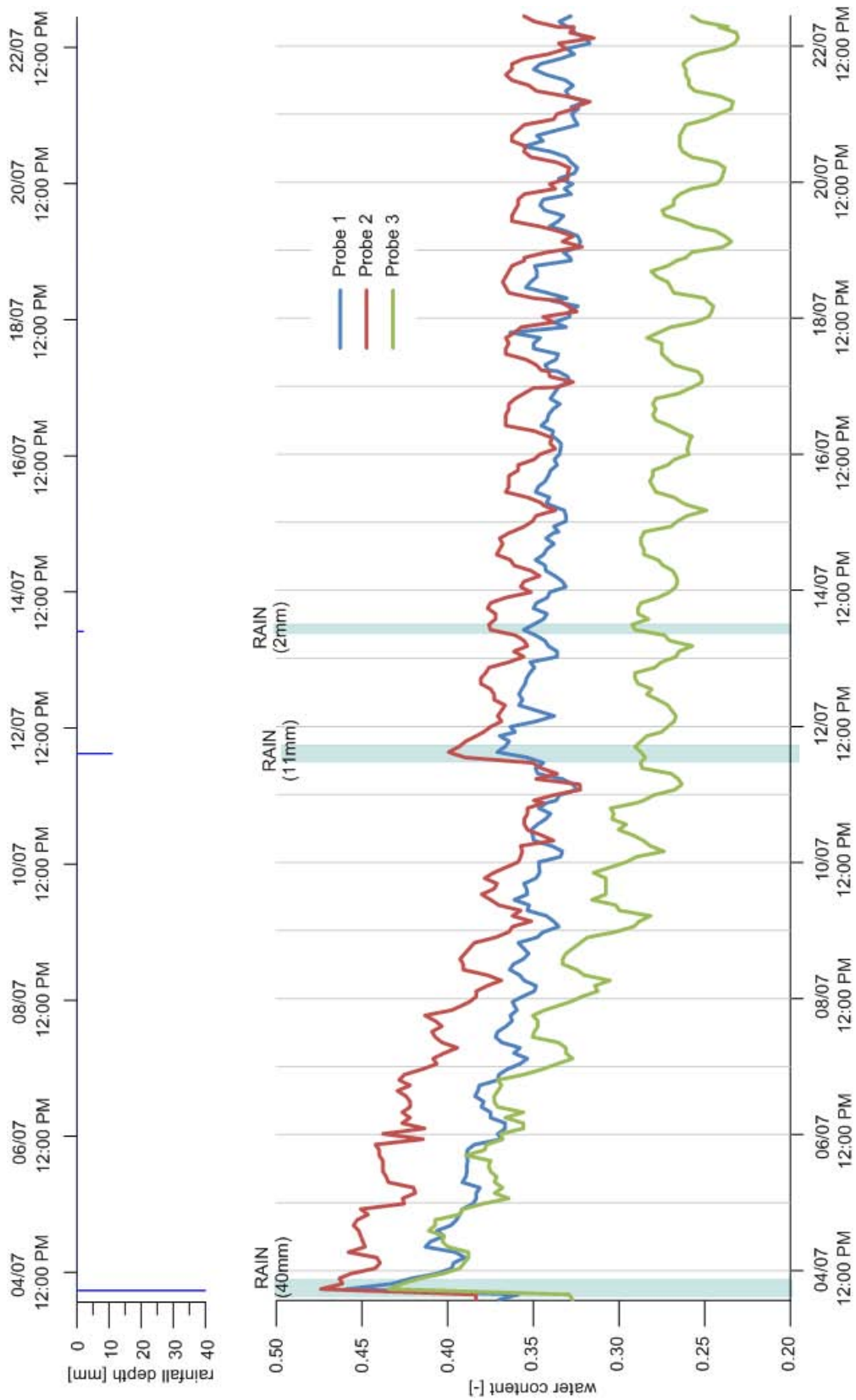


Figure 4.20: Second period; informed probes

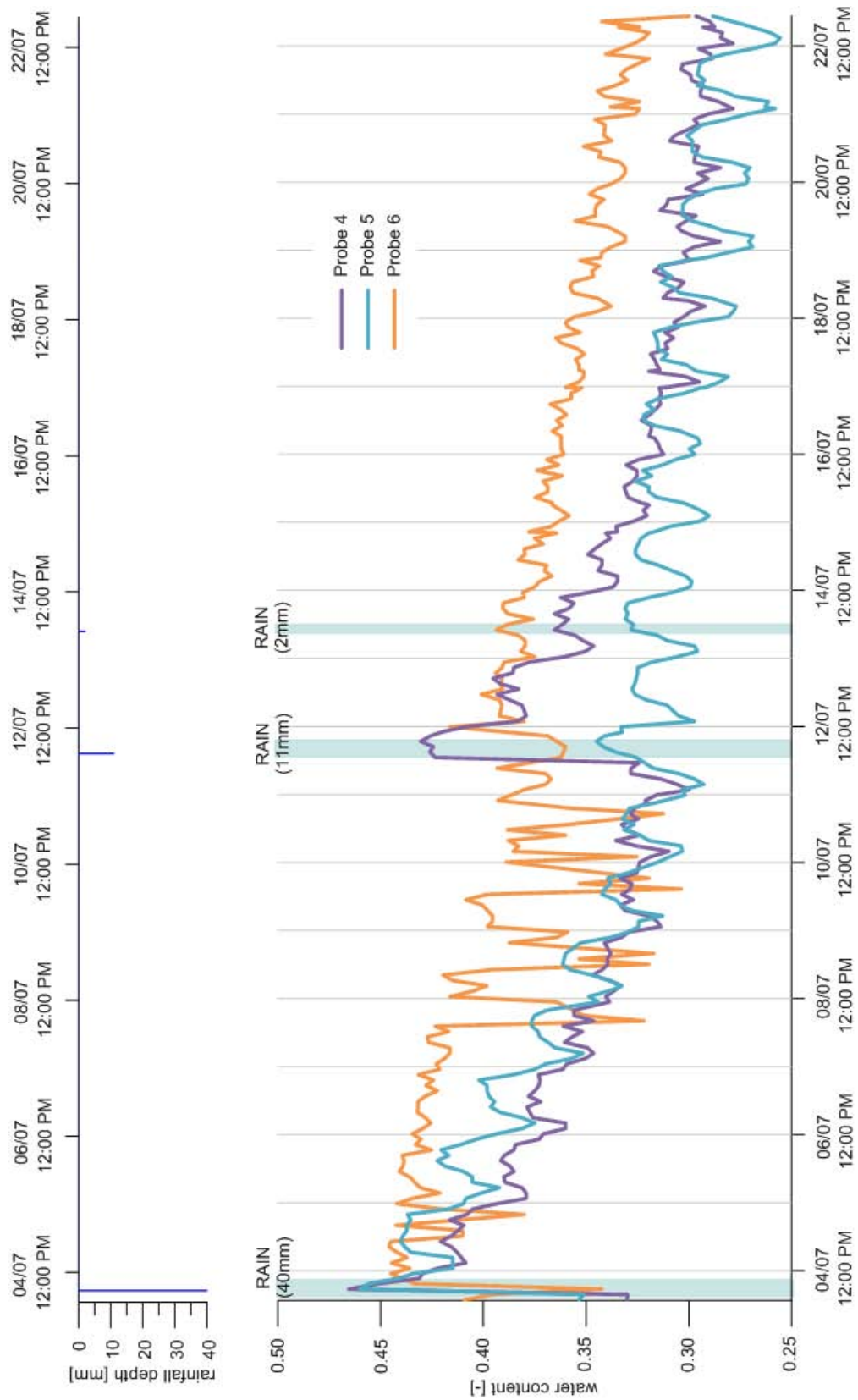


Figure 4.21: Second period; uninformed probes

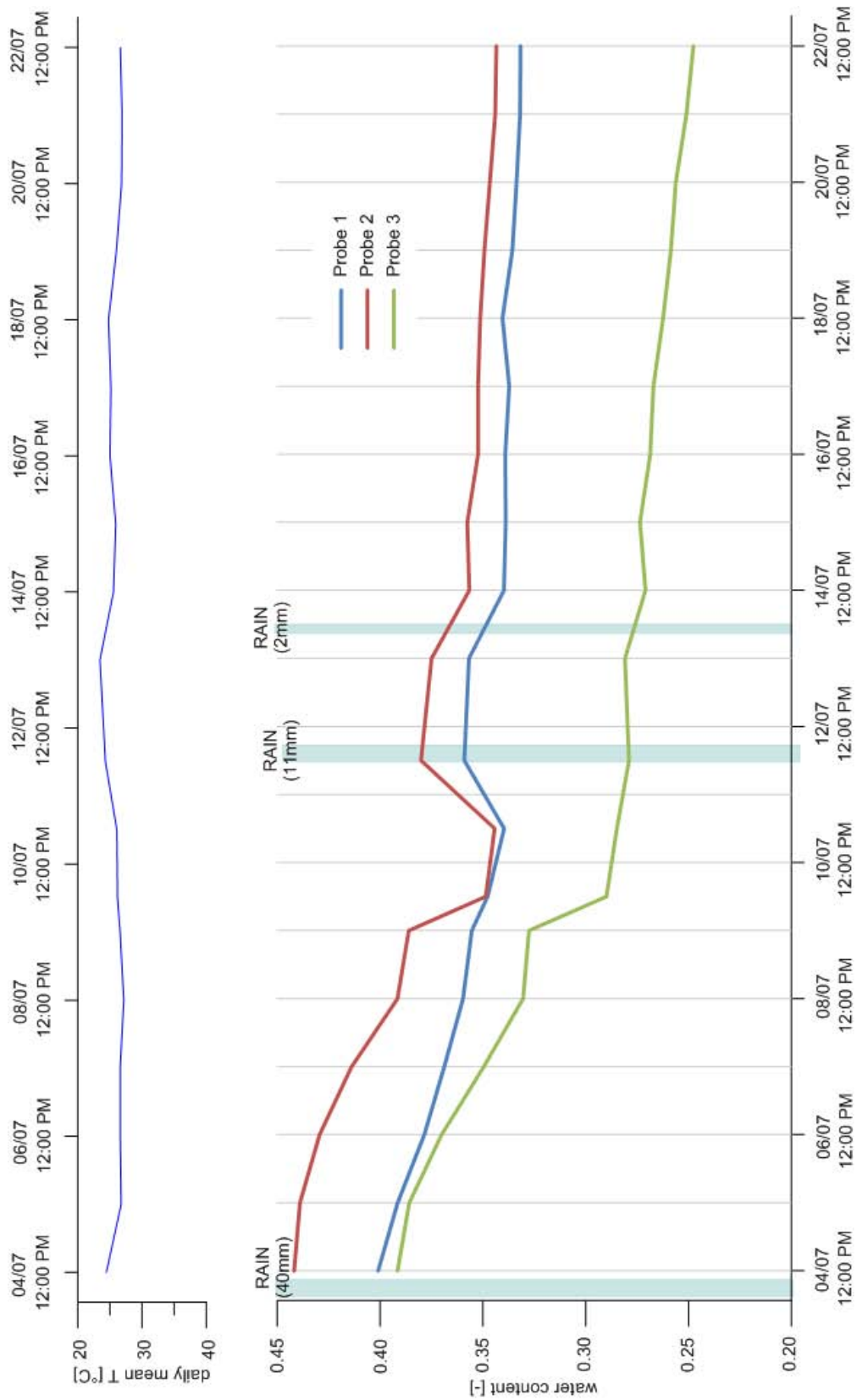


Figure 4.22: Second period; daily means for informed probes

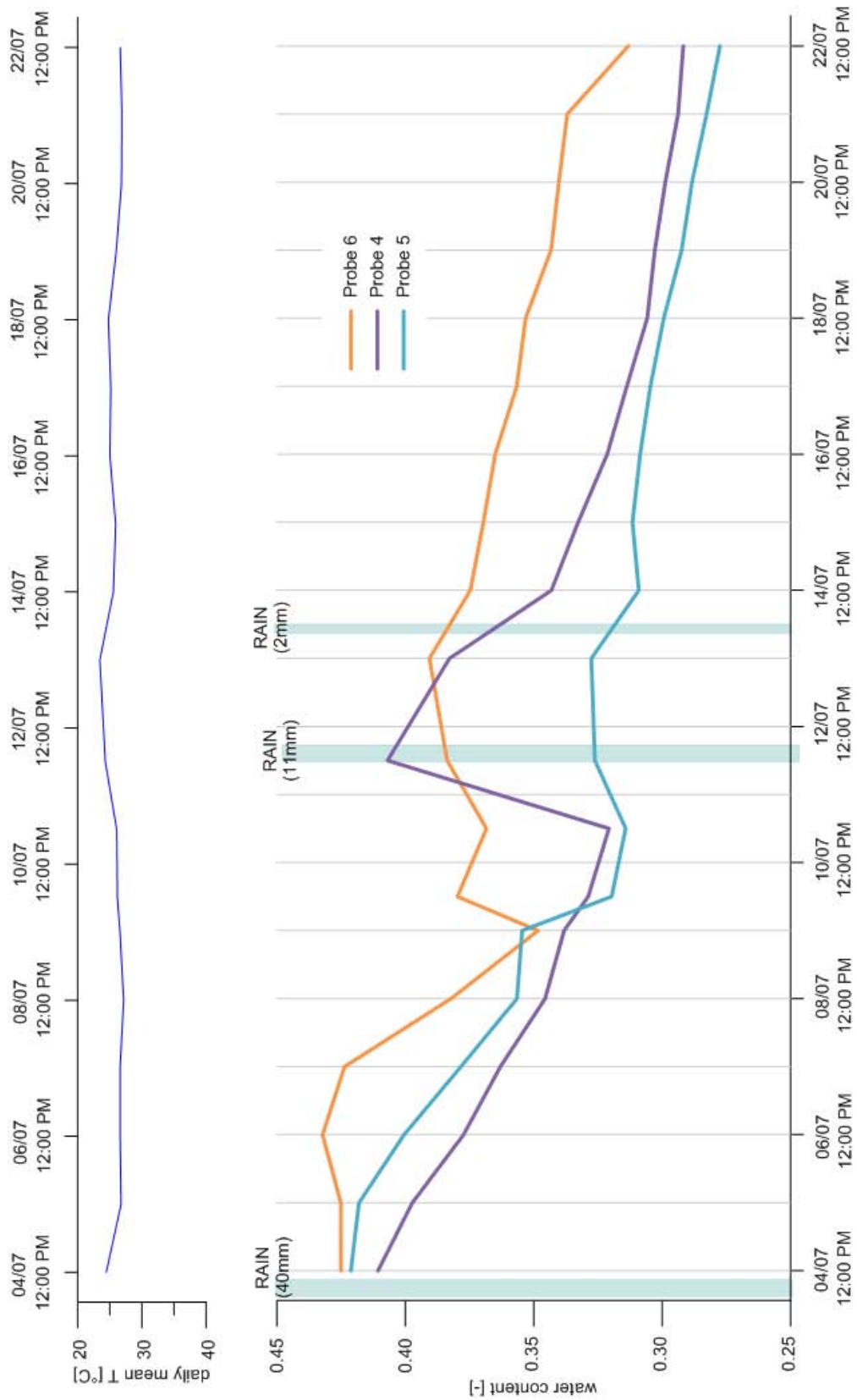


Figure 4.23: Second period; daily means for uninformed probes

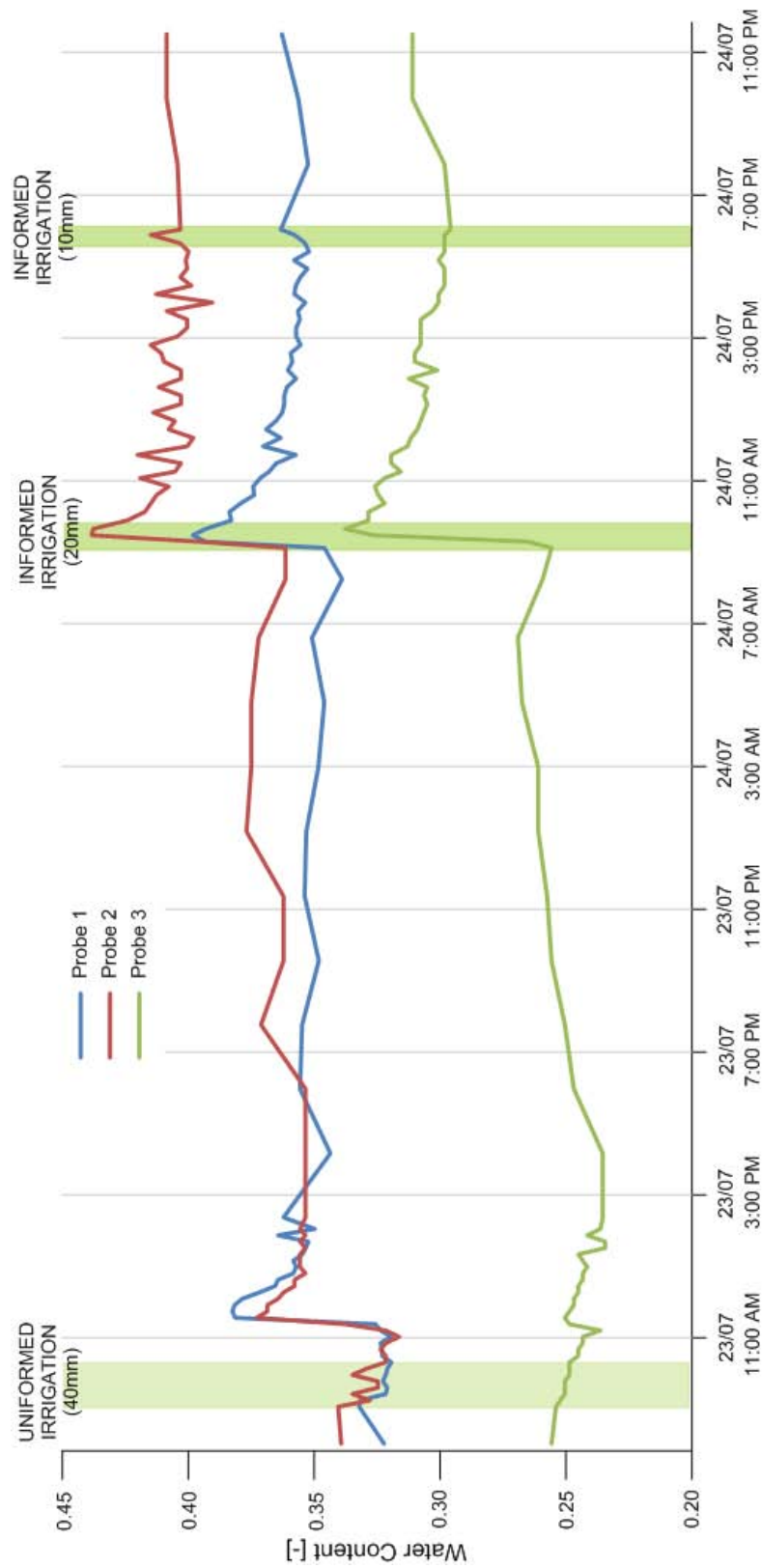


Figure 4.24: Detail of the second irrigation; ‘informed’ probes

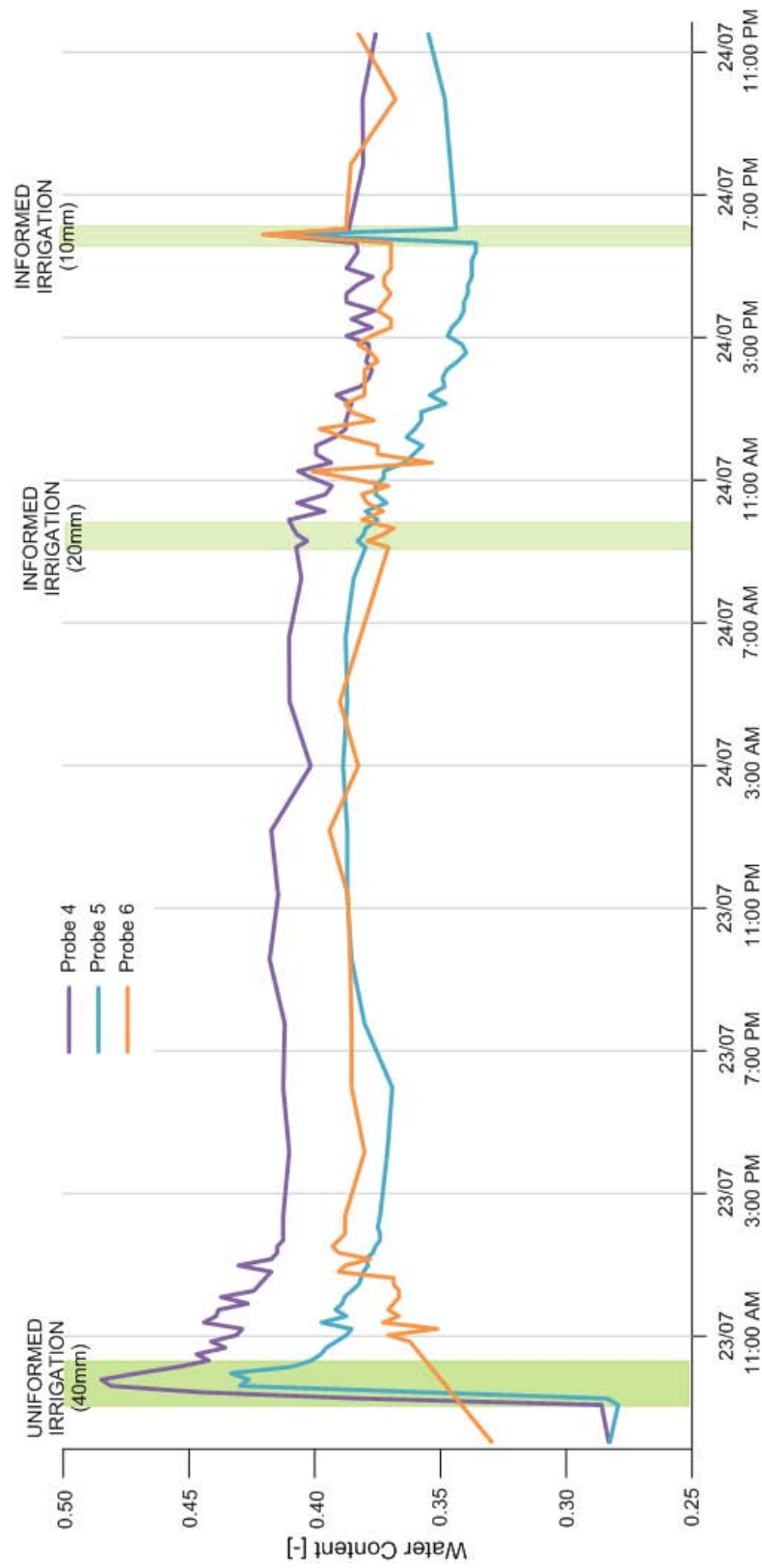


Figure 4.25: Detail of the second irrigation; ‘uninformed’ probes

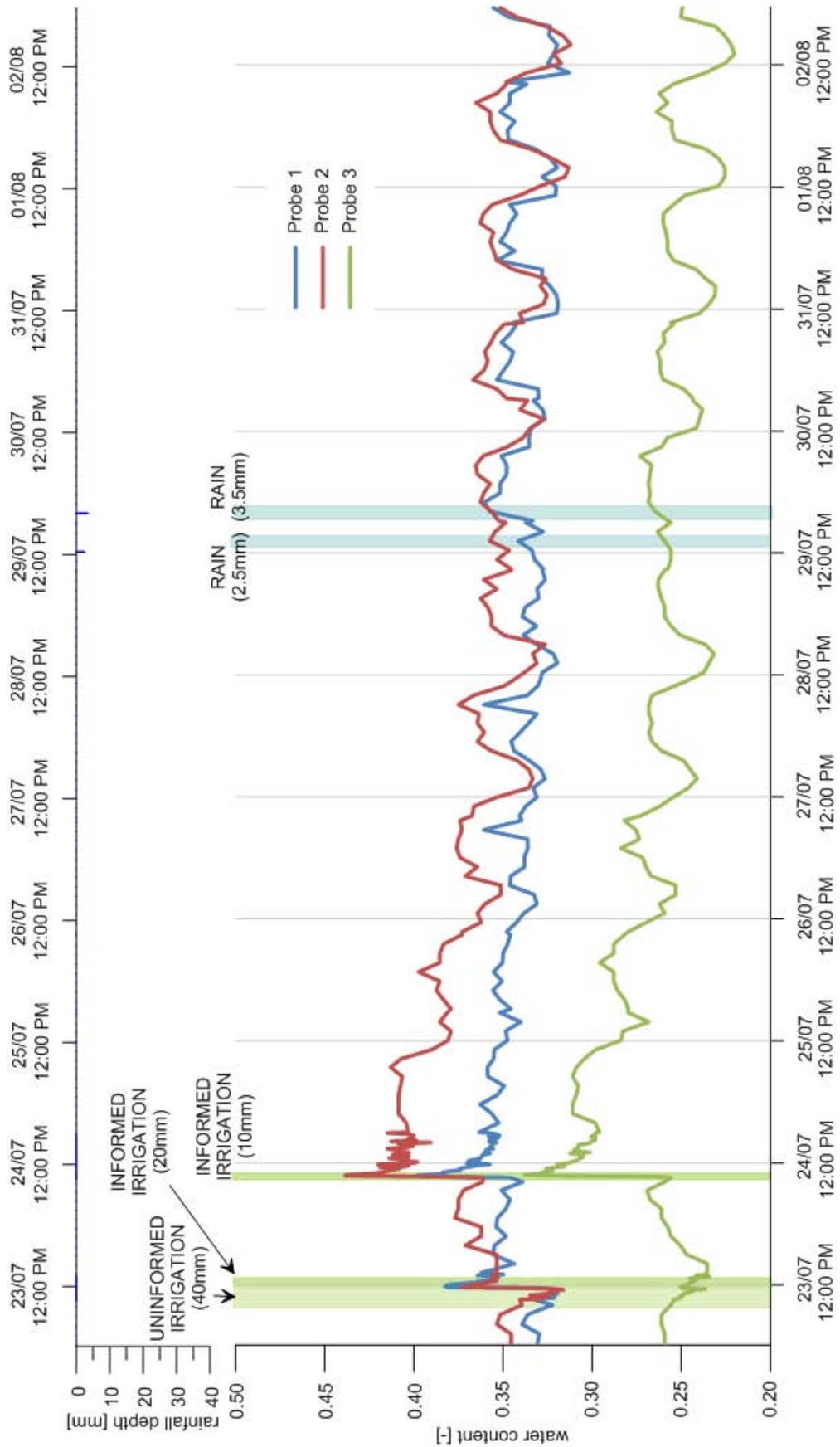


Figure 4.26: Second irrigation; informed probes

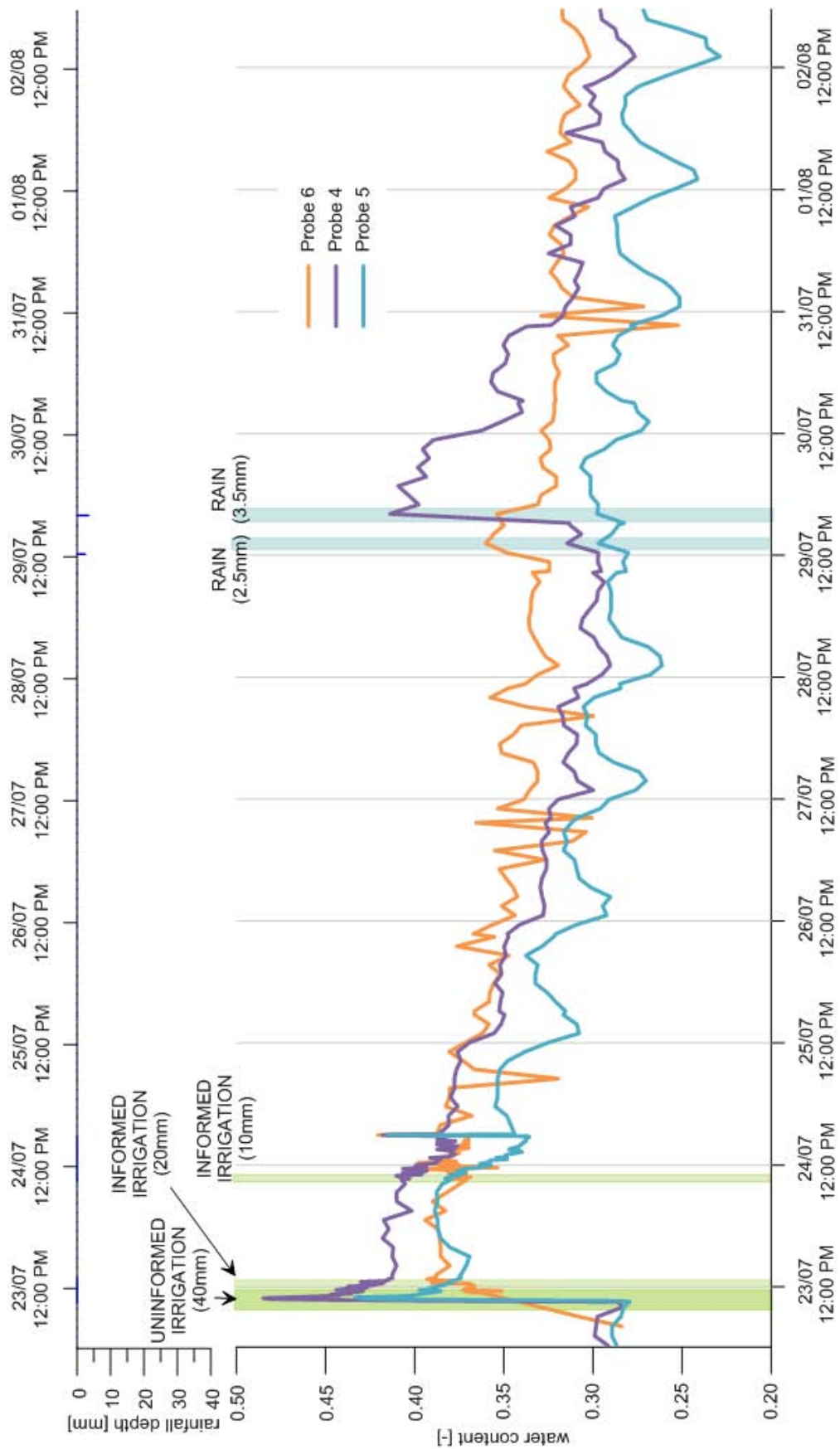


Figure 4.27: Second irrigation; uninformed probes

<i>Probe</i>	θ_{before}	s_{before}	θ_{after}	s_{after}	$\Delta\theta$	Δs
1	0.319	0.710	0.398	0.885	0.079	0.175
2	0.316	0.703	0.438	0.974	0.122	0.271
3	0.243	0.541	0.338	0.751	0.094	0.210
average	0.293	0.651	0.391	0.870	0.098	0.219
4	0.286	0.636	0.485	1.077	0.199	0.442
5	0.279	0.621	0.430	0.955	0.150	0.334
6	0.330	0.733	0.362	0.805	0.032	0.072
average	0.298	0.663	0.426	0.946	0.127	0.283

Table 4.7: Water content and soil moisture values before and after the second irrigation

slightly increased the water contents of the probes, except for the probe 4 which shows a larger increase during the second event (i.e. the 3.5mm). After these rainfall events, there has been a dry period until August 2 during which the water contents measured by the ‘informed’ probes has remained fairly constant. Meanwhile, the value of water content in the ‘uninformed’ probes show a slow decrease (Figures 4.28 and 4.29), which possibly suggests water stress.

4.3.5 Third irrigation

This period comprises the third irrigation of the maize field and three rainfall events. Daily external temperature was around 30C in the first part of the period and ranging between 27C and 20C in the last part. The third irrigation of the maize field started on August 3 at 12PM for the ‘uninformed’ probes and at 4:40PM for the ‘informed’ probes. The uninformed probes received 40mm, while 23mm to the informed site. The informed probes show a very large increase of the water content (Figure 4.32), with a consequent sharp decrease which reveals the occurrence of deep percolation. Similarly, the probes ‘uninformed’ show a quite large increase in their water content during the irrigation (Figure 4.33), followed by a sharp decrease. Due to the limited distance among the two groups of probes, also the water content measured by the uninformed probes is influenced by the water delivered to the informed site. Moreover, surface runoff has been observed during irrigation in the ‘informed’ probes, which enhanced the influence on the

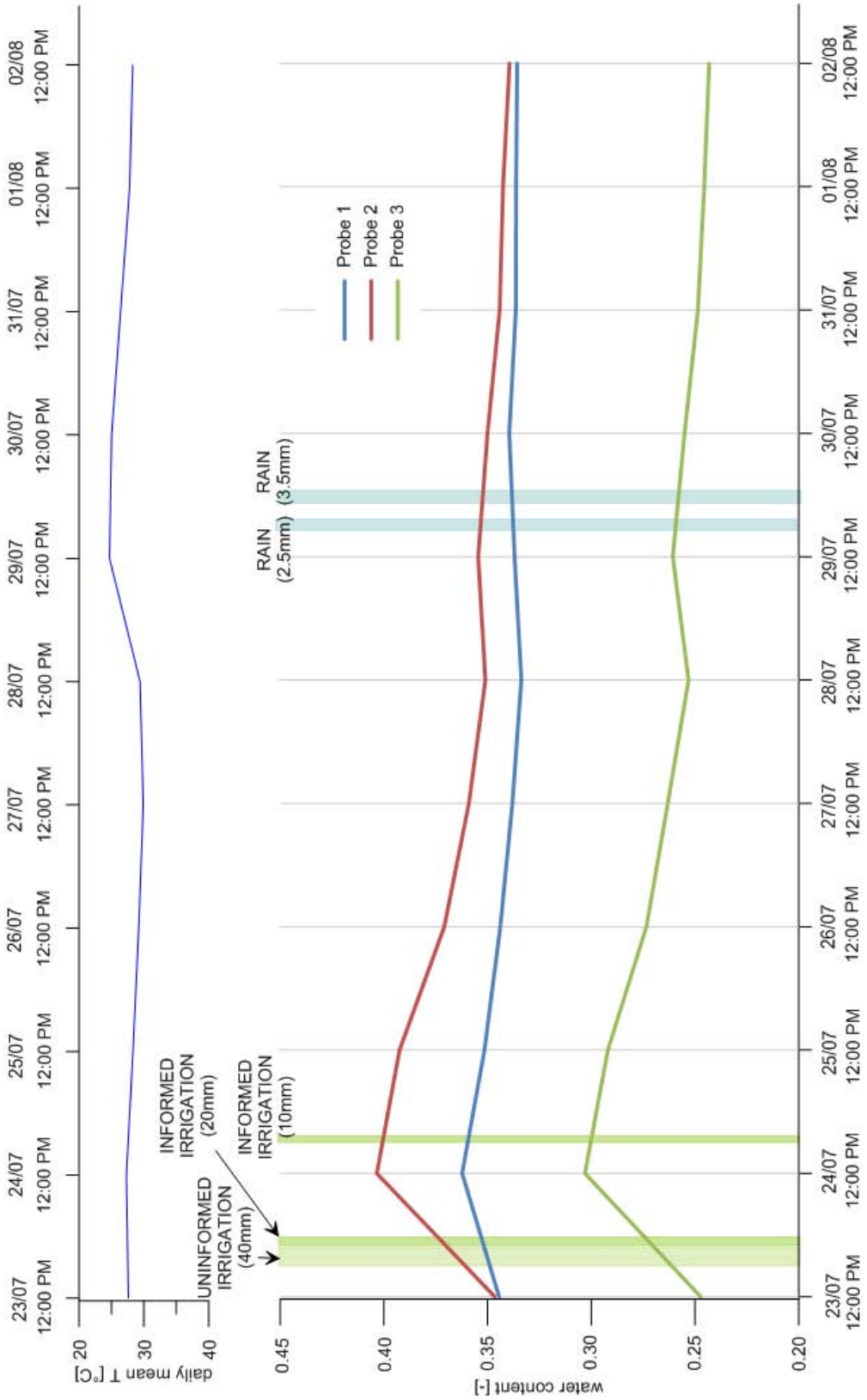


Figure 4.28: Second irrigation; daily means of informed probes

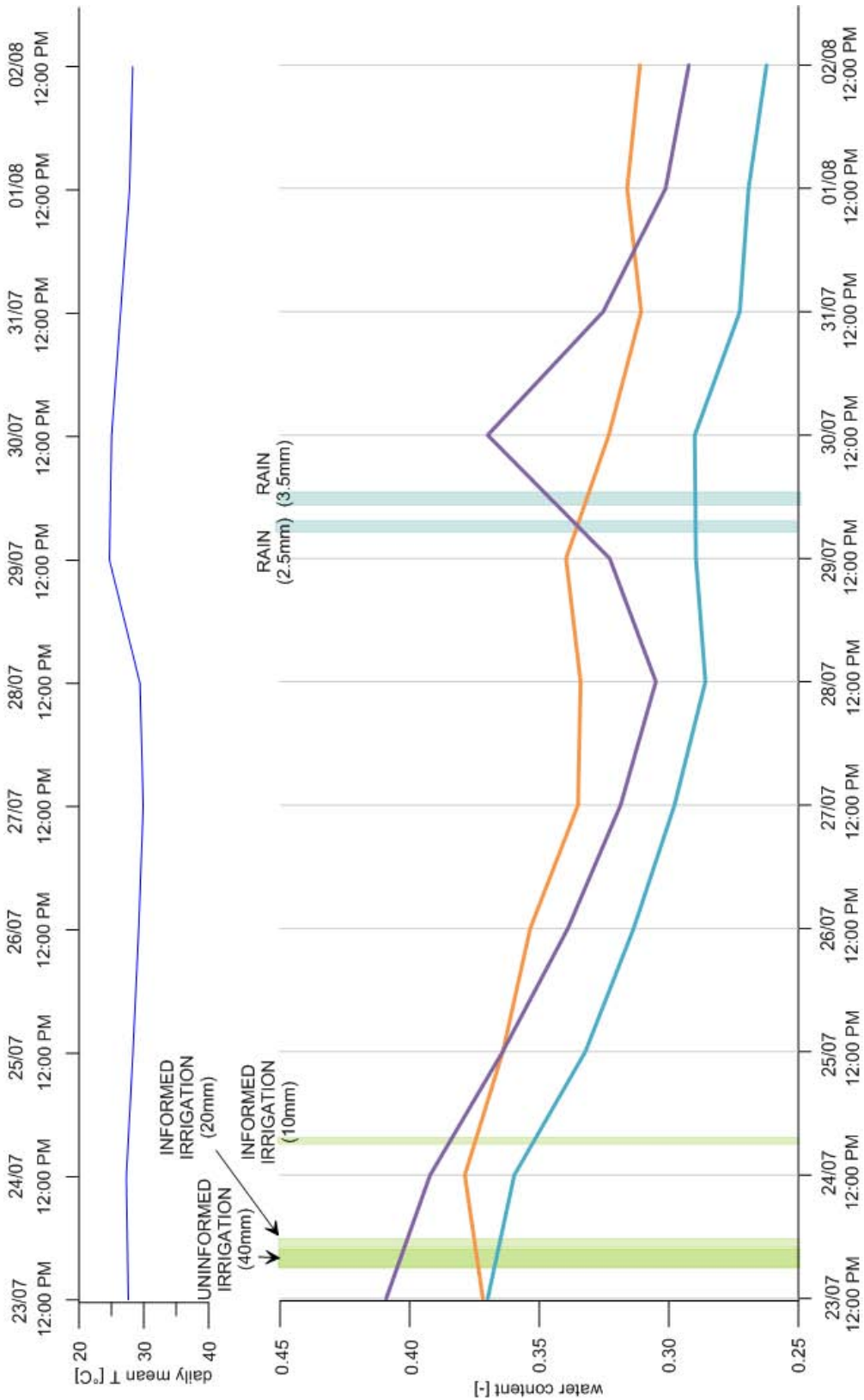


Figure 4.29: Second irrigation; daily means of uninformed probes

water content of the other probes. In fact, during the irrigation of the informed probes, the uninformed site shows a visible increase of soil moisture. Also the informed probes were influenced by the irrigation of the uninformed site, but to a lesser extent. Figures 4.30 and 4.31 show the temporal evolution of the water content dynamics during the third irrigation. The soil water contents (and the corresponding relative soil moisture) measured by the six probes before and after the third irrigation are reported in Table 4.8.

<i>Probe</i>	θ_{before}	s_{before}	θ_{after}	s_{after}	$\Delta\theta$	Δs
1	0.310	0.689	0.482	1.072	0.172	0.383
2	0.314	0.698	0.519	1.154	0.205	0.455
3	0.222	0.493	0.477	1.061	0.255	0.568
average	0.282	0.627	0.493	1.095	0.211	0.469
4	0.235	0.607	0.491	1.090	0.218	0.483
5	0.279	0.523	0.474	1.053	0.239	0.530
6	0.289	0.642	0.470	1.044	0.181	0.402
average	0.266	0.591	0.478	1.063	0.212	0.472

Table 4.8: Water content and soil moisture values before and after the third irrigation

From Figures 4.34 and 4.35 it can be seen that, after the irrigation, the water contents of the probes 2, 3 and 6 decrease linearly, while the remaining probes (i.e. 1, 4 and 5) show a slower decrease of s until August 9. On that day, 1mm of rain was observed during the morning, with negligible effect on the six probes. 4mm of rain were then recorded arrived in the afternoon, causing an evident increase in the water content only for the surface probes (i.e. probes 1 and 4). Some days later (on August 14) a rainfall arrived at 12:00PM bringing 16mm which affected significantly the values of the water contents. The probes 1, 2 and 4 were affected immediately by the rain, while the increment of the water contents for the remaining probes is delayed a bit and it is lower than for the other three probes. All the six probes show a slow decrease of the measured water content after the rain event of August 14 until August 23.

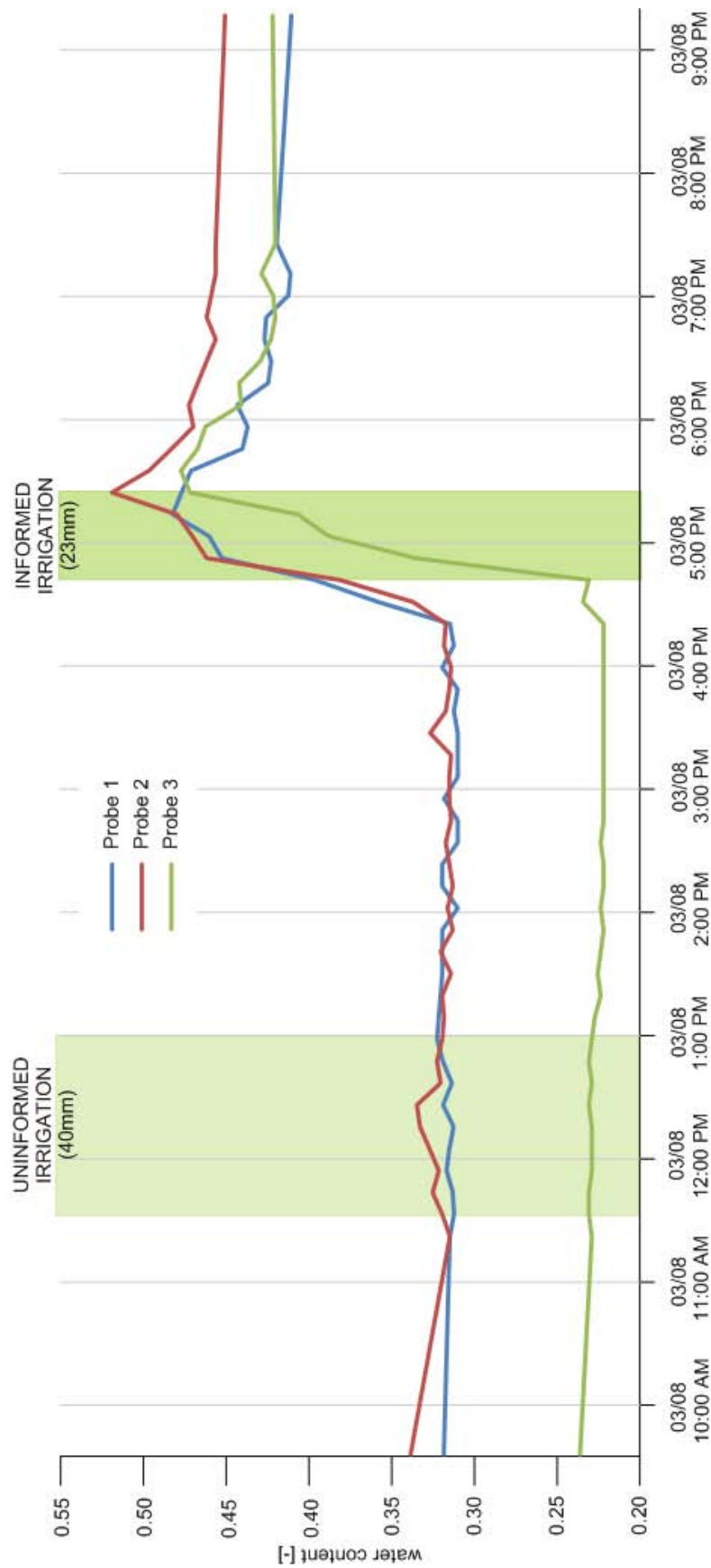


Figure 4.30: Detail of the water content dynamics during the third irrigation; ‘informed’ probes

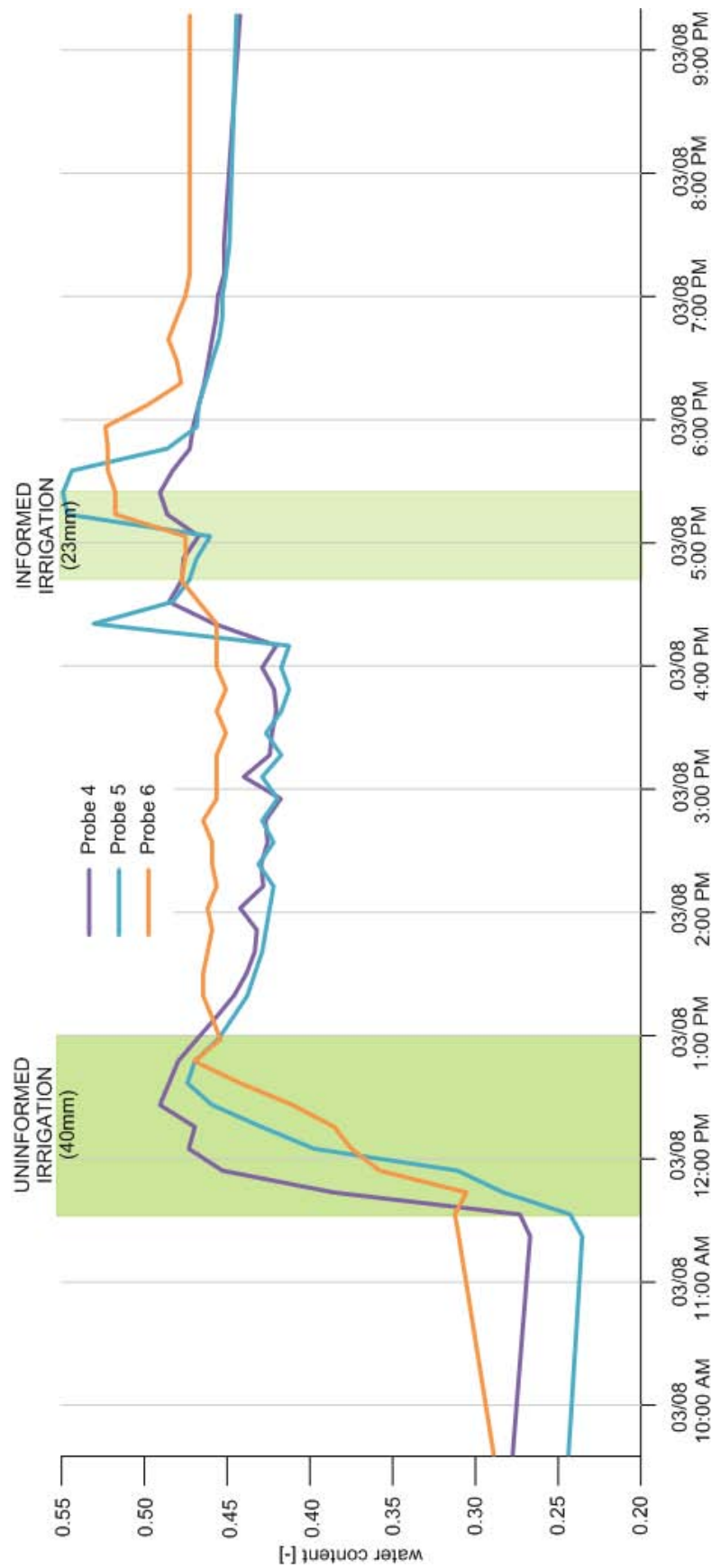


Figure 4.31: Detail of the water content dynamics during the third irrigation; ‘uninformed’ probes

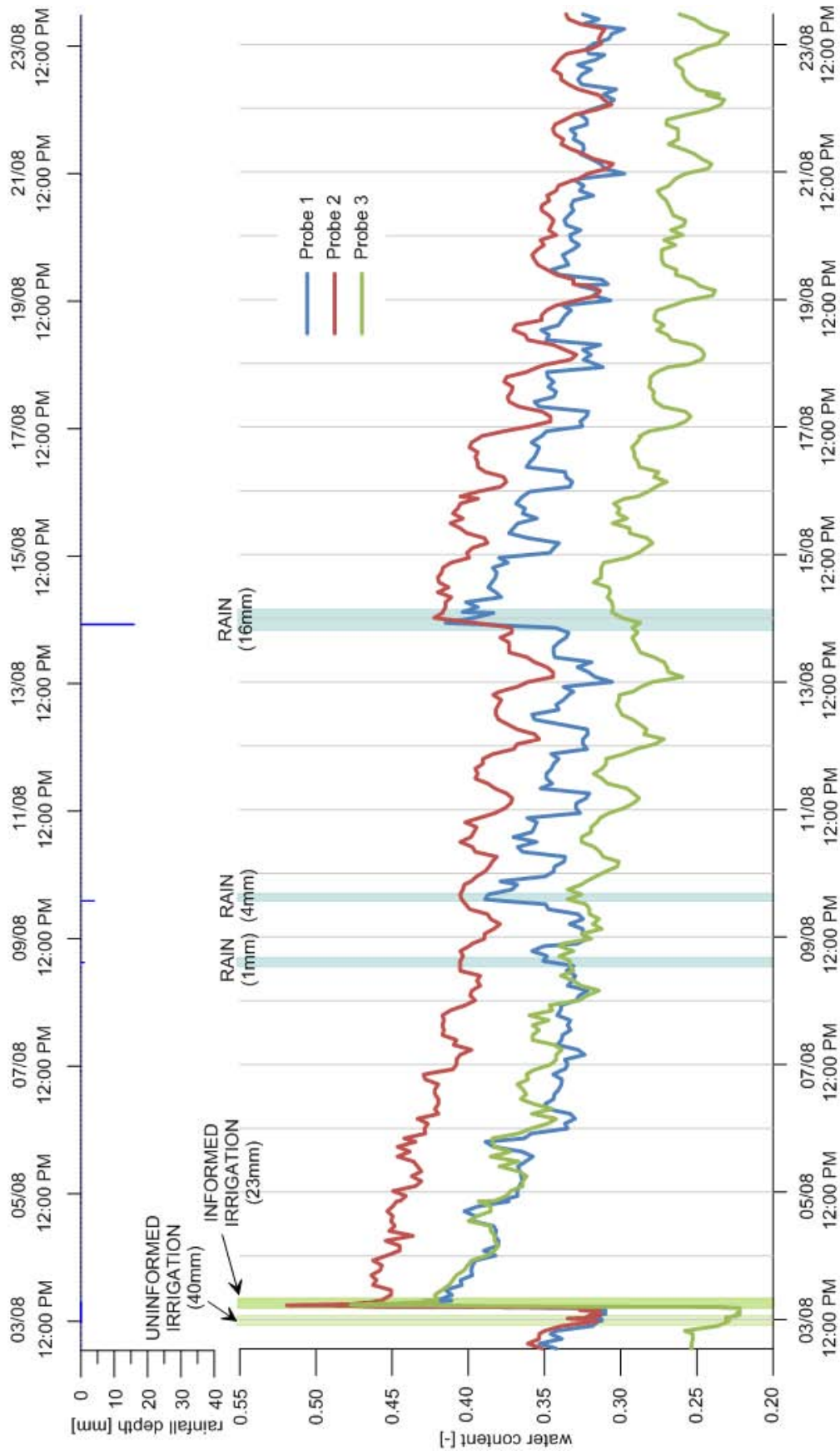


Figure 4.32: Third irrigation; ‘informed’ probes

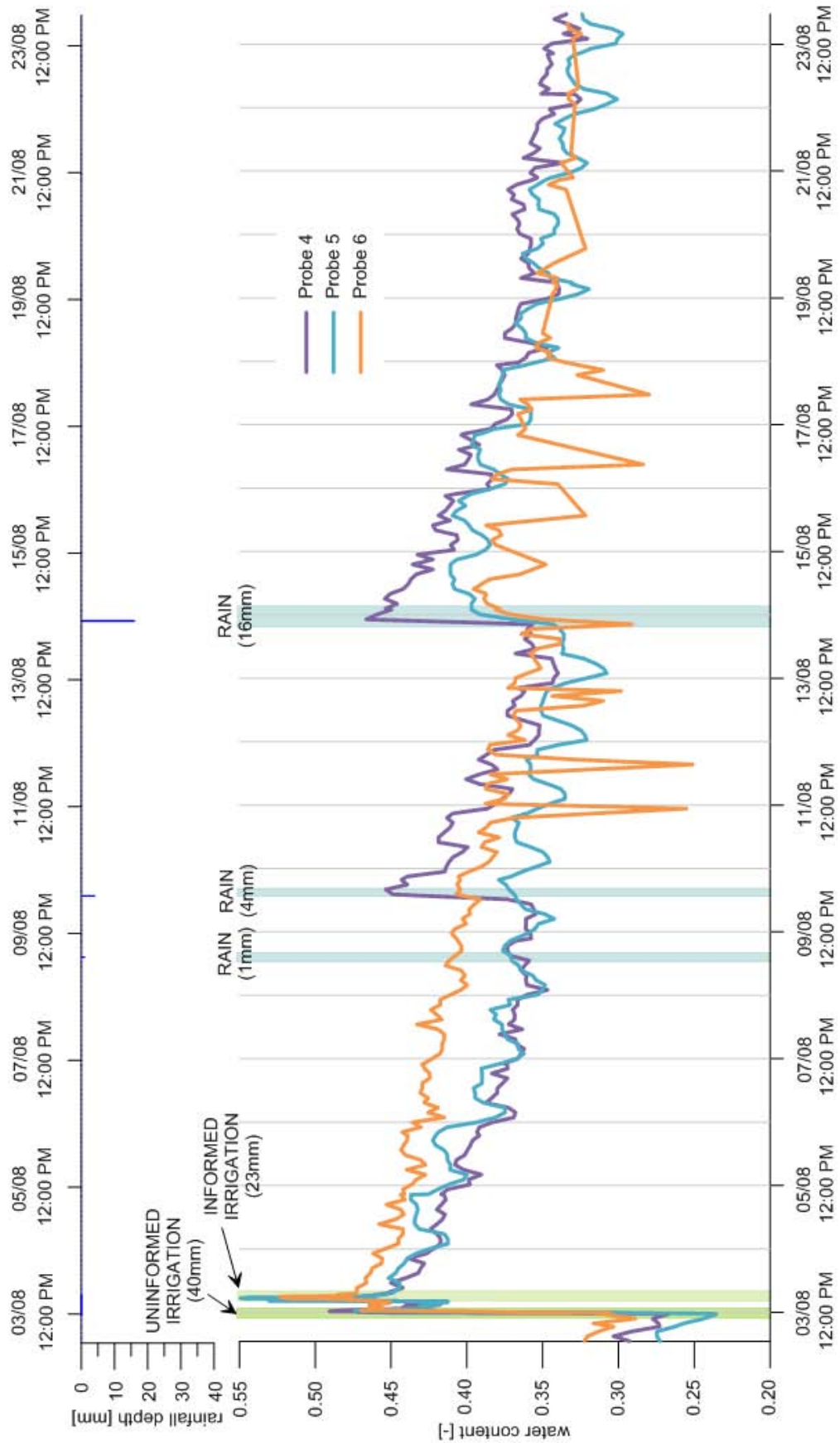


Figure 4.33: Third irrigation; 'uninformed' probes

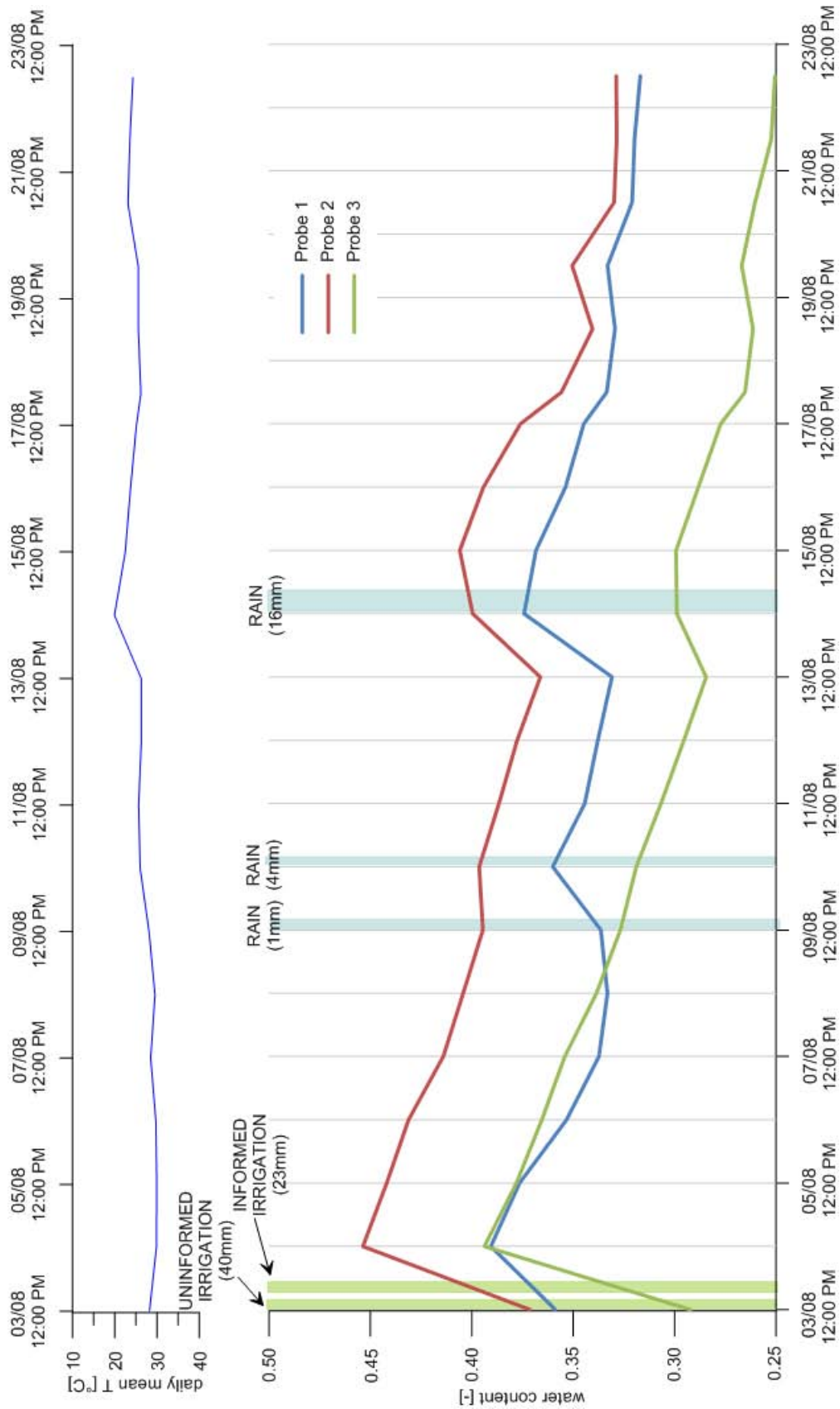


Figure 4.34: Third irrigation; daily means of the ‘informed’ probes

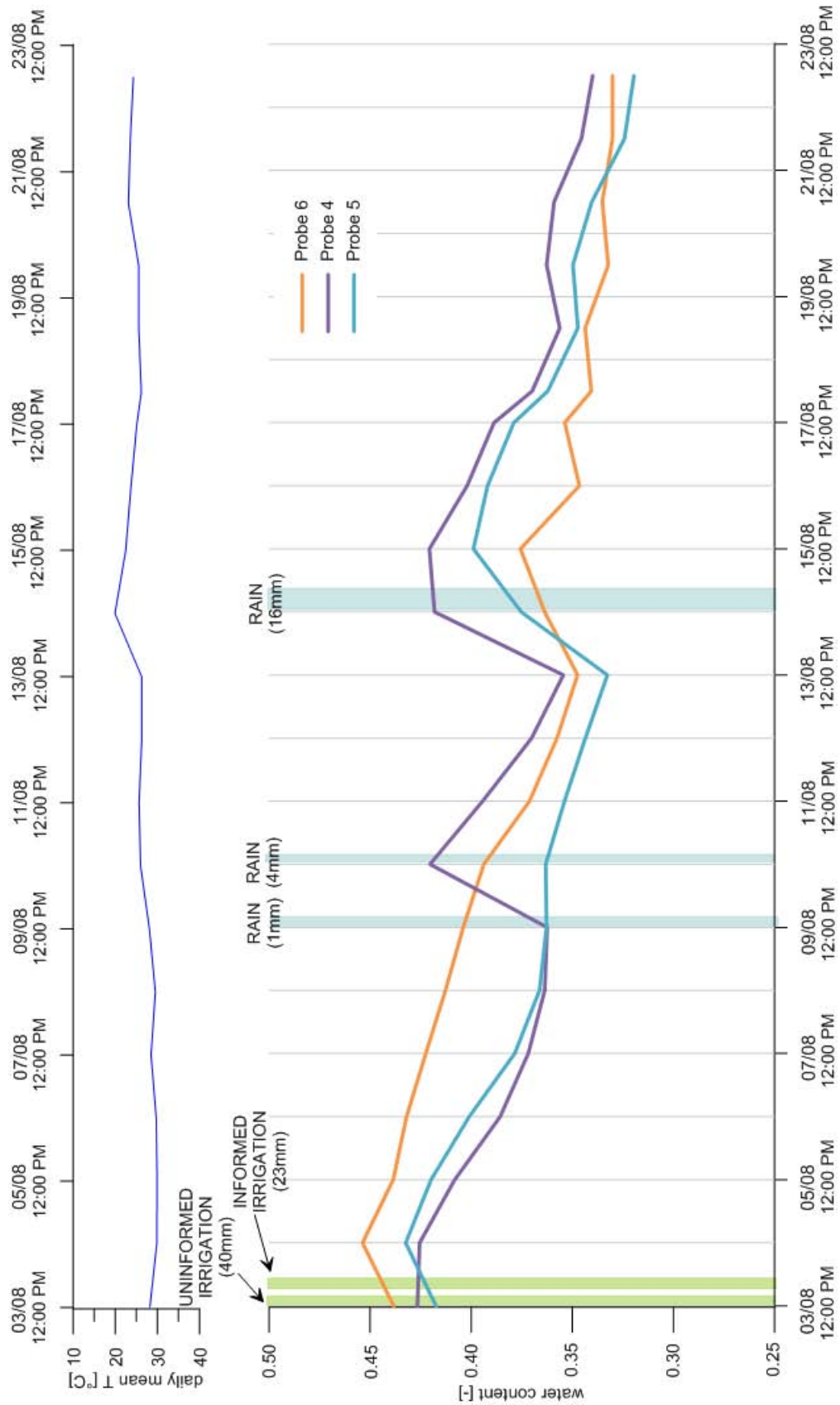


Figure 4.35: Third irrigation; daily means of the ‘uninformed’ probes

4.3.6 Third period

This last period of acquisitions is the most rainy period of the experiment. In fact seven rainfalls were observed, which brought 69.5mm of rain in all. Moreover, daily external temperatures started to decrease and maize plants are going to die. Two rainfalls were observed on August 25: the first one just after midnight brought 12mm of water, causing a sharp jump in the water content measured by probe 1, while the water content measured by probe 2 increased a bit later. Probe 6 shows a very limited increase. Probe 4 had a large jump just after the rainfall and probe 5 shows a water content increase a bit delayed. The second rainfall was observed in the evening and brought 33mm of water which caused a large increase of the water contents measured by probes 1, 2, 3 and 5, while the probe 4 shows a smaller increase of soil moisture content with respect to the remaining probes. Then, 3.5mm of rain were observed on August 26 and 7mm on the following day leading to an increase of the water content measured from all the probes. Thereafter, the water contents measured by the six probes started to decrease linearly until September 2 when a new rainfall was observed, which brought 10mm of water. The water contents of the two superficial probes (i.e. probes 1 and 4) increased more than the other probes. Moreover, the increase of the water contents measured by the probes 2, 3 and 5 was a bit delayed. From September 2 to 10 the water contents decreased linearly for the uninformed probes and more than linearly for the informed probes.

On September 10 and 15 two rain events were observed which brought 1mm and 3mm of water respectively with negligible effects on the values of the water contents measured by the probes. From September 11 until the end of the experiment the water contents of the probes decreased at a very slow rate more likely to the reduced metabolic activity of the plants at this stage.

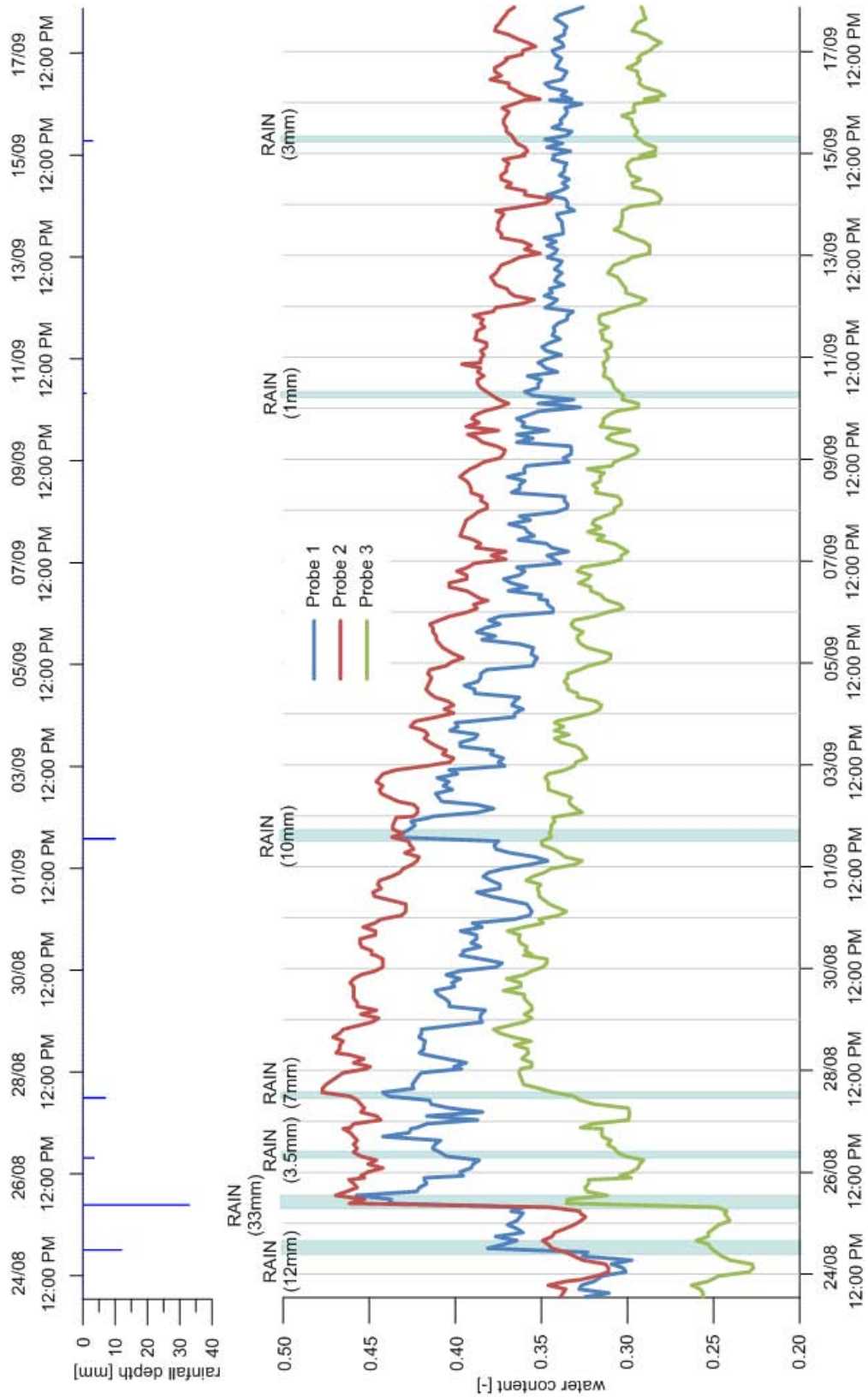


Figure 4.36: Third period; water contents of the ‘informed’ probes

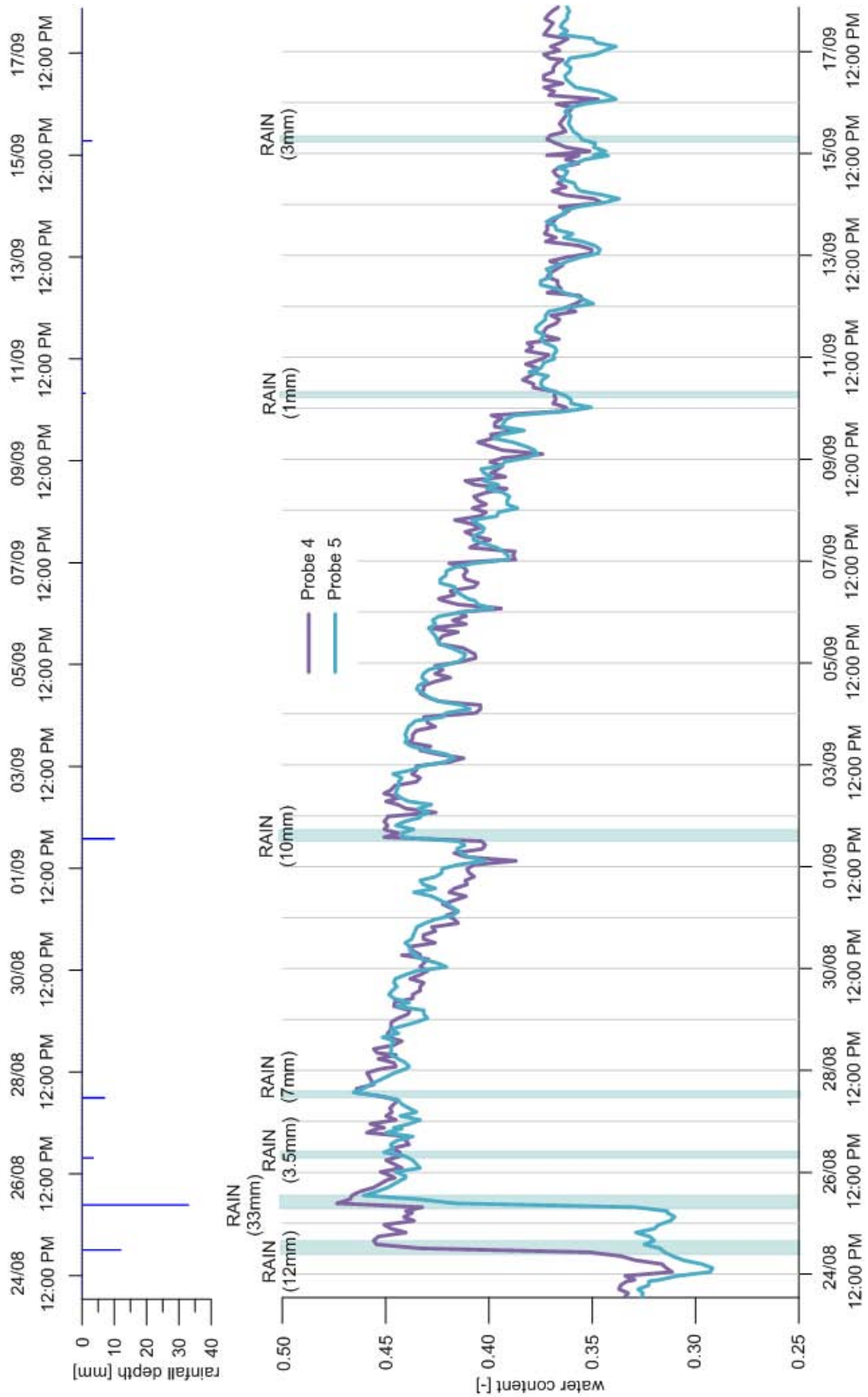


Figure 4.37: Third period; water contents of the ‘uninformed’ probes

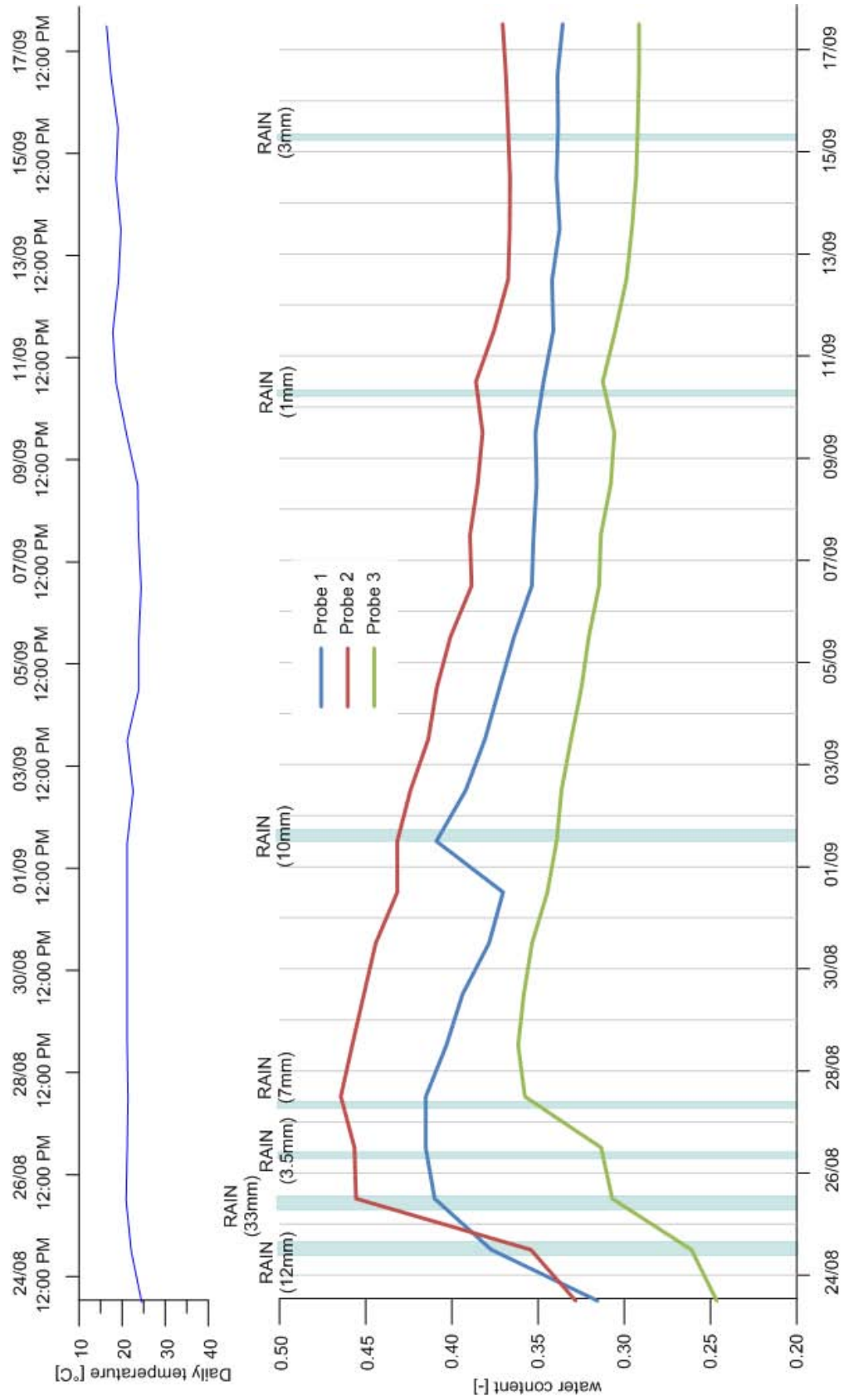


Figure 4.38: Third period; daily means of the water contents of the 'informed' probes

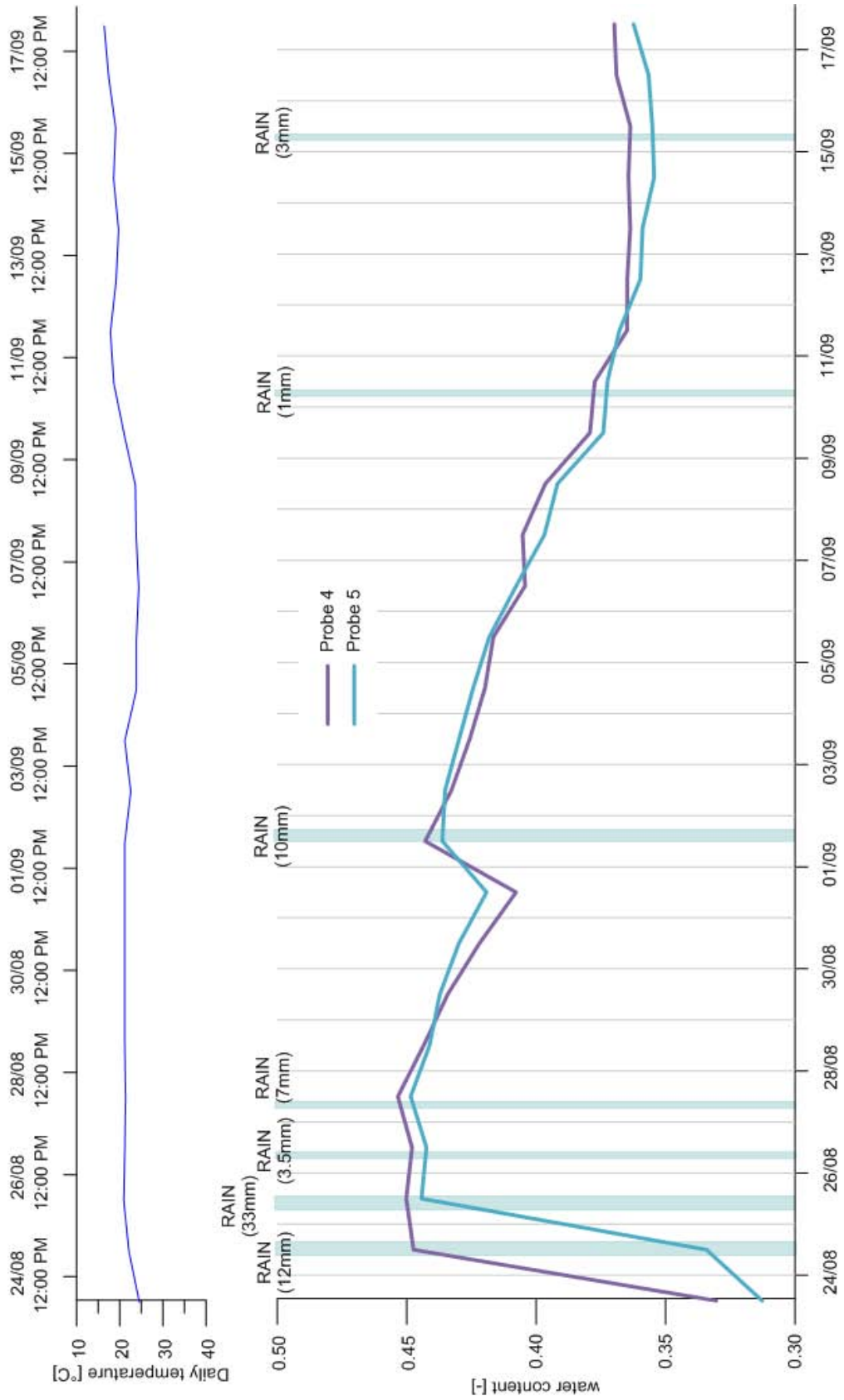


Figure 4.39: Third period; daily means of the water contents of the ‘uninformed’ probes

Chapter 5

Interpretation of the results and discussion

The water content in the maize field has been measured for 101 days, during which rainfall events and irrigations have supplied water to the field as detailed in chapter 4. The amount of water received from the two parts of the field from rainfall is the same, while the irrigation has furnished a different amount of water to the two groups of probes (87mm for the informed site and 120mm for the uninformed). Due to the different amount of water received and to the different features of the field in the two sites, also the water losses due to deep percolation and/or surface runoff shall be different. This hypothesis can be tested starting from the integration of the water balance equations in the two sites:

$$Z_r(t)\Delta\theta_1(t) = \int_0^t P(\tau)d\tau + \int_0^t I_1(\tau)d\tau - \int_0^t LOSS_1(\tau)d\tau \quad (5.1)$$

$$Z_r(t)\Delta\theta_2(t) = \int_0^t P(\tau)d\tau + \int_0^t I_2(\tau)d\tau - \int_0^t LOSS_2(\tau)d\tau \quad (5.2)$$

$LOSS_1$ and $LOSS_2$ represent the losses due to evapotranspiration and to deep percolation of the ‘informed’ and ‘uninformed’ sites respectively. For the sake of convenience, in this chapter the informed site will be denote through the subscript 1, while the uninformed site will be denoted by the subscript 2. By subtracting equations 5.1 and 5.2, the following equation is obtained:

$$Z_r(t)(\Delta\theta_1(t) - \Delta\theta_2(t)) = \int_0^t (I_1(\tau) - I_2(\tau))d\tau - \int_0^t (LOSS_1(\tau) - LOSS_2(\tau))d\tau \quad (5.3)$$

Where $\Delta\theta_1(t)$ and $\Delta\theta_2(t)$ are defined as

$$\Delta\theta_1(t) = \theta_1(t) - \theta_1(0) \quad (5.4)$$

$$\Delta\theta_2(t) = \theta_2(t) - \theta_2(0) \quad (5.5)$$

$\theta_1(t)$ and $\theta_2(t)$ representing the average water content at day t for the informed and the uninformed sites respectively, while $\theta_1(0)$ and $\theta_2(0)$ represent the initial water content for the site considered. Since the amount of rain received from the two sites is the same, as written above, their difference is zero, therefore the integral of their difference has been neglected in equation (5.3). Were the losses of the two sites equal, their integral would be zero and could be omitted as well. Under these assumptions, equation (5.3) can be rewritten as

$$Z_r(t) = \frac{\int_0^t (I_1(\tau) - I_2(\tau))d\tau}{\Delta\theta_1(t) - \Delta\theta_2(t)} \quad (5.6)$$

According to equation (5.6), the ratio between the integral difference of the input and the corresponding difference in the storage provide a proxy for the temporal pattern of Z_r . The resulting graph is reported in Figure 5.1.

Figure 5.1 shows that, under the assumption done, Z_r results would increase in time, as highlighted by the linear regression. This is meaningless from a physical point of view, because the soil tends to compact in time, with an expected decrease of the depth of the rootzone. This demonstrates that the basic assumption $LOSS_1(t) = LOSS_2(t)$ should be neglected. Moreover, Figure 5.1 also suggests that it is not possible to investigate the long term dynamics of Z_r , because they are overwhelmed by the short term dynamics of the losses (fluctuations in Figure 5.1 are dominant).

Provided that it is not possible to track possible dynamics of the rootzone in time, Z_r is set equal to 40cm for the entire period. Based on this assumption the dynamics in time of the losses for the two sites can be estimated.

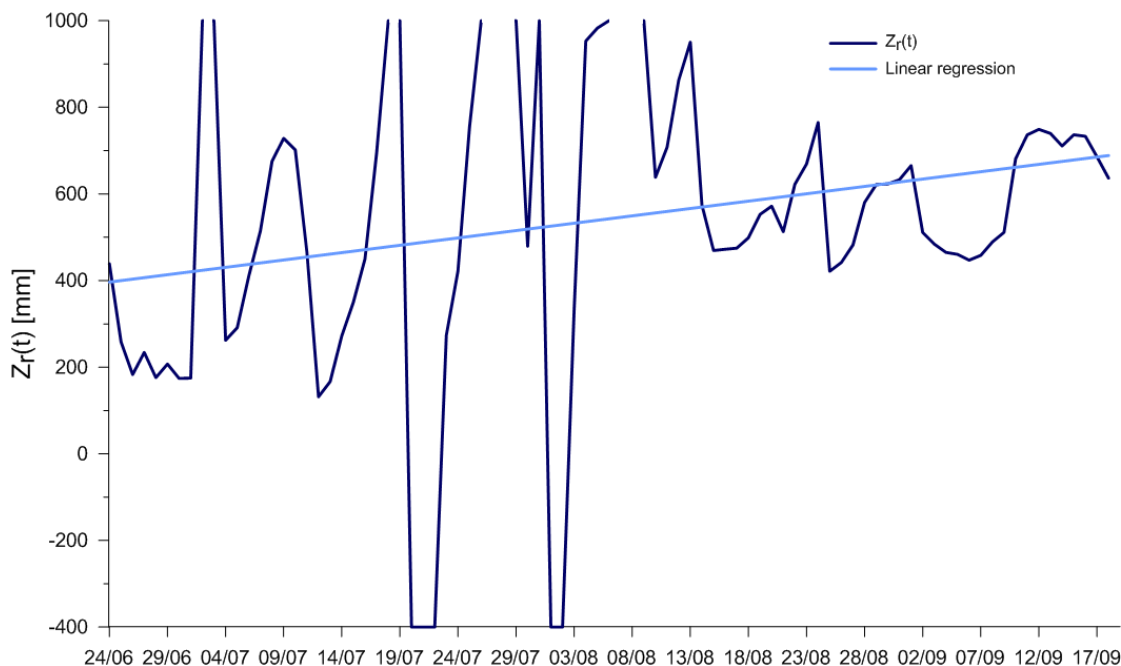


Figure 5.1: Trend of Z_r in time

The dynamics of the losses for the informed and the uninformed sites can be obtained from the following equations.

$$\int_0^t L_1(\tau) d\tau = \int_0^t P(\tau) d\tau + \int_0^t I_1(\tau) d\tau - Z_r(\theta_1(t) - \theta_1(0)) \quad (5.7)$$

$$\int_0^t L_2(\tau) d\tau = \int_0^t P(\tau) d\tau + \int_0^t I_2(\tau) d\tau - Z_r(\theta_2(t) - \theta_2(0)) \quad (5.8)$$

All the terms appearing in these equations have been defined above and the two integrals are plotted in Figure 5.2, while in Figure 5.3 the integrals are reported in a 3D graph.

In the first period of acquisitions, the integrals of the losses for the two sites are very similar, then they start to be different after the second irrigation.

From the plot it can be observed that the curve relative to site 1 jumps only when rainfall events bring a large amount of water. The losses of site 2, instead, are more sensible to smaller rainfall events. Moreover, observing the soil moisture contents for the two sites during the third irrigation (Figures 4.30 and 4.31), it can be seen that the uninformed site is much influenced by the irrigation of the informed site, while the influence of irrigation of the informed site on the uninformed one is very

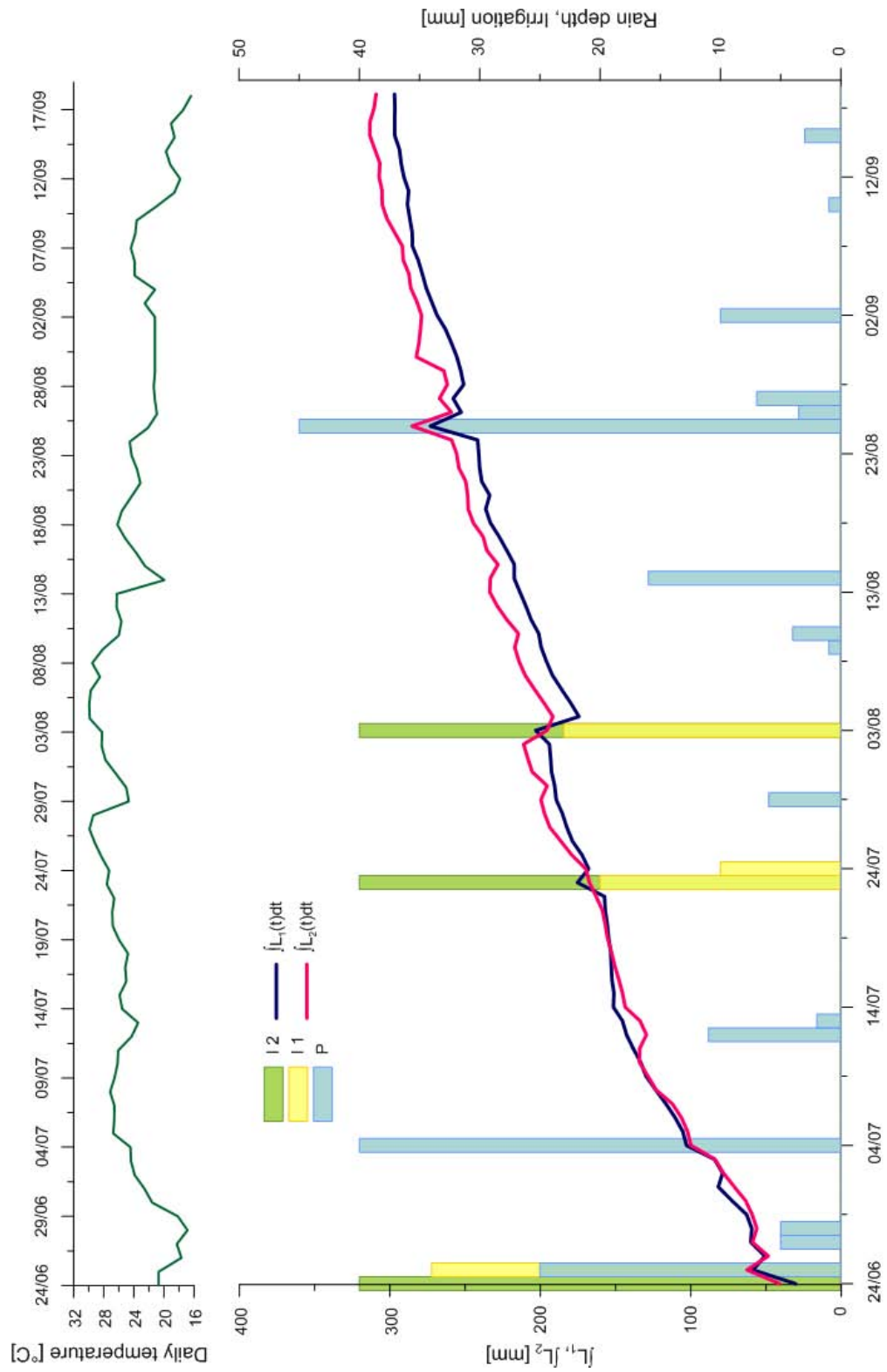


Figure 5.2: Integrals of the losses in time

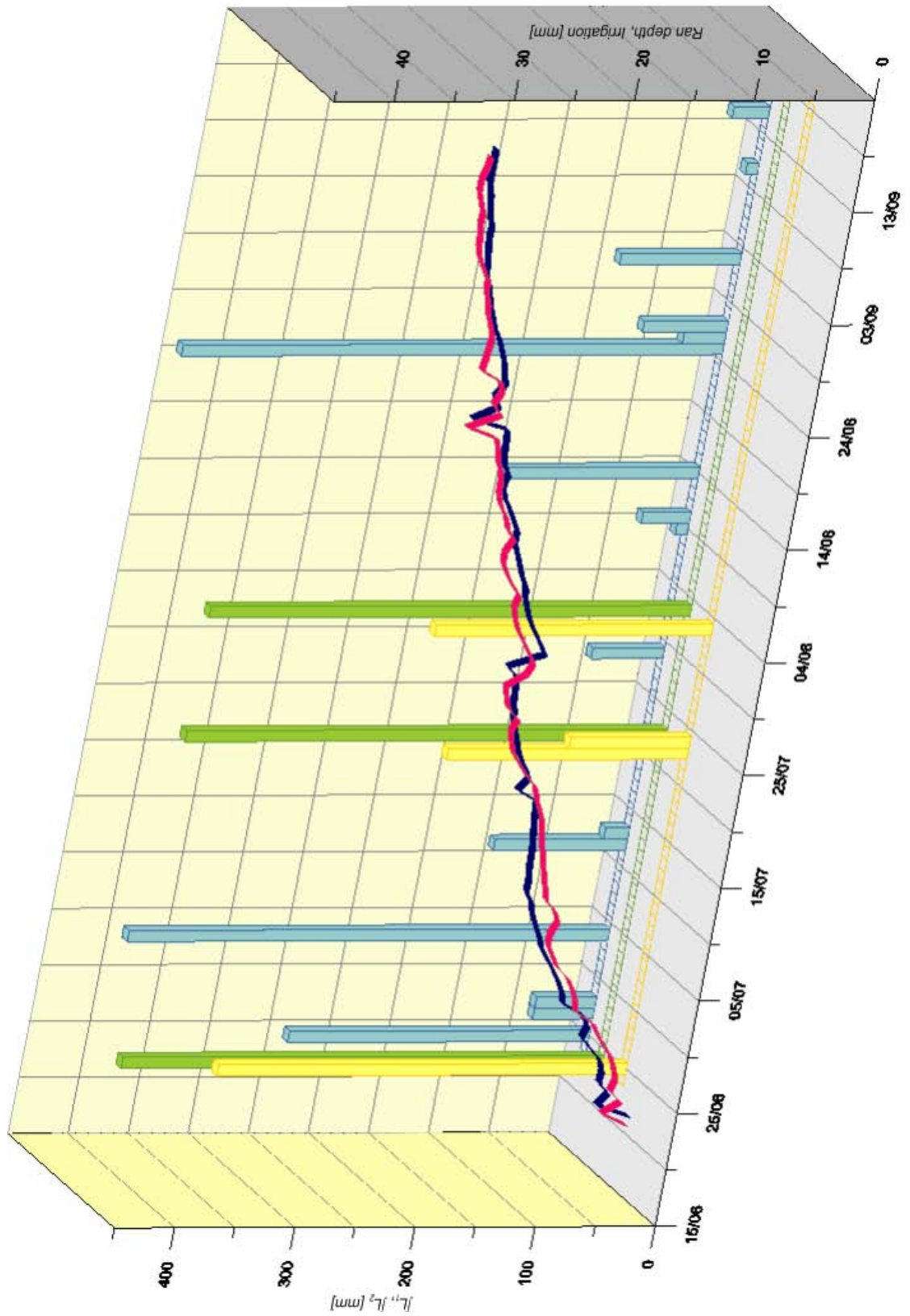


Figure 5.3: Integrals of losses in time; 3D plot

slight. These facts highlight the hydraulic connectivity between the two sites, with a preferential flow direction from site 1 to site 2. In fact, site 1 is characterized by the presence of a large number of fractures which redistribute water in the surrounding area, helped by the gentle slope of the field, and promotes the water flow towards the uninformed site. The integral of the losses of the uninformed site has larger (positive and negative) jumps than the informed site also because of the larger contribution area. The curve relative to the losses of the informed site, tends to flatten when the maize is suffering water stress conditions and ET is low. This does not happen in the uninformed site, because it had received a larger amount of water than informed site during irrigation, and also due to water redistribution processes. Hence, site 2 is characterized by a larger water availability which prevents from water stress conditions.

Considering the periods during which there are no significant water inputs, it is possible to obtain the rate at which the water content changes in time as $(\theta(t_{in}) - \theta(t_{fin}))/\Delta t$. $\theta(t_{in})$ represents the water content measured when the curve starts to be almost linear, while $\theta(t_{fin})$ is the water content value before a significant event. During the whole period of acquisitions, there are 4 periods in which the integrals of the losses are almost linear: from July 5 to 22, from July 25 to August 2, from August 4 to 24 and from August 26 to September 9. The water contents considered are the average of each site. Tables 5.1 and 5.2 report the values calculated.

<i>Informed site</i>			
<i>Period</i>	$\theta(t_{in})$	$\theta(t_{fin})$	$(\theta(t_{in}) - \theta(t_{fin}))/\Delta t$ [1/d]
5/07 - 22/07	0.405	0.308	0.005752
25/07 - 2/08	0.345	0.306	0.004901
4/08 - 24/08	0.413	0.297	0.005798
26/08 - 18/9	0.391	0.333	0.002535

Table 5.1: Rates at which water contents change in time, informed site

These values suggest that the ET rates are larger in the uninformed site, and that in both sites the evapotranspiration rate is decreasing in time during the season, most likely due to seasonal patterns of climate variables (e.g. the average daily temperature starts decreasing from August, 2).

<i>Uninformed site</i>			
<i>Period</i>	$\theta(t_{in})$	$\theta(t_{fin})$	$(\theta(t_{in}) - \theta(t_{fin}))/\Delta t$ [1/d]
5/07 - 22/07	0.408	0.285	0.007236
25/07 - 2/08	0.348	0.277	0.008864
4/08 - 24/08	0.429	0.322	0.005372
26/08 - 18/9	0.447	0.366	0.003528

Table 5.2: Rates at which water contents change in time, uninformed site

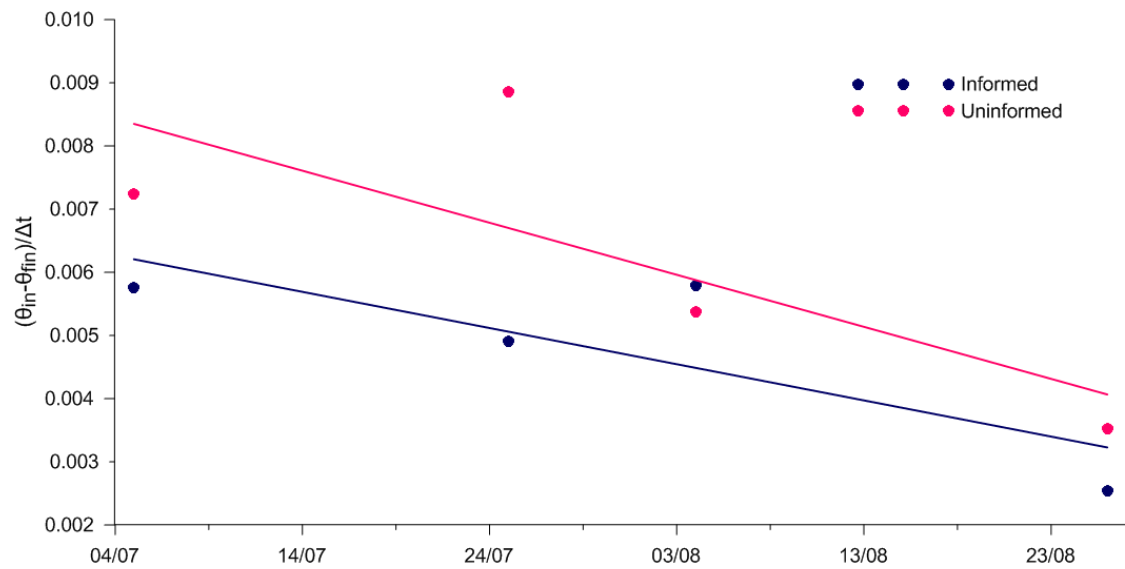


Figure 5.4: Water content change in time

The amount of water present in the root zone for the informed and for the uninformed sites during the acquisition period depends on external inputs and also on the different response to these inputs of the two sites.

Figure 5.5 reports the amount of water available in the root zone for the two sites. The informed site is referred as number 1, while number 2 refers to the uninformed site. Also in this case, the curves of the two different sites have a different behavior: the curve 2 is more sensitive than curve 1 to the external inputs. The water content relative to site 2 jumps more than site 1 when water arrives through rainfall which provides the same amount for both sites and also decreases faster than for site 1. This behavior means that in site 1 there is a more efficient redistribution of water, with lower losses.

When the two curves go above the zero line of the $Z_r\Delta\theta$ axis, it means that the water received exceeds the water needed from the two sites. For rainfall water nothing can be done, while, regarding irrigation water, a lot of water could be saved especially for the uninformed site for which the exceedance is more relevant. The last period of acquisitions is the one in which maize plants are dying, so the two curves start to be parallel and remain so until the end of the experiment.

During the whole period of the experiment, it is possible to identify 5 significant water input events: three irrigations and two rainfall events (observed in July 4 and August 25). The two different sites are considered separately in a comparative perspective. For each event, it has been considered the ratio among the amount of water h received from the site and the response of the same site in terms of change in the water content $Z_r\Delta\theta$. Figures 5.6 and 5.7 show the spatial and temporal pattern of the ratio $h/(Z_r\Delta\theta)$ during the 5 events in the two sites.

In the cases in which $h > (Z_r\Delta\theta)$, the change in the soil water content is lower than what expected from the mass balance and the amount of water provided. This means that water has been stored right after the application and redistributed to the plants in the following days. Fractures most likely play a key role in this process thanks to their ability to act as reservoirs. The ratio among h and $(Z_r\Delta\theta)$ is significantly larger than 1 only for probe 4 during the rain observed on August 25.

When the ratio between h and $(Z_r\Delta\theta)$ is lower than 1, the water content measured by the probes has a larger increase with respect to the amount of water provided.

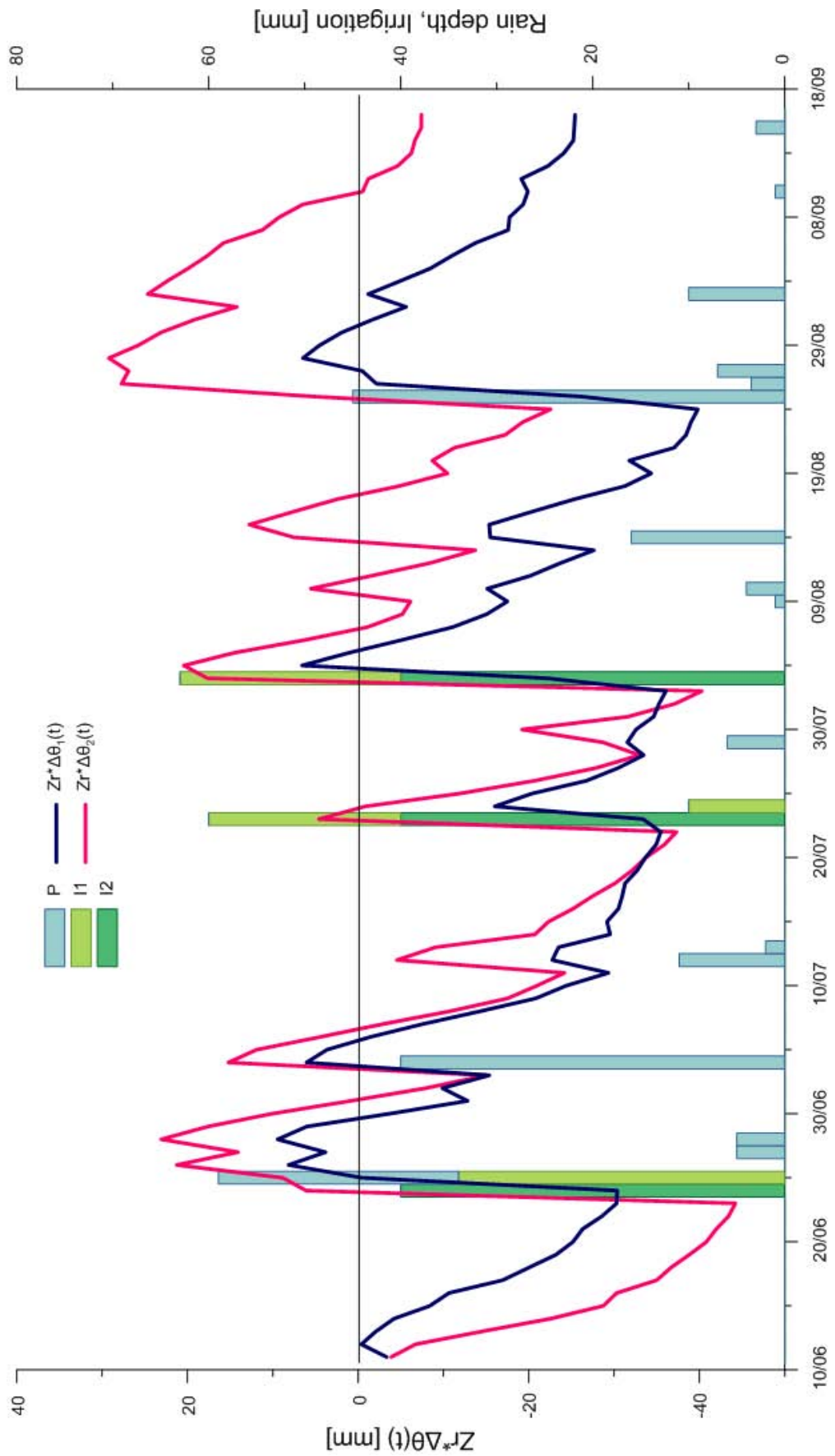


Figure 5.5: Water content dynamics in the rootzone

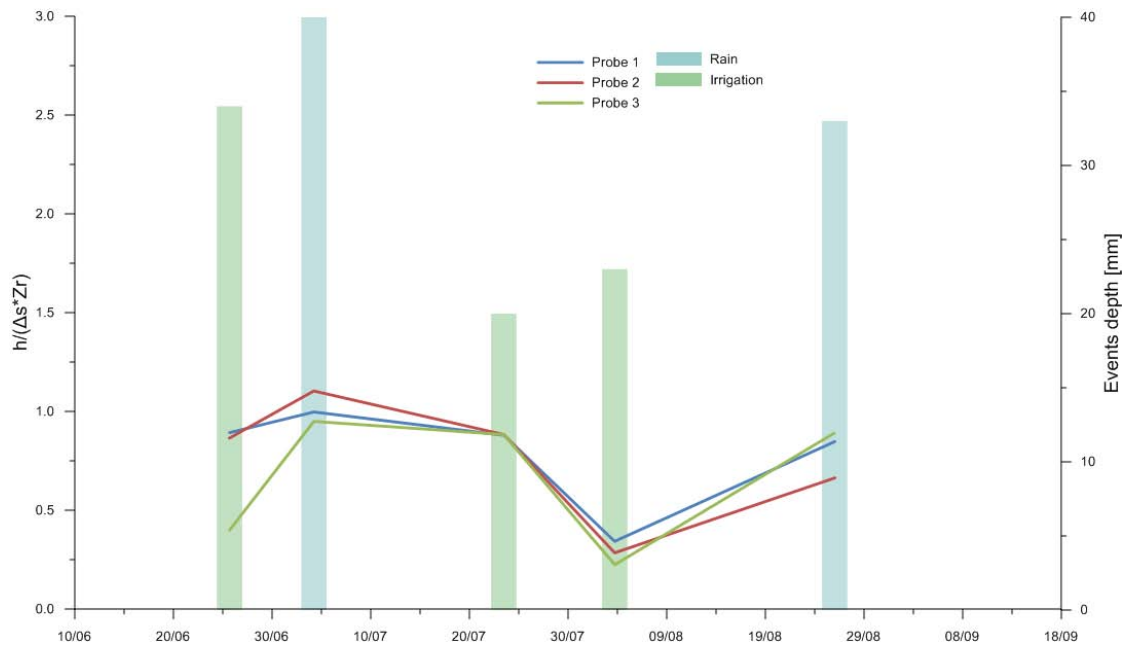


Figure 5.6: Response of the informed site to the significant events

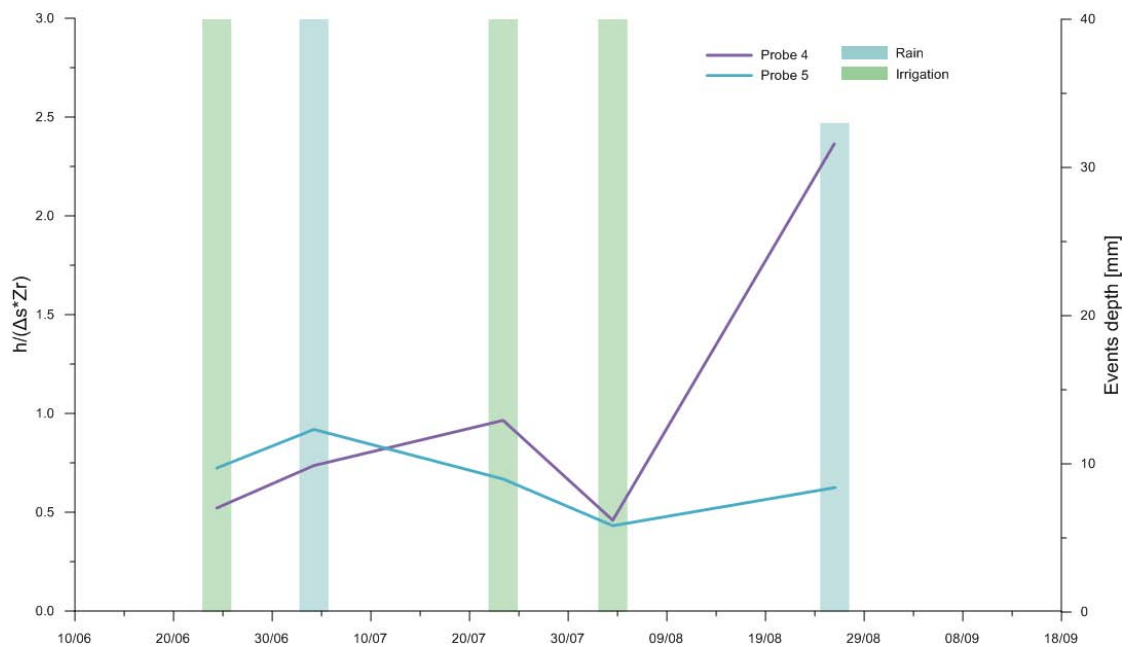


Figure 5.7: Response of the uninformed site to the significant events

In these instances, the water content decreases just after the event, meaning that there have been leakage losses from the root zone. This happens for the uninformed probes during the first irrigation, for probe 5 during the second and the third irrigation and for the rain observed on August 25. During the third irrigation, the ratio is lower than 1 for all the informed probes. During the first irrigation, probe 3 measures a water content change much lower than the amount of water received probably because of its depth to the surface which delays the increase of s with respect to the application.

Figures 4.6 and 4.7, suggest that the amplitude of the daily fluctuations of the water contents measured by the six probes changes in time. The daily fluctuations of the water contents are indeed wider in the first periods and become progressively more tight during the last stages of the experiment. The decrease in the fluctuations of s are well agrees with the pattern of plant evapotranspiration which is maximum during the months of June and July but progressively decreases after the begin of August until the death of the maize plants. Hence, daily fluctuations of soil moisture are most likely induced by hydraulic redistribution through the plants roots. This behavior is evidenced also by the daily variance of soil moisture (equation (5.9)) that measures the dispersion of a set of values around the mean:

$$VAR = \frac{\sum(\theta - \theta_{mean})^2}{N} \quad (5.9)$$

θ represents the soil water content at each acquisition, θ_{mean} represents the average water content of the considered day and N is the number of measurements per day. The variance is equal to zero when all the values are equal, while a small variance implies that the measured values tend to be very close to the mean. Conversely, high variance indicates a significant spreading of the water content around the mean. Since the variance is the sum of squared terms, only positive values are expected. Figures 5.8 and 5.9 show the variance of soil moisture as a function of time for probes 1 and 4. Similar patterns can be obtained for the other probes. The daily variance of the water content measured by probe 4 in the uninformed site has larger long-term fluctuations compared to probe 1. Furthermore, the variance relative to probe 4 decreases more significantly in time. Probe 1, however, in the last days of acquisitions measures values for the soil water content almost constant (Figure 4.6). For this reason the variance in these days is very small (Figure 5.8).

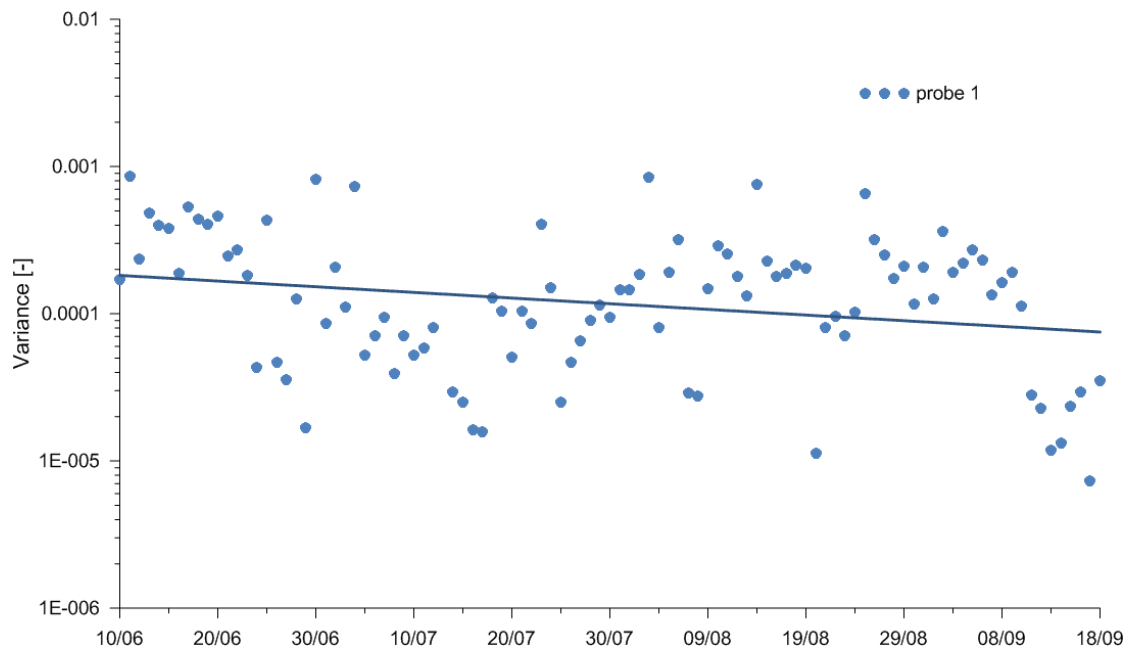


Figure 5.8: Variance of probe 1

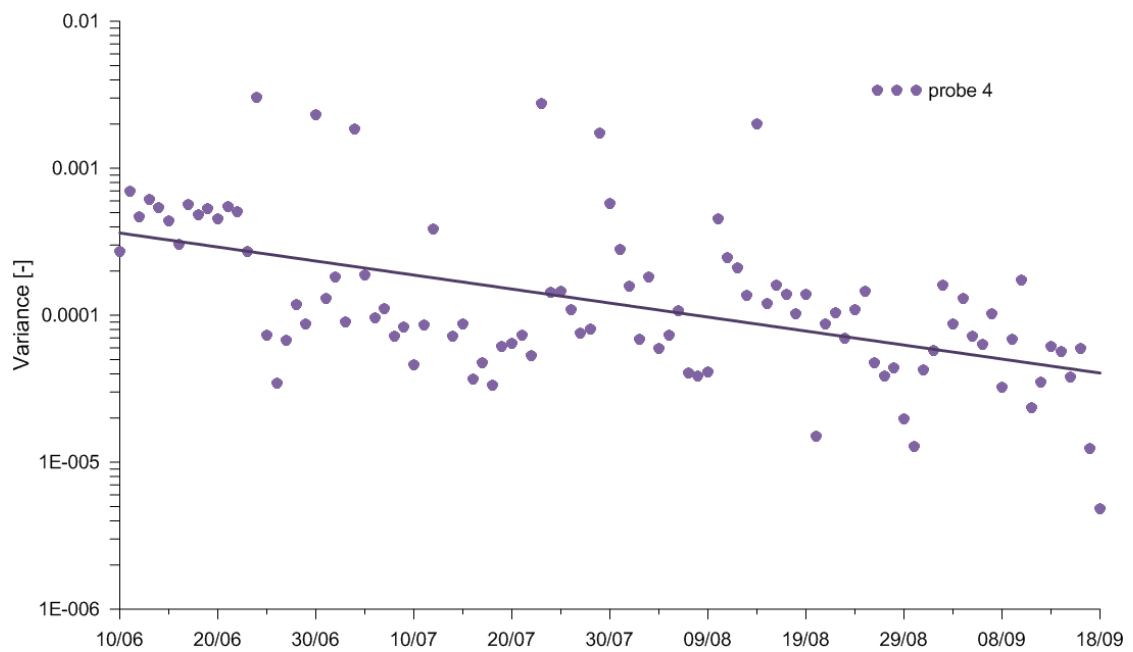


Figure 5.9: Variance of probe 4

The coefficient of variation CV is another statistic function useful to evaluate the behavior of the fluctuations of the soil water content. The coefficient of variation is a dimensionless measure of the dispersion of the values around the mean, and it is defined as the ratio between the square root of the variance VAR and of the mean μ :

$$CV = \frac{\sqrt{VAR}}{\mu} \quad (5.10)$$

Figures 5.10 and 5.11 show the coefficient of variation for probes 1 and 4 during the period of acquisitions.

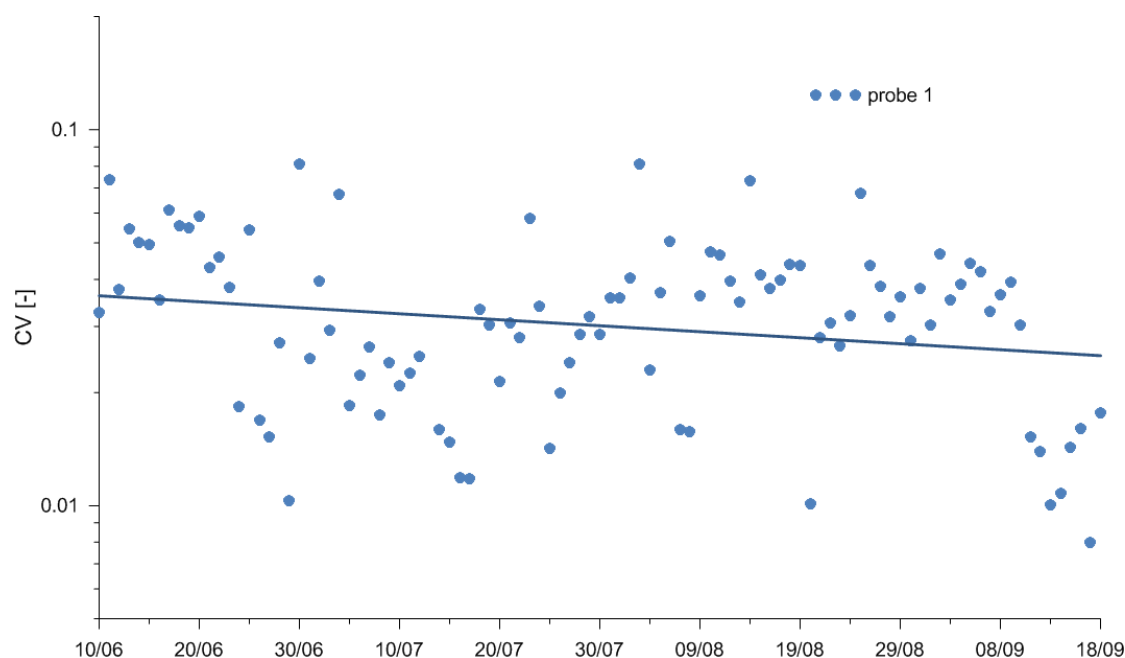


Figure 5.10: Coefficient of variation for probe 1

After normalizing the values to their mean the two sites result to be closer one to each other in terms of intra-seasonal variability. The reduction of the amplitude of the fluctuations of the water content toward the end of the acquisition period clearly emerges, especially for the informed site.

The period of acquisitions stopped on September 18 in the morning. Right after the switch off of the TDR instrument, a sample of corn has been collected from each site. The harvesting was performed by collecting the maize row above the probes and the two adjacent rows, so as to cover an area of about 4m^2 . Plants

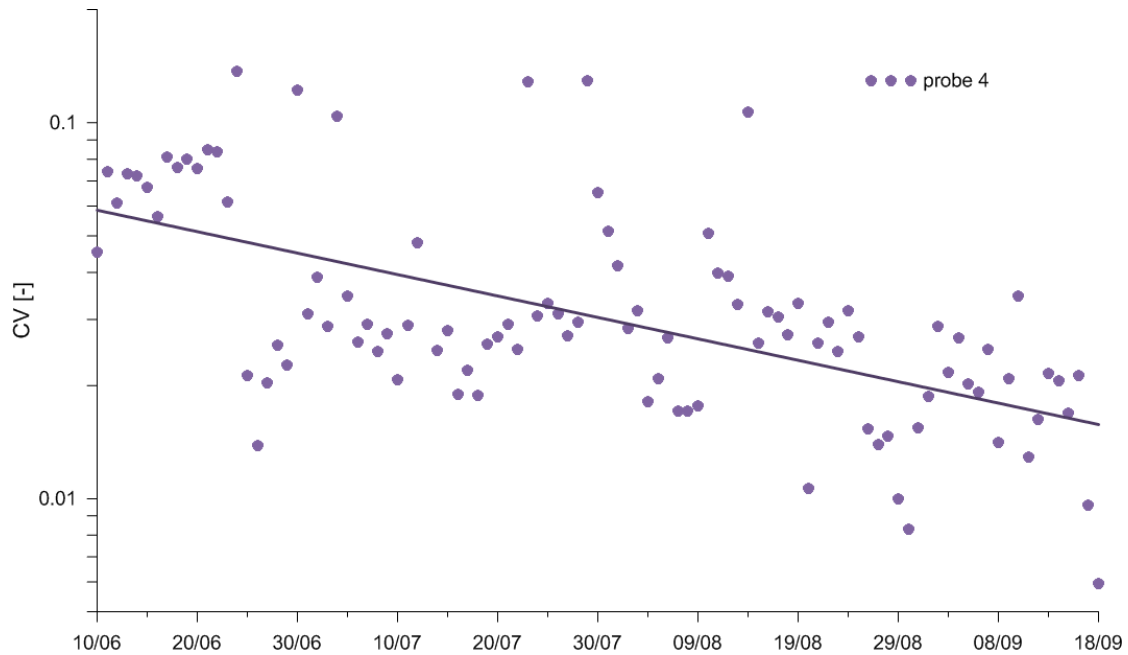


Figure 5.11: Coefficient of variation for probe 4

have been weighted separately for the two sites, before removing and weighting the corncobs. The number of grains of a representative number of corncobs were calculated for each site before removing the cobs and weight the grains. A sample of grains for each site was analyzed in the laboratory to estimate the specific weight and relative humidity of the two samples. All the information derived from the laboratory analysis are reported in Table 5.3, which shows that no significant differences were observed between the two samples derived from the two sites.

The difference between the amount of water provided to the two sites through irrigation is 33mm. This means that, using an informed water balance scheme, about 30% of water has been saved compared to the uninformed irrigation. Conversely, the analysis of the samples collected, suggests that difference in grain production is minimal. In fact, in the uninformed site the productivity (kg of corm for each plant) was only 5% larger than that in the uninformed site. The small difference of productivity between the two sites can be explained by small-scale differences in the fertility of the soil, but it can be also related to the sampling procedure adopted. Hence, the use of an informed water balance scheme allows a significant saving of irrigation water (with some advantages also in terms of irrigation costs)

	<i>Informed site</i>	<i>Uninformed site</i>
Number of plants	27	26
Number of corncobs	29	29
Total weight of the plants [kg]	12.5	15.5
Total weight of the corncobs [kg]	9	9
Average number of grains per corncob	619	639
Total weight of the grains [kg]	7.3	7.4
Seed temperature [C]	20	19
Relative humidity	25.7%	25.9%
Specific weight [kg/hl]	72.8	72.6
kg grains/plant	0.270	0.285
Total amount of irrigation water [mm]	87	120

Table 5.3: Harvest data

without compromising field productivity, suggesting the usefulness of hydrologic measurements for irrigation management.

Chapter 6

Conclusions

Hydrologic measurements could significantly help agriculture to reduce water waste during irrigation without compromising crop productivity. In fact, information on soil water content dynamics allows an optimization of the timing and amount of water supplied to the field, avoiding water losses through leaching and water stress for plants.

For this study, a maize field was monitored through a TDR instrument designed to measure soil water content during an entire growing season (from June 10 until September 18 2013). The TDR is provided with six probes, which have been subdivided into two groups and positioned at variable depths in two separate parts of the same maize field. In the first site traditional irrigation procedure were performed, relying on the farmer's experience, ('uninformed' site), while in the second site an informed water balance irrigation scheme accounting for the available hydrologic measurements was carried out ('informed' site). In both sites water was delivered through sprinkler irrigation: in the uninformed site a hose reel was used, while in the informed site fixed sprinklers were employed. The two sites were at a distance of about 30m one from each other, so as to avoid huge interferences between the two sites during irrigation. Unfortunately, the interaction between the two sites in some cases has not been negligible. In particular, the uninformed site seems to be significantly influenced by the irrigation of the informed site due to water redistribution and drainage. Soil water balance schemes revealed a different response of the two sites to rainfall events in terms of water losses (leakage and *ET*). The different responses of the two sites evidence an hydraulic connection among

them with a preferential direction toward the uninformed site. This phenomenon is helped by the fractures observed in the field and by the gentle slope of the terrain allowing water movement toward the uninformed site, which therefore has a larger flow basin.

During the acquisition period there have been three irrigation applications for both sites: 120mm of water were delivered to the uninformed site, while the informed site received 87mm of water, 27.5% less than the uninformed site. To check whether the informed water balance irrigation scheme has allowed to save water during irrigation without compromising crop productivity, samples of maize from both sites have been taken and then analyzed. To compare the productivity of the two sites, the kilograms of grains produced per plant were calculated for each site. In the informed site the productivity was 0.270kg of grains per plant, while in the uninformed site the productivity was of 0.285kg of grains per plant, only a few percent larger than that of the informed site. This difference can be explained by errors during sampling and measurement procedures. The experiment performed in this study demonstrates that the availability of hydrologic measurements has allowed a significant water resources saving without compromising crop productivity, thus suggesting a potential large-scale applicability of this irrigation method.

Future developments of the informed water balance irrigation scheme can include a numerical modeling able to include the available hydrologic measurements, climate forecasts and crop type with the aim of inform farmers about the timing and amount of water required to plants. Technical improvements in irrigation water management could be also achieved by exploiting modern irrigation methods, such as drip irrigation, which (jointly with hydrologic measurements) could further reduce water waste and even increase crop productivity.

Ringraziamenti

Finalmente raggiungo questa importante tappa nella mia vita e, se ci sono arrivata, devo ringraziare molte persone che mi hanno aiutato.

Innanzitutto devo ringraziare la mia famiglia: mamma Alberta e papà Michele, che non mi hanno mai fatto mancare affetto e sostegno (anche economico), e un grazie anche al mio 'fratellino' Elia per aver sacrificato l'udito del suo orecchio destro. La mia famiglia è davvero speciale per me per tutto l'amore e la serenità che riesce a darmi.

Ringrazio i miei nonni Angelo, Rosa e Franca perché mi hanno sempre dato una parola di conforto e per le tante candele accese durante gli esami. Un grazie speciale anche per il nonno Renzo che non è più qui con noi, ma che da lassù mi protegge e mi sta vicino anche quando tutti gli altri devono rimanere fuori. Devo ringraziare anche la zia Ginevra, che ogni volta che viene a trovarmi riesce a farmi sorridere! Grazie anche allo zio Sergio per tutte le volte che ha riparato le mie biciclette.

Un ringraziamento molto speciale al mio Alessandro, perché mi sprona sempre a fare meglio e mi incoraggia nei momenti di sconforto, mi sta vicino e mi sopporta anche se non è cosa facile e con cui spero che, dopo questo importante traguardo, potremo iniziare a costruire una vita insieme.

Devo ringraziare molto anche le mie amiche Alessandra, Alessandra, Fiorenza, Francesca e Michela per i bei momenti trascorsi assieme, per avermi sopportato e per l'appoggio su cui sono certa di poter contare anche se le nostre vite ci hanno un portato a vederci un po' di meno. Grazie ad Arianna e Mattia per le 'avventure' vissute assieme! Spero continueranno ad essercene ancora per molti anni.

Grazie a Mirella e Silvia con cui la laurea triennale è sembrata meno pesante! In particolare grazie a Silvia per il sostegno morale pre-esami e a Mirella per essere riuscita a sopportarmi come compagna di collegio!

Un grazie di cuore a Ilaria e Katia per tutti i progetti portati avanti assieme e per avermi sempre aspettato mentre finivo di mangiare in mensa. Lo so, sono una piaga!

Questa tesi non sarebbe stata relizzata senza l'aiuto del prof. Botter, del prof. Putti e di Enrica. Vi ringrazio davvero molto.

Ringrazio la famiglia Crivellaro Giuseppe per la disponibilità ad installare lo strumento nella loro corte e i tecnici Pioneer Andriolo Giuliano e Beltrami Isaia per i numerosi dati forniti.

Padova, 16/10/2013